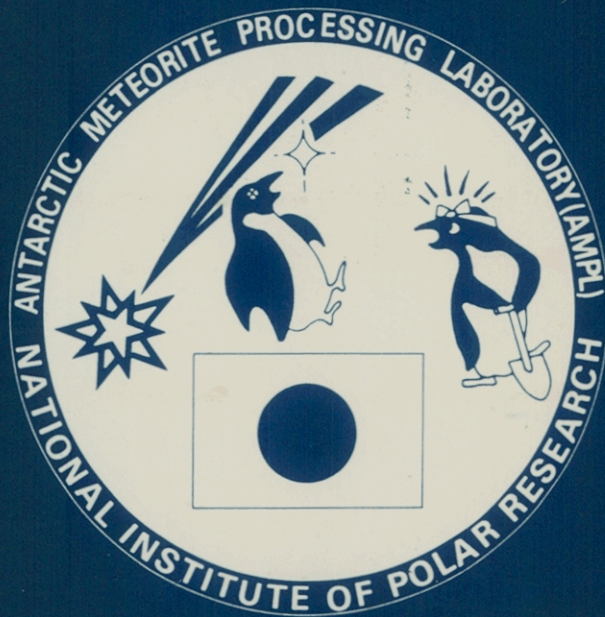


Papers presented to the
SIXTH SYMPOSIUM
ON ANTARCTIC METEORITES



19-20 February 1981

NATIONAL INSTITUTE OF POLAR RESEARCH,
TOKYO

国立極地研究所
南極隕石処理室

- 12 1345 Kitamura M.* Watanabe S. Morimoto N.
Study of Allende Meteorite by Analytical Transmission
Electron Microscopy
- 13 1400 Takeda H.* Mori H. Yanai K.
Mineralogy of the Yamato Diogenites of Possibly Pieces
of a Single Fall
- 14 1415 Sato G.* Takeda H. Yanai K.
A Mineralogical Examination of Some Allan Hills
Polymict Eucrites
- 15 1430 Masuda A.* Nakamura N. Shimizu H.
Did Diogenites form from Diogenites?
- 16 1445 Matsumoto Y.* Hayashi M. Daishi M. Miura Y.
Homogeneity of the Yamato-75110 Chondrite

1500-1515 Tea Time

Chairmen: Hiroshi Takeda and Kosuke Ohnuma

- 17 1515 Fujimaki H.* Aoki K. Sunagawa I. Matsu-ura M.
Study on Some Minerals in ALH-77015(L3) Chondrite
- 18 1530 Ikeda Y.* Kimura M. Takeda H.
Major Chemical Composition of Matrices of Unequilibrated
Ordinary Chondrites
- 19 1545 Nagahara H.
Petrology of Chondrules in ALH-77015(L3) Chondrite
- 20 1600 Matsu-ura M.* Sunagawa I. Aoki K. Fujimaki H.
Petrology of ALH-77015 Chondrite
- 21 1615 Tsuchiyama A.* Nagahara H.
Experimental Reproduction of Textures of Chondrules; II
Effect of Residual Crystals
- 22 1630 Fukuoka T.* Ishii T. Nakamura N. Takeda H.
Chemical and Petrological Studies of ALH-77302 Meteorite
- 23 1645 Onuma N.* Hirano M.
Sr-Ba Systematics in Antarctic Ca-rich Achondrites
- 24 1700 Shimizu H.* Masuda A.
REE, Ba, Sr and Rb Abundances in Some Unique Antarctic
Achondrites
- 25 1715 Biswas S. Ngo H. T. Walsh T. M. Lipschutz M. E.*
Does Weathering Affect Trace Element Contents of
Antarctic Meteorites?

1800-1930 Reception (Lecture Room, 2nd Floor in Research Building)

Friday, February 20, 1981

Chairmen: Akimasa Masuda and Naoki Onuma

- 26 1000 Nishimura H.* Okano J.
Magnesium Isotopic Ratios of Yamato Meteorites
- 27 1015 Nishiizumi K.* Imamura M. Arnold J. R. Honda M.
Cosmogenic ^{53}Mn in Yamato and Allan Hills Meteorites
- 28 1030 Imamura M.* Honda M. Nishiizumi K. Nitoh O.
Takaoka N.
Extraterrestrial History of Antarctic Meteorites
Recorded in the Cosmogenic Nuclides
- 29 1045 Honda M.*
Terrestrial History of Antarctic Meteorites Recorded in
the Cosmogenic Nuclides
- 30 1100 Unruh D. M. Patchett P. J. Tatsumoto M.*
U-Pb and Lu-Hf Systematics of Antarctic Meteorites
- 31 1120 Nakamura N.* Ito A. Masuda A. Tatsumoto M.
Rb-Sr and Sm-Nd Systematics of the Antarctic Chondrites
(ALH-74640, ALH-769) and Achondrite (ALH-77302)
- 32 1135 Kaneoka I.* Ozima M...
 $^{40}\text{Ar}/^{39}\text{Ar}$ Ages of Antarctic Meteorites
- 33 1150 Nagao K.* Saito K. Ohba Y. Takaoka N.
Rare Gas Studies of the Antarctic Meteorites

1205-1300 Lunch

Chairmen: Ichiro Sunagawa and Nobuo Takaoka

- 34 1300 McFadden L.A. Gaffey M.J. Takeda H.*
The Layered Crust Model and the Surface of Vesta
- 35 1315 Fujimura A.* Kato M. Kumazawa M.
Preferred Orientation of Phyllosilicate in Yamato-74642
and -74662(C2)
- 36 Cancel Ponnampereuma C.*
Organic Matter in Carbonaceous Chondrites from the
Antarctic

- 37 1350 Yamaji M.* Matsumoto T.
The Structures of Olivines in Yamato-74 Meteorites
- 38 1405 Chang Ziwen
On the Falling Frequency and Geographical Distribution
of Chinese Historical Meteorites
- 39 1420 Chang Shuyuen.* Yu Zhi-Jun
Historic Records of Meteorites in China and Their Time-
Series Analysis
- 40 1435 Chang Shuyuen.*
The Fissure of Kirin Meteorite

1455-1510 Tea Time

Chairmen: Masatake Honda and Hiroichi Hasegawa

- 41 1510 Hasegawa H.*
Shape of the Meteorites
- 42 1525 Funaki M.* Nagata T. Momose K.
The Composition of Natural Remanent Magnetization of
an Antarctic Chondrite, ALH-76009(L6)
- 43 1540 Nagata T.* Funaki M.
Magnetic Analyses of Metallic Phases of Yamato-74115(H5),
-74190(L6), -74354(L6), -74362(L6) and -74646(LL6)
- 44 1555 Nagata T.*
Paleointensity of Antarctic Achondrites
- 45 1610 Miyamoto M.* Mito A. Takano Y. Fujii N.
Spectral Reflectance(250-2500nm) of Powdered Samples
of Antarctic Meteorites
- 46 1625 Miura Y.* Matsumoto Y.
A Classification of Some Yamato-75 Chondrites (III)
- 47 1640 Yomogida K.* Matsui T.
Physical Properties of Meteorites
- 48 1655 Karato S.* Matsui T.
Dislocations in Olivines from Pallasite Meteorites
-
- 49 1330 Akai J.
Mineralogy of the Matrix Phyllosilicates of Carbonaceous
Chondrite by High Resolution Electron Microscopy

JAPANESE ANTARCTIC METEORITE SEARCH IN 1979-1980 SEASON

Yanai Keizo*, Kojima Hideyasu*, Nishida Tamio***

* National Institute of Polar Research, Kaga, Itabashi-ku, Tokyo 173.

** Inst. of Mining Geology, Mining College, Akita Univ. Tegata, Akita 010.

*** Inst. of Earth Science, Faculty of Education, Saga Univ. Honjo-Machi, Saga 840.

The Japanese party visited the Yamato Mountains in the 1979-1980 season to search for Antarctic meteorites. Over 3,000 new specimens were collected between October 1979 and January 1980 on the bare ice areas adjacent to the Yamato Mountains where about 1,000 meteorite specimens had been recovered by Japanese Antarctic Research Expedition Teams in the past. The same party collected few specimens on the bare ice near the Belgica Mountains located about 200 km west from the Yamato Mountains.

The collected specimens are chondritic meteorites in majority, and the finds included less than 10 irons, over 20 carbonaceous chondrites (type 2 in majority), about 100 achondrites (eucrites and diogenites in majority) and many possible unique specimens.

The total number of original meteorites in this finds is believed to present 300 to 400 individual meteorites.

This collection are processing initially and examine preliminarily in order of findings in the Antarctic Meteorites Processing Laboratory, National Institute of Polar Research. After preliminary examination for about six hundreds the collection includes ten eucrites (polymict), two diogenites, five carbonaceous chondrites and one ureilite, and many possible unique specimens.

These collections were named officially as Yamato-79 meteorites and Belgica-79 meteorites, and the specimens were designated initially as Yamato-790001 to Yamato-79XXXX and Belgica-79X1 to Belgica-79XX respectively in order of discovery.

2

A POSSIBLE RATIO OF THE APPEARANCE OF METEORITES FROM THE ANTARCTIC ICE

Yanai K.* and Matsumoto Y.*

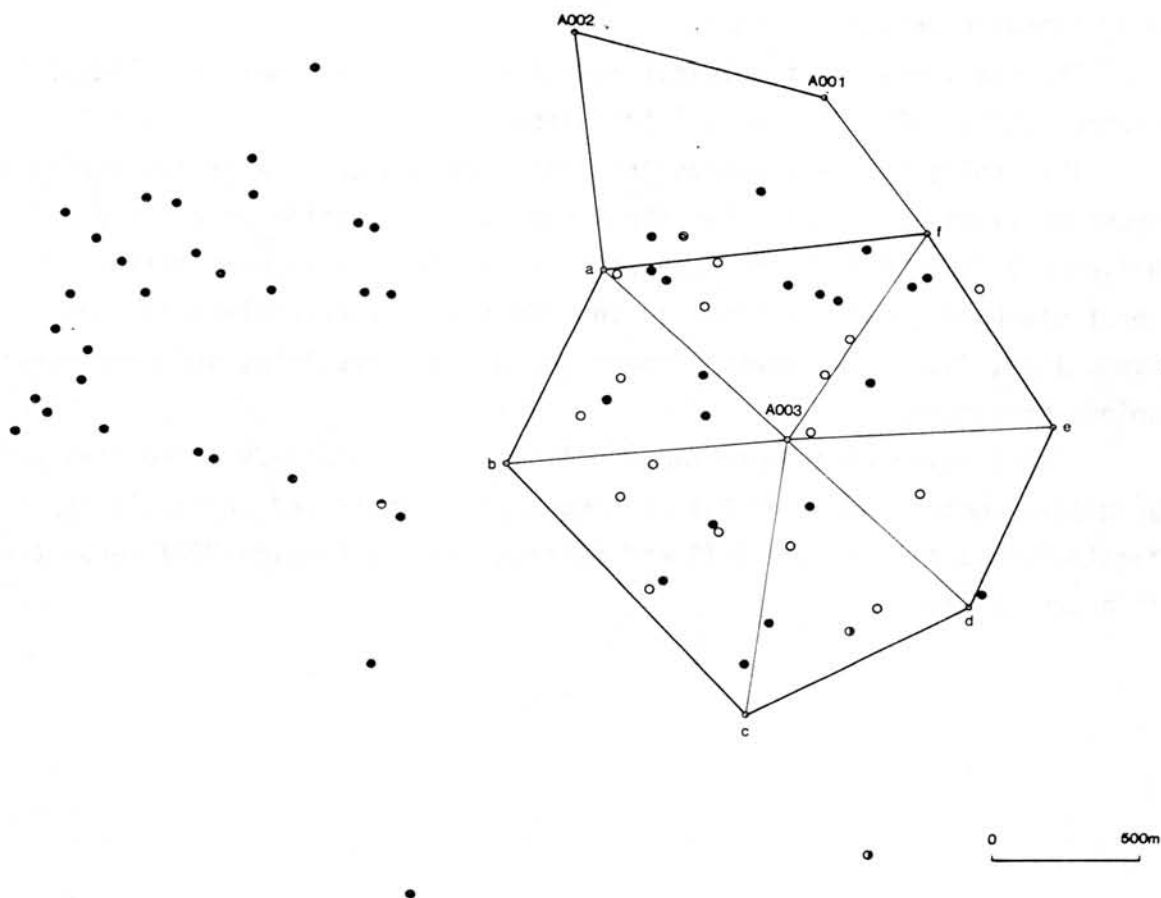
* National Institute of Polar Research, Kaga, Itabasi-ku, Tokyo 173.

** Department of Mineralogical Sciences and Geology, Faculty of Science, Yamaguchi University, Yamaguchi 753.

Seventeen new specimens of meteorites were collected in a grid which is hexagonal form with each side being about 800 m and about 2 square km. At January 1976, the grid was set up on the bare ice field around A003 control point near the Motoi Nunatak, at the southend of the Yamato Mountains, Antarctica. Then all meteorite specimens exposed on the bare ice surface in the grid were collected.

After four years, Japanese Antarctic Research Expedition party re-visited and re-searched rigorously meteorites in the grid. As the result, seventeen specimens contained two diogenites and two carbonaceous chondrites were recovered on the bare ice which is ablating at the rate of 9-32 cm in four years. As a result of the ablation ratio of the ice, meteorite come up to the it's surface at the rate of two pieces per year and the square km.

The figure shows the localities of the meteorites recovered near the Motoi Nunatak. Open circle: newly found specimens. Others: meteorites collected 1969-1976. A003: Motoi Nunatak.



ON SHOWER OF THE ANTARCTIC METEORITES

Yanai Keizo: National Institute of Polar Research. Kaga, Itabashi-ku, Tokyo 173.

About 5,000 meteorite specimens grouped into some different kinds are distributed in the several small area of the bare ice field in the Antarctic continent. Some explanations may be given to such distribution: These are meteorite showers, mechanical fractionation by weathering on the bare ice surface and concentration of meteorites by transportation and ablation effect for ice.

Following specimens may be explained as shower or fractionation.

<u>Diogenite Type "A"</u>		<u>Eucrite</u>	
Y-692	138.0 grms.	Y-75159	98.2 grms
Y-74005	3.8	356	10.0
10	298.5	450	235.6
11	206.0	Y-75011	121.5
13	2,059.5*	15	166.6
31	6.1	295	8.8
37	591.9*	296	8.6
96	16.1	307	7.9
97	2,193.9*	Y-79XXXX	about 40 specimens
109	43.5	Allan Hills eucrites	over 7 specimens
125	107.0		
126	14.5	<u>Carbonaceous Chondrites</u>	
136	725.0*	Y-693 (C4)	150
150	33.4	Y-74641 (C2)	4.5
151	49.1	642 (C2)	10.6
162	3.9	662 (C2)	150.9
344	1.4	Y-75013 (C2)	1.5
347	7.8	260 (C2)	4.0
368	4.1	293 (C2)	8.1
448	17.7	Y-79XXXX	about 20 specimens
546	7.3		
606	2.9	<u>Chondrites</u>	
648	185.5	Y-74048-046(H)	17 pieces 2-135 grms
Y-75001	4.1	Y-74138-142	5 4-30
4	37.1		
7	2.6	Y-74194-342	149 1-10
14	3.0	379-416	38 "
285	3.1	Y-79XXXX	about 50 "
299	9.1		
Y-79XXXX	about 10 specimens	Y-74418-436(H6)	19 500 max, -20
		Y-74459-602	144 1,719 max
		Y-79XXXX	about 10 about 10
<u>Diogenite Type "B"</u>			
Y-75032	189.1,		
Y-79XXXX	about 10 specimens	Y-75108-257	150 600-800 X 8 about 40
<u>Ureilites</u>		<u>Porous Specimens</u>	
Y-74123	69.9	Y-79XXXX	
130	17.9		
659	18.9		
Allan Hills Ureilites			

Possibility of detecting meteorite buried within the ice
by radio echo sounding

Fumihiko NISHIO, Makoto WADA and Shinji MAE

National Institute of Polar Research

1. Introduction To elucidate the concentration mechanism of a large number of meteorites in the bare ice area, it is very significant to find meteorites buried within the ice in the bare ice area where many meteorites are concentrated. From the observed results of the movements and the ablation rate of ice sheet surface in the bare ice area, it may be generally concluded that the ice mass is coming upwards from the ice sheet interior and it is continuously scraped out by the ablation effect. The ice flow is continuously carrying a number of meteorites with it to the bare ice surface, and many meteorite pieces may be buried within the ice. This suggests that meteorite piece within the ice may probably be on its way to come out to the bare ice surface. It is also believed that such a finding of meteorite buried within the ice could be of importance in that an independent method for dating the earth residence time of the meteorite would then be possible. That is, the ice surrounding the meteorite could be dated and compared with the date determined from element decay ratio measurements made on the meteorite. Although there may be many methods to find meteorite buried within the ice, radio echo sounding could have been used practically as a technique for detecting buried meteorites in the ice sheet interior.

2. Power reflected from meteorite within the ice.

For the purpose of calculating the power reflected from the meteorites within the ice, we begin by assuming that meteorite pieces are sphere in shape though they are very complicated shape, and that the dielectric constant of stony meteorite is given by that of granite ($\epsilon_s = 8.0$) and iron meteorite conductive sphere. It is also assumed that isolated meteorite piece is buried within the ice and the strength of the electric field throughout the ice is not attenuated for simplicity. So we could obtain three models to calculate the power reflected from meteorite piece according to relation between the wavelength of the radio echo-sounding apparatus and the diameter of meteorite piece. This will be considered in more detail later.

2.1. Size distribution of meteorite piece in diameter.

A histogram of the frequency distribution of diameter of the Yamato stony meteorites and the world recognized iron meteorites with respect to diameter is illustrated in Fig. 1, where diameter is calculated with using the meteorite density given by 3.6 gm/cm^3 as stony meteorite and 7.8 gm/cm^3 as iron meteorite respectively. The maximum values of diameter are numerically given as about 10 cm for the Yamato stony meteorites and as about 70 cm for the world recognized iron

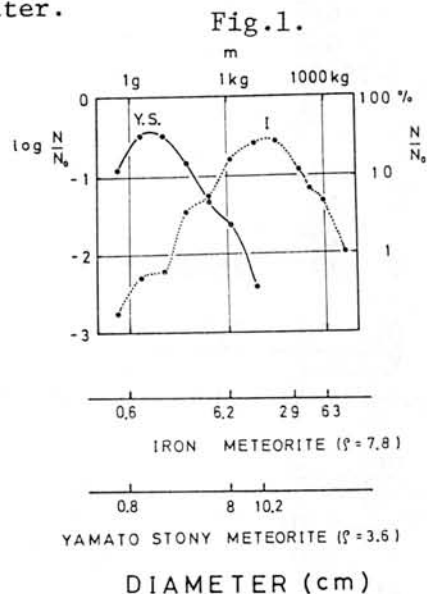


Fig.1. Frequency spectrum of diameter of Yamato meteorites(Y.S.) and the world recognized iron meteorites(I). Diameter is calculated with using the density of stony meteorite(3.6 gm/cm^3) and iron meteorite(7.8 gm/cm^3) respectively.

meteorites, and the maximum frequency of the diameter of them is about 1 cm and 20 cm respectively.

2.2. Back scattering crosssection of spherical meteorite.

By a function of diameter of spherical meteorite (d) and wavelength of pulsed radar (λ), three models for the back scattering power depending on the variation of back scattering crosssection of spherical meteorites will be considered as illustrated in Fig. 2.

(1) Optical scattering as the diameter (d) is greater than the wavelength (λ).

(2) Mie scattering as the diameter is nearly equal to the wavelength.

(3) Rayleigh scattering when the diameter is very much smaller than the wavelength.

Therefore, the power reflected from the spherical meteorite can be computed by applying the radar equation.

2.3. Calculation of the power reflected from the spherical meteorite.

The back-scattered power from the spherical meteorite will be given by applying the radar equation as follows:

$$\frac{P_r}{P_t} = \frac{G_0^2 \lambda^2}{64\pi^3 D^4} \sigma \quad (1)$$

where P_r is the power reflected from spherical meteorite, P_t the transmitted power, G_0 the antenna gain, λ the wavelength of radio echo power, D the depth which meteorite is buried in the ice sheet and σ the back scattering crosssection for the variation of the wavelength (λ) with the diameter of meteorite (d). Taking $G_0 = 2$ as the antenna gain and $P_r/P_t = 10^{-10}$ as the intensity of power received by the present apparatus, we have the following equation to solve the problem to detect meteorite in the ice from equation (1):

$$d^6 \geq C_0 \lambda^2 D^4 \quad \text{for stony meteorite} \quad (2)$$

where C_0 is constant. This equation (2) means that at a given depth (D) we could detect meteorite piece greater than the diameter of spherical meteorite (d) with a pulsed radar operating at the wavelength of λ as the stony meteorite will have Rayleigh scattering crosssection. On the other hand, since the most of iron meteorites have larger diameter than the stony meteorites as illustrated in Fig.1, it will be expected that besides Rayleigh scattering the iron meteorite as a conductive sphere will show Mie scattering and also optical scattering. The equation is given for the optical scattering in the following:

$$d^2 \geq C_1 \cdot D^4 / \lambda^2 \quad (3)$$

where C_1 is constant.

3. Possibility of detecting meteorite in the ice.

Using equations of (2) and (3), the relation between the depth of ice and the diameter of spherical meteorite is obtained as shown in Fig.3. As illustrated in the figure, it is generally considered that with a pulsed radar operating at the shorter wavelength (higher frequency) it will be able to detect the smaller meteorite in diameter and it deeper in depth within the ice. Since there is a small number of the Yamato stony meteorites more than 10 cm in diameter, it is, therefore, difficult to find the stony meteorite deeper

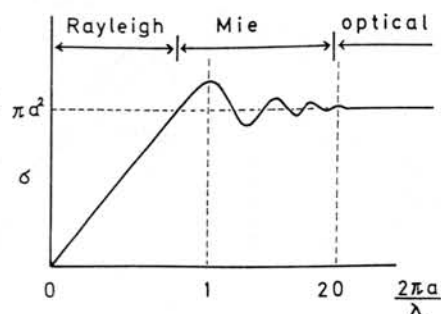


Fig.2. A schematic illustration of back scattering crosssection the sphere.

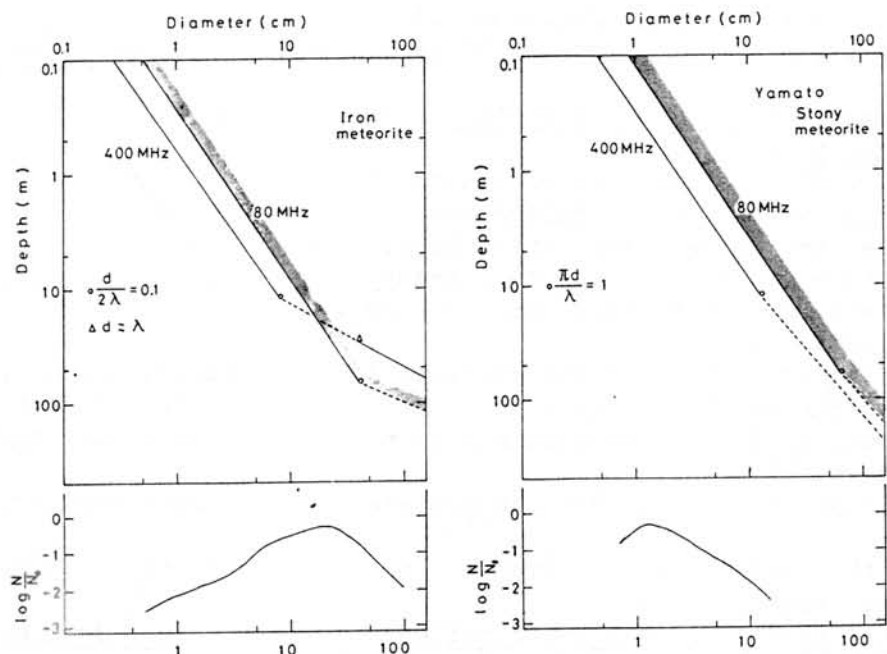


Fig.3. Relation between the depth of ice and diameter of spherical meteorite for the world recognized iron meteorites and the Yamato stony meteorites with a pulsed radar operating at the frequency of 400 MHz and 80 MHz. In the lower part of the figure, frequency spectrum of diameter of the Yamato stony meteorites and the world recognized iron meteorites are also shown. The relation dependent on Mie scattering is shown as the dashed straight lines.

than 10 m in depth as reflections from the meteorite piece in the ice are far too weak to be detected with the present radio echo sounding apparatus. In the case of the iron meteorites it may be able to detect it within the depth of 100 m with the radio frequency of 400 MHz.

References

- KOVACS, A. (1980): Radio-echo sounding in the Allan Hills, Antarctica, in support of the meteorite field program. CRREL Special Report, 80-23, 9p.
- NAGATA, T. (1978): A possible mechanism of concentration of meteorites within the Meteorite Ice Field in Antarctica. Mem. Natl Inst. Polar Res., Spec. Issue, 8, 70-92.
- NISHIO, F. (1980): Studies on the ice flow in the bare ice area near the Allan Hills in Victoria Land, Antarctica. Mem. Natl Inst. Polar Res., Spec. Issue, 17, 1-13.

RADIO ECHO SOUNDING IN THE AREA OF YAMATO MOUNTAINS

Wada, M., Yamanouchi, T., Mae, S. and Kusunoki, K.
National Institute of Polar Research, Tokyo 173

In December 1969, a glaciological party of the Japanese Antarctic Research Expedition (JARE) found and collected nine pieces of meteorite in the blue ice area (between $71^{\circ}48'S$ and $71^{\circ}52'S$ and between $36^{\circ}10'E$ and $36^{\circ}30'E$) at the southeast of the Yamato Mountains. Since then a lot of meteorites were found in the blue ice area near the Yamato Mountains (Yanai, 1979).

A mechanism of concentration of meteorites was discussed by Nagata (1978). Reports of geology, meteorology and glaciology were carried out in the bare ice area around the Yamato Mountains were presented (Kobayashi, 1979, Yoshida and Mae, 1978).

In the summer of 1979/80, observations of bedrock topography were carried out over the Yamato Mountains (between $71^{\circ}10'S$ and $72^{\circ}10'S$ and between $34^{\circ}35'E$ and $37^{\circ}25'E$) by JARE-20 in co-operation with JARE-21. A new airborne radio echo sounder was used in this survey. This sounder with a 179 MHz transmitter was developed by the National Institute of Polar Research, and it was installed in a Pilatus Porter PC-6. The peak power of the sounder was about 1 kW and the penetration depth was designed to be about 2000 m.

In 28 January 1980, airborne radio echo soundings were carried out over the Yamato Mountains. Since the navigation instruments aboard the aircraft were limited, the position of the aircraft were determined by terrestrial navigation, thus the error in position is about 10 km. The aircraft flew with a constant altitude of 3000 m above sea level. The total flight distance was about 500 km and the flight lines are shown in Fig. 1. Some parts of obtained continuous records are shown in Fig. 2, and an A-scope record is shown in Fig. 3. The bedrock topography along the flight lines are shown in Fig. 4,

Fig. 1

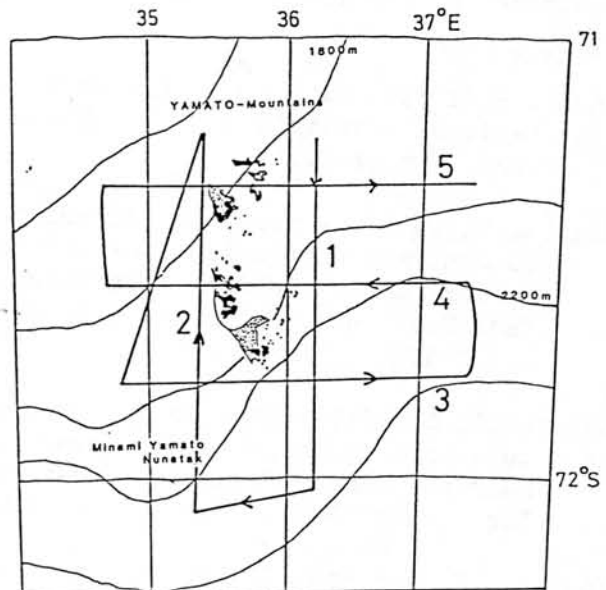
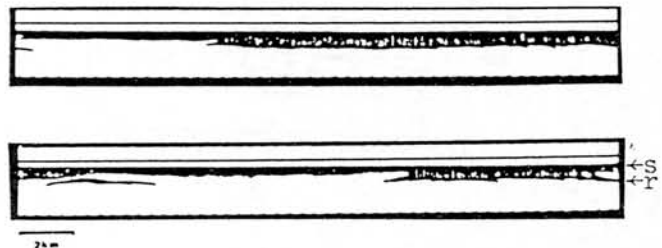


Fig. 2



5 - 2

using the value of wave velocity in ice is 169 m/ μ s and 300 m/ μ s in air.

The snow surface elevation of the eastern side of Yamato Mountains area was higher than that of the western side. The rock surface elevation of the eastern side was about 1500 m and that of the western side was about 1000 m. It is suggested that the deep valleys are existing where no clear echos were obtained. Considering from the topographic feature of the bedrock along the five flight lines in this area, it is suggested that the ice sheet flows from southeastern side to northwestern side and many meteorites were found out at the southeast of the Yamato Mountains.

References

Yanai, K.(1979): Catalog of Yamato Meteorites. National Institute of Polar Research, Tokyo, pp.ix-xviii

Nagata, T.(1978): A possible mechanism of concentration of meteorites within the meteorite ice field in Antarctica. Mem. Natl Inst. Polar Res., Spec. Issue, 8, 70-92.

Kobayashi, S.(1979): Some features of the turbulent transfer on the bare ice field near the Yamato Mountains. Mem. Natl Inst. Polar Res., Spec. Issue, 12, 9-18.

Yoshida, Y. and Mae, S.(1978): Some information on topographic features and the ice sheet around the Yamato Mountains. Mem. Natl Inst. Polar Res., Spec. Issue, 8, 93-100.

Fig. 3

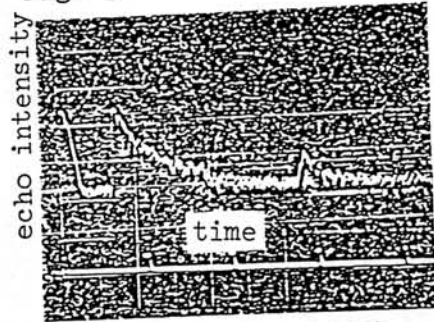
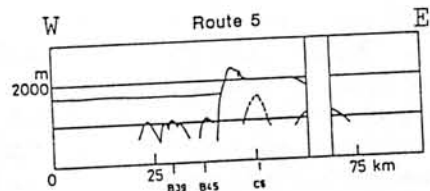
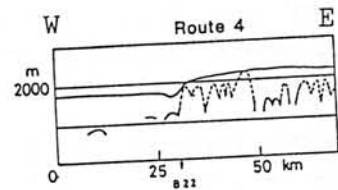
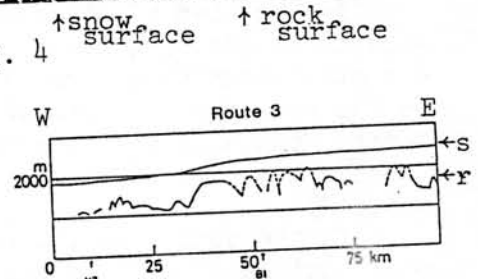
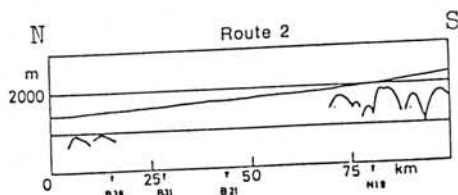
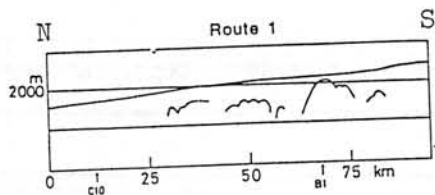


Fig. 4



s shows snow surface.
r shows rock surface.



CURATORIAL ASPECTS OF THE ANTARCTIC METEORITE PROGRAM IN THE
UNITED STATES: Duke, M. B.; Bogard, D. D.; Annexstad, J. O.:
NASA, JOHNSON SPACE CENTER, HOUSTON, TEXAS 77058

The curation of Antarctic Meteorites has three distinct phases: (1) initial processing and preliminary examination; (2) preparation and distribution for study; and (3) preservation and storage.

Procedures have been fashioned after those used for lunar samples, but are simplified in keeping with different requirements for the meteorites. The preliminary description of large numbers of smaller meteorites has been expedited by arranging with individual meteorite scientists to perform these descriptions in return for the exclusive opportunity to study any unusual meteorites that turn up in the course of their study. At this time, all meteorites from the 1977-1979 collections have been initially processed and all meteorites > 150 gm have been described in the Antarctic Meteorite Newsletter. Preliminary descriptions of the smaller "pebbles" will be completed in early 1981. Sample requests are reviewed by a Meteorite Working Group consisting of scientists and curators, who recommend sample distribution to the National Science Foundation Office of Polar Programs. Based on the approved recommendations, over 900 samples have been distributed to 85 laboratories in 13 countries since October 1978.

7 - 1

ANTARCTIC CARBONACEOUS CHONDRITES

Moore, Carleton B., Center for Meteorite Studies
Arizona State University, Tempe, Arizona 85281 U.S.A.

At least ten carbonaceous chondrites have been collected in Antarctica. Of these ten the majority are reported to be in the C2 classification. One C3, one C4 and no C1 chondrites have been reported. The proportionately small number recovered and absence of C1 chondrites may indicate a selection process in the Antarctic ice, whereas other meteorite types may have been moved from their original place of fall by ice movement the carbonaceous chondrites may have been collected where they fell.

Analyses of the carbonaceous chondrites show that they are pristine specimens. They show no evidence of terrestrial contamination by organic material or leaching of components from them during their terrestrial lifetime. Evidence for this is shown in Table I for chemical composition and Table II for amino acids from an interior and exterior piece of the ALHA 77306 C2 chondrite.

Table I. Element abundances in the Antarctic chondrite ALHA 77306 (Analysis by M.S. Ma and R.A. Schmitt, June 1980; written communication to author).

	EXTERIOR ALHA 77306,8	INTERIOR ALHA 77306,16
TiO ₂ (%)	<0.2	<0.2
Al ₂ O ₃	2.1	2.1
FeO	25.4	25.6
MgO	18.3	18.5
CaO	1.9	1.8
Na ₂ O	0.521	0.564
K ₂ O	0.045	0.038
MnO	0.211	0.208
Cr ₂ O ₃	0.378	0.386
Sc (ppm)	7.5	7.4
V	63	66
Co	514	520
Ni	10580	10930
La	0.32	0.34
Sm	0.21	0.21
Yb	0.20	0.20
Lu	0.031	0.027
Au (ppb)	114	126
Ir	609	551

Table II. Amino acids in meteorite extracts (nanomoles per gram) (from J.R. Cronin , S. Pizzarello and C.B. Moore, Science 206, p. 335, 1979).

Allan Hills		
Amino Acid	EXTERIOR (77306.8)	INTERIOR (77306.16)
Asp	3.2	1.0
Glu	1.6	1.8
Gly	26.3	18.3
Ala	5.4	3.8
Aib	2.8	2.6
Abu	1.3	1.4
Val	0.4	0.6
Iva	0.6	1.2
Aeb	0.3	0.8
Ple	0.2	0.1
$\alpha\beta M_2ab$	0.4	1.6
βAbu	1.4	1.1
βAla	5.1	3.3
βAib	0.9	0.6
γAbu	1.7	1.8
Total	51.6	40.0

8

ALLAN HILLS A77283: AN ANTARCTIC IRON METEORITE CONTAINING
PRETERRESTRIAL IMPACT-PRODUCED DIAMOND AND LONSDALEITE

Roy S. Clarke, Jr., Daniel E. Appleman, and Daphne R. Ross
Department of Mineral Sciences, National Museum of Natural History,
Smithsonian Institution, Washington, DC 20560.

Only nine of the many meteorites recovered so far from the Allan Hills, Antarctica, have been iron meteorites. One of these, ALH A77283, contains a number of troilite(FeS)-graphite(C)-schreibersite((Fe, Ni)₃P)-cohenite(Fe₃C) inclusions that are rich in the carbonado-type diamond-lonsdaleite 'nodules' previously described from the Canyon Diablo meteorite. The Canyon Diablo, Arizona, meteorite, the excavator of Meteor Crater, is the only other iron meteorite known to contain these high-pressure minerals, and their occurrence in that meteorite has been explained as the result of shock-induced transformation of graphite, most probably at the moment of terrestrial impact and disintegration of the projectile during crater formation. Virtually identical diamond-lonsdaleite-containing material in ALH A77283 occurs in a meteorite specimen with a well-developed heat-altered zone produced by atmospheric ablation. It appears, therefore, that the diamond and lonsdaleite were present in the meteoroid prior to its final ablative passage through the atmosphere and soft landing on the ground. The shock event that produced these high pressure phases, therefore, must have taken place on its parent body or have been associated with the disruption of that body. Metallographic and X-ray diffraction studies provide the data on which this conclusion is based.

9

A PRELIMINARY REPORT ON THE ACHONDRITE METEORITES IN THE 1979 U. S.
ANTARCTIC METEORITE COLLECTION

Reid, Arch M., Dept. of Geology, Univ. of Cape Town, Rondebosch, S. Africa
Score, Roberta, Northrop Services Inc., P.O. Box 34416, Houston, TX. USA

The 1979 U.S. Antarctic meteorite collection comprises 73 meteorites, 7 of which are achondrites. The achondrite collection consists of one eucrite (390 g.) three polymict eucrites (86, 310, 451 g.), one howardite (716 g.) one shergottite (7.9 kg.), and one diogenite (2.8 kg.). Also present in the 1979 collection is a unique iron meteorite (10 kg.) with abundant silicate (orthopyroxene) inclusions.

The most interesting meteorite is the shergottite in which two distinct lithologies are joined along what appears to be an undisturbed igneous contact. The fine grained lithology present at one end of the sample is texturally and mineralogically similar to Shergotty but is finer-grained and appears to lack the high Ca pyroxene that coexists with pigeonite in Shergotty. The major portion of the meteorite consists of large complex zoned pyroxenes in a groundmass of pyroxene and maskelynite. The overall pyroxene to feldspar ratio is higher than in the Shergotty-like portion and the pyroxenes are more Mg-rich and Ca-poor. Plagioclase has been converted to maskelynite in both lithologies and glass veinlets and pockets of black glass occur throughout the meteorite.

Five of the seven achondrites were found in a new collection site, Elephant Moraine (EET). This site will be further investigated in 1980-81.

10 - 1

STUDIES ON THE LITHIFICATION OF METEORITES (II).

Naoyuki Fujii(*), Masamichi Miyamoto(#), Keisuke Ito(*), and Yoji Kobayashi(*)
: (*)Dept. Earth Sci., Kobe Univ., Kobe 657; (#)Dept. Pure & Appl. Sci., Tokyo Univ., Tokyo 153.

Planetesimals evolved from the dust layer collide with each other and a limited number of planetoids grows among them. Mechanical properties of mutually colliding bodies are of importance in the early stage of the growing process by collision as well as the relative impact velocities. As the initial size of planetesimals are about 5km in radius (1) and their central pressure is very low (about 0.1~1 bar), they should be loosely consolidated aggregates (2). Though the melting compaction was one of the most important process at the early stage of planet formation (2), chondritic meteorites (e.g. ordinary chondrites or carbonaceous chondrites) had not experienced widely remelting process. The melting process has not played an important role in the lithification of these meteorites. However, the extraterrestrial materials now observed are evidently lithified to some extent, although experimental studies on the strength of meteorites have been very few (3). Mechanical properties, especially the adhesive strength, of loosely consolidated aggregates depend strongly on the presence and nature of the fine-grained materials such as ice, hydrous minerals, and amorphous materials which fill up the grain boundaries (4,5). Therefore, both approaches to clarify the mechanisms of the lithification of loosely consolidated aggregates (simulated planetesimals) and the degree of the lithification of chondrites are obviously important.

VIBRATIONAL FRACTURING RATE — A new strength measure named "vibrational fracturing rate", which is suitable for small rocks, is applied to ordinary chondrites from Antarctica (6). A fragment of chondrites was embedded in resin and made at least 5mmx5mm flat surface. Using a ultrasonic machine, the sample surface is excavated by a vibrating 2mm-diameter steel rod (Fig. 1). The rate of excavation is measured by a differential transformer (D.T.) and recorded on a strip chart, under a constant normal stress ($\sigma_n \sim 0.6\text{MPa}$) and mechanical impedance matching condition (6). Excavation experiments were made several times on each sample. We take the average gradient for each excavated depth versus time curve as the vibrational fracturing rate of the sample. Because the absolute value of the vibrational fracturing rate would be affected by normal stress, size of tool tip, and amplitude of vibration, only a relative value has its meaning. Figure 2 shows logarithmic ratios of the vibrational fracturing rate of calcite (V_0) relative to those (V) of single crystals (\square), terrestrial rocks (\diamond) and chondrites (\odot). Data are from (6) with the addition of the measurements for Allende (C3).

Examples of excavated depth versus time curves are shown in Fig. 3. An inclusion with about 2mm-diameter is found in the border of the surface of Allende. Allende (m) and (i) in the figure 3 indicate the difference of the location of excavation in the same specimen. Excavation versus time curve of Allende (i) is obtained at the location of excavation within a few millimeter distance from the inclusion. The highest rate of excavation with large variation for the curve of Allende (m), which is obtained in other part of the specimen, indicates that this portion is highly heterogeneous and loose. At the moment of a steep gradient of the curve, small fragments are often removed from the excavated hole, suggesting the occurrence of large fracture nearby the hole. In contrast, Allende (i) shows a smooth and low rate of excavation which is similar to that of Yamato-74191(L3), Yamato-75258(LL6) and ALHA 77231(L6) show intermediate rate of excavation. Single crystal of calcite with the excavation direction perpendicular to $\{10\bar{1}1\}$ shows a similar rate of excava-

tion to that of ALHA 77231. Furthermore, basalt shows about half a rate of excavation when compared to those of Allende (i) and Yamato-74191. It is obvious that the higher rate of excavation is always associated with the larger variation of the excavation depth versus time curve. Gradients of the curves obtained for each sample show relatively small variations within $\pm 10\%$ except Allende (m). Fragments of sample itself hit the sample surface vertically and behave as grinding power at the resonant vibration condition. The vibrational fracturing rate corresponds well with the relative hardness (6). Cleavages, cracks, and adhesion between grains would play an important role in the vibrational fracturing process. Pouring of water between sample surface and the tip of steel rod is necessary in this measurement to keep good matching of mechanical impedance. So the application of this method would be limited to the samples with too high porosity or including water-soluble minerals such as clay unless further improvements are made.

RELATIVE STRENGTH DIFFERENCES AMONG CHONDRITES — It is considered that petrologic types are caused by thermal metamorphism (7). It seems concordant with the observations of grain boundaries by scanning electron microscope (SEM) that large grains ($\geq 50\mu\text{m}$) are rounded and fitted each other in Yamato-75258 (LL6) and ALHA 77231(L6) whereas in Yamato-74191(L3) they are embedded with fine angular grains (6). It may be expected that the strength of chondrites becomes high as the thermal metamorphic grade becomes high and the porosity of chondrites decreases. The vibrational fracturing rates for chondrites, however, show the lowest rate for L3 (Yamato-74191) and the highest and lowest rates in the same specimen of C3 (Allende). The strength represented by the vibrational fracturing rate is likely to depend on grain-to-grain adhesion and cementing condition among grains. When large grains (or accumulation of grains) are sparsely disturbed, the vibrational fracturing rate would be high for the matrix and low for the large grains. This may be the case for Allende sample. Crushing strength of several ordinary chondrites has wide variety from 380MPa to unmeasurable small value. They are crushed between thumb and fingers (3). Effects of shock and fragmentation history may differ among chondrites both in space and on the earth. Unless mechanisms and physical processes of these effects on the lithification of chondrites are solved, there will be little confirmation whether the strength of chondrites would closely relate to petrologic types or not. It is, however, apparent that the presence of intergrain fine material in chondrites causes significant change in adhesive strength as well as other mechanical properties (5,6).

SIGNIFICANCE OF AMORPHOUS MATERIALS IN ADHESIVE STRENGTH OF LOOSELY CONSOLIDATED AGGREGATES — Presence of once molten ice of only 5 wt% can make the strength of loosely consolidated aggregate of olivine powder ($\approx 250\mu\text{m}$) as high as that of pure ice (5). It may indicate that the adhesive nature of once wetting material around grains causes the increase of strength. At the temperature range in which the thermal metamorphism has occurred as expected for ordinary chondrites, the hydrous minerals (clay, serpentine, etc.) or glassy materials seem to be likely candidates for intergrain fine materials to expedite the low temperature sintering or lithification process. In Fig. 4., the dropping experiments of spherical projectiles ($\approx 1.5\text{cm}$ in diameter) of olivine powder with 20 wt% soda glass powder ($\approx 10\mu\text{m}$) are demonstrated. Fig. 4 shows the ratio of the mass of the largest fragment after dropping to the original mass for various temperatures (≈ 15 hrs.) as a function of impact velocity. The dotted lines show the results of Hartmann's experiments (8). Significant change of strength occurs between 550°C and 600°C which corresponds the annealing temperature of soda glass. It may suggest that the annealing of glass powder

#10-3

(effective viscosity $\sim 10^{13}$ Poises) among olivine grains plays an important role for the strength of such a loosely consolidated aggregate. Adhesive condition by small fraction of amorphous material and hydrous minerals at grain boundaries affects the strength of chondrites and lithification of planetesimals and chondrite parent bodies in the case when they had not undergone the melting of silicate minerals (2,4,6). Further investigations for different petrologic types of chondrites and for the effects of intergrain fine materials on the mechanical properties are obviously indispensable.

We express our thanks to the National Institute of Polar Research, Japan, for offering chondrites from Antarctica and to Dr. N. Nakamura for Allende sample.

References:

- (1) Goldrich, P. and Ward, W.R. (1973) *Astrophys. J.*, **183**, 1051-1061.
- (2) Fujii, N., Miyamoto, M. and Ito, K. (1978) *Proc. 11th Lunar Planet. Symp.* Tokyo Inst. Space Aeronaut. Sci., Univ. Tokyo, 262-267.
- (3) Wood, J.A. (1963) *Physics and Chemistry of Meteorites*, In The Solar System IV, p337-401, Chicago Press, Chicago.
- (4) Fujii, N., Ito, K. and Miyamoto, M. (1979) *Proc. 12th Lunar Planet. Symp.* Tokyo Inst. Space Aeronaut. Sci., Univ. Tokyo, 145-150.
- (5) Miyamoto, M., Ito, K., Fujii, N. and Kobayashi, Y. (1980b) *Proc. 13th Lunar Planet. Symp.*, Tokyo Inst. Space Aeronaut. Sci., Univ. Tokyo, 232-238.
- (6) Fujii, N., Miyamoto, M. and Ito, K. (1981) *Mem. Natl. Inst. Polar Res.*, Spec. Issue, **18**, 258-267.
- (7) Miyamoto, M., Fujii, N. and Takeda, H. (1980a) *Lunar Planet. Sci. XI*, Houston, Lunar and Planetary Institute, 737-739.
- (8) Hartmann, W.K. (1978) *Icarus*, **33**, 50.

Fig. 1. Schematic diagram of the vibrational fracturing measurement, D.T.: Differential transformer, P.U.: pick-up, (6).

Fig. 2. Logarithmic ratios of the vibrational fracturing rate (V_0) of calcite relative to those (V) of single crystals (\square), rocks (\diamond) and chondrites (\odot). Allende (i) and (m) indicate the location of excavation nearby an large inclusion and other part of matrix, respectively.

Fig. 3. Examples of excavation depth versus time curves for chondrites. As a reference, curves for calcite and basalt (6) are also indicated.

Fig. 4. The ratio of masses of the largest fragment after dropping to the original one as a function of impact velocity. Spherical projectiles (olivine + 20 wt% soda glass powder) are heated for 15 hrs at temperatures indicated in the figure.

#11

A PRELIMINARY CLASSIFICATION OF YAMATO-79 METEORITES

Kojima Hideyasu* Yanai Keizo**

* Inst. of Mining Geology, Mining College, Akita University, Tegata Akita 010.

** National Institute of Polar Research, Kaga, Itabashi-ku, Tokyo 173.

About 3,000 meteorites have been collected in the area surrounding the Yamato Mountains, East Antarctica in the 1979 - 1980 season. These meteorite specimens were stored in the freezer maintained 20°C at the National Institute of Polar Research.

For the processing, each meteorite specimen was taken out of the freezer and transferred at room temperature in the cabinet that filled with dry nitrogen. Each meteorite specimen was weighed, measured by three dimensions, and photographed from the six orthogonal faces with both colour and black & white films in the processing laboratory.

About 1,000 meteorites were processed, and 500 specimens were classified preliminary. These specimens were classified into 9 eucrites, 3 diogenites, 1 ureilite, 5 carbonaceous chondrites, many ordinary chondrites, and 23 possibly unique specimens. The achondrites and carbonaceous chondrites are similar to the specimens that have been recovered around the Yamato mountains in the past.

These possibly unique specimens are classified two groups by the feature of hand specimen. The group to which 13 specimens belong is characterized by presence of many pores as the same of volcanic rocks, greenish gray in colour, less fusion crust, no obvious chondrules, and less metals.

The other group to which 8 specimen belong, is characterized by compact property, dark greenish grey in colour, less fusion crust, no obvious chondrules, and less metals.

Two specimens seem to be strongly recrystallized ones.

STUDY OF ALLENDE METEORITE BY ANALYTICAL TRANSMISSION ELECTRON MICROSCOPY
 Kitamura, M., Watanabe, S. and Morimoto, N.
 Dept. Geology & Mineralogy, Fac. Science, Kyoto Univ., Sakyo, Kyoto, 606

Allende meteorite is a carbonaceous chondrite and has been studied by many workers. In addition to the petrographic studies (cf. Clark et al., 1970), a few studies on the fine textures such as dislocation structure have been carried out using electron microscopes (Green et al., 1971; Ashworth and Barber, 1975). In the present study, an analytical transmission electron microscope has been used to study the fine textures and chemical compositions of the meteorite.

Thin sections of the Allende meteorite were observed under an optical microscope and studied by EPMA. Then, the boundary region between the chondrule (~ 0.4 mm ϕ) and the matrix of the thin section was ion-thinned. This ion-thinned specimen (Figure 1) was studied under the 200 kV transmission electron microscope (Hitachi-700H) with an analytical mode, in the same manner as described by Morimoto and Kitamura (1981). The results are as follows:

Chondrule: The chondrule mainly consists of olivine crystals with a size of ~ 50 μm . $\{hk0\}[001]$ slip system (Ashworth and Barber, 1975) and "black-spot structure" (Green et al., 1971) were observed (Figure 2). The chemical compositions of the olivine crystals vary in a range of Fo_{85} - Fo_{55} . The precipitates (~ 0.1 μm) along the sub-grain boundaries in the olivine show some Cr contents, suggesting that the phase is Cr-spinel. Fine particles of clinopyroxene, $(\text{Fe,Ni})\text{S}$ and FeAl_2O_4 are also observed at the grain boundaries among the olivine.

Matrix: The matrix also consists mainly of olivine crystals with a size of a few μm in length and about 1 μm in width (Figure 3). The dislocation structures are observed, where the slip system is $\{hk0\}[001]$ as described by Ashworth and Barber (1975). Crystal shapes of the olivine seems to follow the theoretical morphology of the crystal ('t Hart, 1978). The chemical compositions of the olivine are in a range of Fo_{60} - Fo_{40} , indicating a definite compositional difference between the olivine in the chondrule and that in the matrix. Clinopyroxene and other fine particles less than a few nm in size are observed at the boundary regions among the olivine. The x-ray spectra from the aggregates of these fine particles show existence of Si, Mg, Fe, Ca, Cr, Ni, S, P. A large olivine crystal (~ 10 μm) is found in the matrix (Figure 4). The central part (~ 6 μm) of the single crystal has no dislocation and is surrounded concentrically by the outer region with high dislocation density. This texture suggests existence of at least two stages of crystal formation. Therefore, this grain seems to have experienced a different process from that of the other olivine common in the matrix.

[References]

- Clark, R.S.Jr., Jarosewich, E., Mason, B., Nelen, J., Gómez, M. and Hyde, J. R. (1970) : *Smithsonian Contrib. Earth Sci.*, 5, 1-53.
 Green, H.W., Radcliffe, S.V. and Heuer, A.H. (1971) : *Science*, 172, 936-939.
 Ashworth, J.R. and Barber, D.J. (1975): *Earth Planet. Sci. Lett.* 27, 43-50.
 Morimoto, N. and Kitamura, M. (1981): *Bull. Minéral.* in press.
 't Hart, J. (1978) : Ph. D. Thesis, Leiden State University.

#12-2

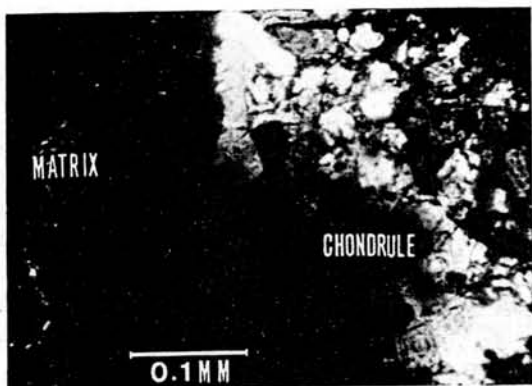


Figure 1. Optical micrograph of ion-thinned specimen of Allende meteorite (cross polars). The chondrule is in the right side and the matrix in the left side. The dark background is an open space.

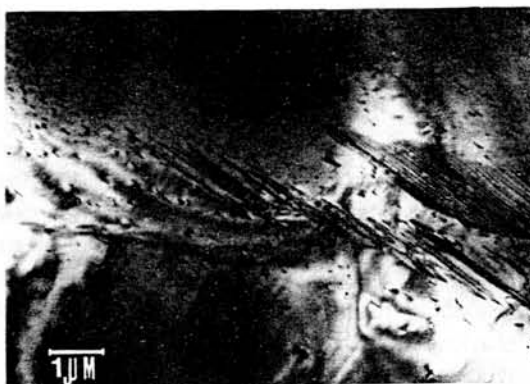


Figure 2. One of the electron micrographs of the dislocation structures of olivine in the chondrule. The "black-spot structure" defined by Green et al. is observed.

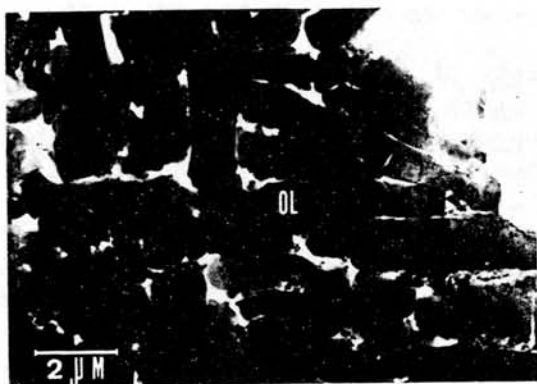


Figure 3. A low magnification electron micrograph of the matrix. Olivine has an enlarged shape. Fine particles are observed at the boundaries among the olivine.

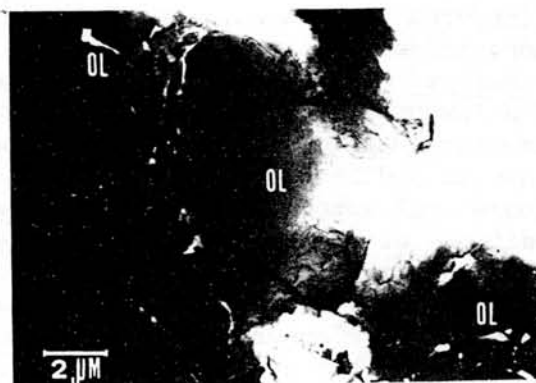


Figure 4. Large olivine crystal in the matrix with dislocation-free core. A wide region with high dislocation density envelops the core.

MINERALOGY OF THE YAMATO DIOGENITES OF POSSIBLY PIECES OF A SINGLE FALL.

Takeda Hiroshi^{1,2}, Mori Hiroshi¹, and Yanai Keizo²¹ Mineralogical Inst., Faculty of Science, Univ. of Tokyo, Hongo, Tokyo 113.² National Institute of Polar Research, Kaga, Itabashi-ku, Tokyo 173.

Among 30 diogenites recovered from the Yamato meteorite field by the JARE parties, 29 meteorites totaling 6775.8g have granoblastic texture distinct from known diogenites. The importance of this characteristic texture was first noted by us in Yamato-6902 (Takeda et al., 1975; 1978). It has been proposed on the basis of their mineralogy and bulk chemistries that we are dealing with pieces of a single fall. Some differences in their isotopes and rare earth elements distribution found among these meteorites have been attributed to the heterogeneity in mineral distribution within a single meteorite (Discussion at 4th Symp. on Antarctic Meteorites, 1980). Yamato-75032 is another unique diogenites with the most Ca and Fe rich pyroxenes (Takeda et al., 1979). In order to clarify their identity, we have reexamined thin sections of Yamato-74013, 74097, 74136, 74648, 74037, 74010 and 74011 by optical, electron optical and microprobe techniques. Petrographic description is represented by that of Yamato-74013 given by Duke in our previous paper (Takeda et al., 1979). It has granoblastic texture as was reported previously. The grain sizes of orthopyroxene is always finer than chromite, which occurs as isolated clots up to 5mm in diameter and in veinlets. Fine-grained orthopyroxenes with grain size 0.1-0.2mm cover areas up to 3cm or more in diameter and seem to be surrounded by coarse-grained areas, giving the fine grained areas the appearance of clots in a network of veins. The round isolated chromites are surrounded by a zone of clear, coarser pyroxene and are foci for radiating coarse-grained veins.

Orthopyroxenes in coarser-grained areas are clear and 0.4-0.5mm in diameter, but at some junctions of coarse-grained veins, a pyroxene crystal reaches up to 3mm in the longest dimension. The TEM observation shows stacking faults parallel to (100), which are thought to be produced by weak shock effects when the meteorite mass was formed. Neither exsolution nor dislocation indicating low strain-rate deformation have been observed. The rims of the large clear orthopyroxenes sometimes are rich in Ca and Fe than the core. In the coarsest portion, there are found plagioclases filling interstices of orthopyroxenes, a silica mineral and coarse grained troilite. Because the coarsest portions with rare-earth-element-rich plagioclase distribute in a few cm intervals, the difference in rare-earth contents may be attributed to the inhomogeneity of sampling.

Finer grained portions have a haze of tiny inclusions of troilite, with yet smaller blebs of metallic iron in some troilite grains. This area shows a subtle parallel structure that transects the granularity (Fig.1). This structure is marked by relative abundance of opaque grains, and short fractures. This linear structure resembles that of planar features produced by shock effect. Such planar feature parallel to (001) of pigeonite has been found in a pyroxene-rich ureilite, Yamato-74659. With reference to our finding of subboundaries decorated by troilite and chromite in many diogenitic pyroxenes, the parallel structure can be interpreted to be decorated linear features produced by shock event. The parallel structures are erased at a clear portion where pyroxenes are recrystallized and opaques were excluded. Orthopyroxenes rich in haze of tiny opaque inclusions have lower Ca and Fe concentration, than the recrystallized portion (Fig. 2).

#13-2

In conclusion, the granoblastic texture and the parallel structure characteristics of the Yamato diogenites except Yamato-75032, may have been formed by recrystallization of a few very large crystals (several cm in diameter) by heavy shock processes, and subsequent thermal annealing. Coarse grained area may indicate intergranular melting and recrystallization. The concentration of the Ca and Fe cations at the rims of crystals in coarse grained areas support this hypothesis. Some differences found in rare-earth abundance of the different masses of the Yamato diogenites may be results of inhomogeneous sampling, and some isotope disturbances may be attributed to the different degree of shock processes and thermal annealings. It is believed that we are dealing with pieces of a single fall, and that the Yamato diogenites with granoblastic textures are one of the most heavily shocked diogenites.

We thank the National Institute of Polar Research for the meteorite samples and Dr. M. B. Duke for processing the sample.

References on the Yamato diogenites:

- Takeda H., Reid A. M. and Yamanaka T. (1975) Crystallographic and chemical studies of a bronzite and chromite in the Yamato (b) achondrite. Mem. Natn'l Inst. Polar Res., Spec. Issue 5, 83-90.
- Takeda H., Miyamoto M., Yanai K. and Haramura H. (1978) A preliminary mineralogical examination of the Yamato-74 achondrites. Mem. Natn'l Inst. Polar Res., Spec. Issue 8, 170-184.
- Takeda H., Miyamoto M., Ishii T., Yanai K. and Matsumoto Y. (1979) Mineralogical examination of the Yamato-75 achondrites and their layered crust model. Mem. Natn'l Inst. Polar Res., Spec. Issue 12, 82-108.
- Takeda H., Duke M. B., Ishii T., Haramura H. and Yanai K. (1979) Some unique meteorites found in Antarctica and their relation to asteroids. Mem. Natn'l Inst. Polar Res., Spec. Issue 15, 54-76.



Fig. 1. Photomicrograph of Yamato-74013. Width is 0.8mm. Parallel structures marked by relative abundance of opaques and short fractures are observed in finer grained areas. This structure transects the granularity. Tiny inclusions are mostly troilites.



Fig. 2. Coarse-grained area with clear large crystals of orthopyroxene. A haze of tiny inclusions of opaque minerals are left in the core of the recrystallized grains. The size of troilites is also larger than that in the finer grained areas. Width is 0.8mm.

A MINERALOGICAL EXAMINATION OF SOME ALLAN HILLS POLIMICT EUCRITES

Gen SATO* Hiroshi TAKEDA** Keizo YANAI***

* Department of Earth Sciences, Faculty of Science, Chiba Univ., Chiba 280

** Mineralogical Inst., Faculty of Science, Univ. of Tokyo, Tokyo 113

*** National Institute of Polar Research, Tokyo 173

The achondrites found in the Antarctic meteorites collection include 12 polymict eucrites. 7 polymict eucrites were discovered in the Yamato Mountains and 5 in the Allan Hills. These facts pose the problems why so many polymict eucrites were found in only Antarctica. ALH-765, -77302 were previously studied precisely (MIYAMOTO et al. 1979). They classified pyroxenes into four groups and concluded that their pyroxene trends are very similar and they suggested that two polymict eucrites may be pieces of a single fall.

We carried out mineralogical examination of polymict eucrites from Allan Hills to check the possibility that they represent pieces of a single fall. Pyroxenes in ALH-78158, -78165 were analysed by the electron microprobe. Some characteristics of their pyroxenes were not found in polymict eucrites from the Yamato Mountains. Our results on ALH-78158 revealed that it is composed of complex breccias of angular fragments of pyroxene and plagioclase, in a matrix of comminuted pyroxene and plagioclase. Pyroxene fragments show a wide range of chemical compositions (Fig. 1). The chemical composition falls in the same fields as those of the pyroxene quadrilateral of ALH-765 and -77302. Namely the presence of chemically zoned pyroxenes of the Pasamonte type and extensively exsolved pyroxenes have been confirmed. However very Mg rich pyroxene $\text{Ca}_3\text{Mg}_5\text{Fe}_3$ with coarsely exsolved augite $\text{Ca}_4\text{Mg}_4\text{Fe}_1$ of ALH-78158 have not been detected in the previous polymict eucrites from the Allan Hills. The exsolved pair is similar to that found in Yamato-75011, -75015. Pigeonites with fine regular exsolved augite, which was previously called the Juvinos type, are abundant in ALH-78165.

The fact observed in ALH-78158 seems to suggest that the chemical and mineralogical trend of pyroxenes are the same as those of the Yamato and Allan Hills polymict eucrite, and that there are some differences in polymict eucrites collected from different localities.

References:

MIYAMOTO M. and TAKEDA H. (1979)
Proc. 9th Lunar Planet. Sci. Conf.,
847-848

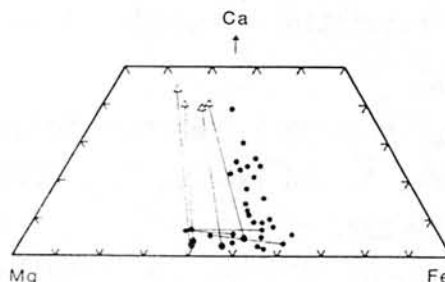


Fig. 1

Akimasa Masuda, Noboru Nakamura and Hiroshi Shimizu

Department of Earth Sciences, Faculty of Science, Kobe University

There are some observations (1) to indicate that Yamato diogenites are fragments of originally the same parental meteorite, although there are conflicting observations. We determined precisely the rare-earth elements (REE) in several Yamato diogenites (2,3). By chance, two chips A and B of Y74010, sizes of which are about 500 mg, were studied. The Y74010B was found to have the highest REE abundances among the samples studied, and there is a considerable difference in REE abundance between Y74010B and Y74010A. Whole rock and hand-picked orthopyroxene separate of Y74013 were also analyzed for REE.

In general, the REE abundance ratios between the two sets studied show simple patterns. The Y74013 orthopyroxene pattern relative to Y74010B is rectilinear over the whole range (Fig. 1). The Y74010A/Y74010B pattern is also linear with a break. Corresponding pattern between Y692 and Y74010B reveals split to two subparallel lines (Fig. 2). The jump shift between these subparallel lines corresponds to two units in terms of the increment per atomic number.

If the whole rock of Y74013 is assumed to be composed of the pyroxene crystals as represented by hand-picked orthopyroxene and the matrix component, it can be concluded that the matrix material in question is almost identical with the material represented by Y74010B. The results can be interpreted to imply that the Yamato diogenites involve two constituents. In view of mutually normalized REE patterns, it may be conceivable that two constituents under consideration stand for the liquid and solid phases which coexisted. Features of those patterns might be considered to suggest that the present orthopyroxene crystals passed once through the state of clinopyroxene in separation from the coexisting diogenitic liquid.

References

- (1) Honda, M. (1980) *Planetary Sciences* 1, No. 3, 106-109. (In Japanese).
- (2) Masuda, A. and Tanaka, T. (1978) *Mem. Natl. Inst. Polar Res., Spec. Issue*, 8, 229-232.
- (3) Masuda, A., Tanaka, T., Shimizu, H., Wakisaka, T. and Nakamura, N. (1979) *Mem. Natl. Inst. Polar Res., Spec. Issue*, 15, 177-188.

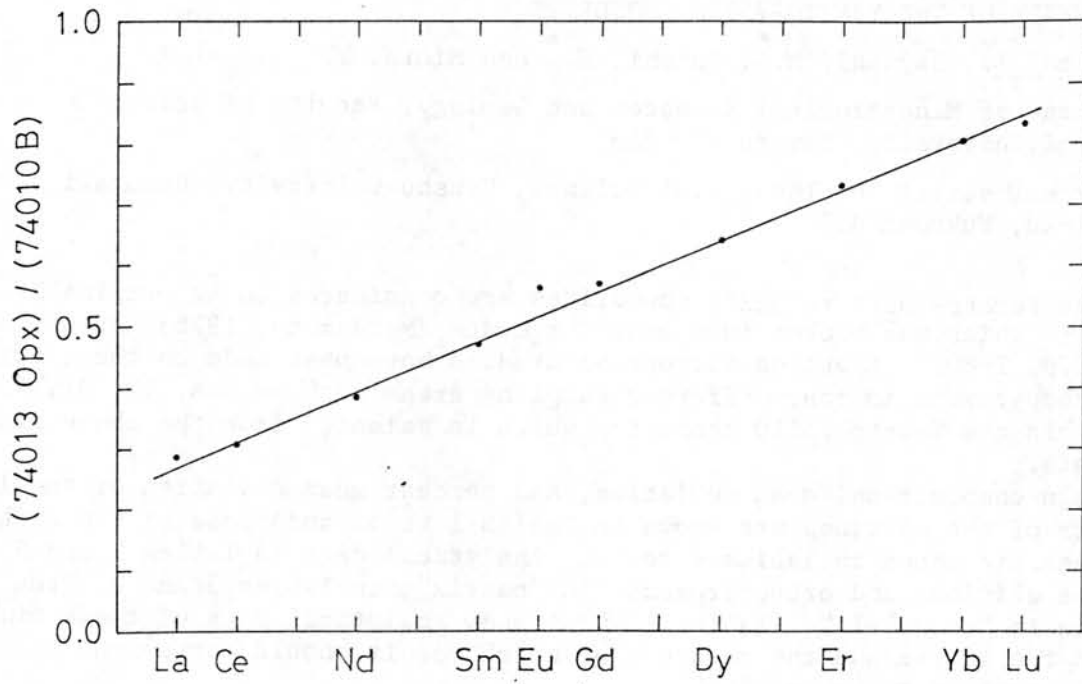


Fig. 1. REE abundance ratio pattern of orthopyroxene separate of Y74013 relative to Y74010B.

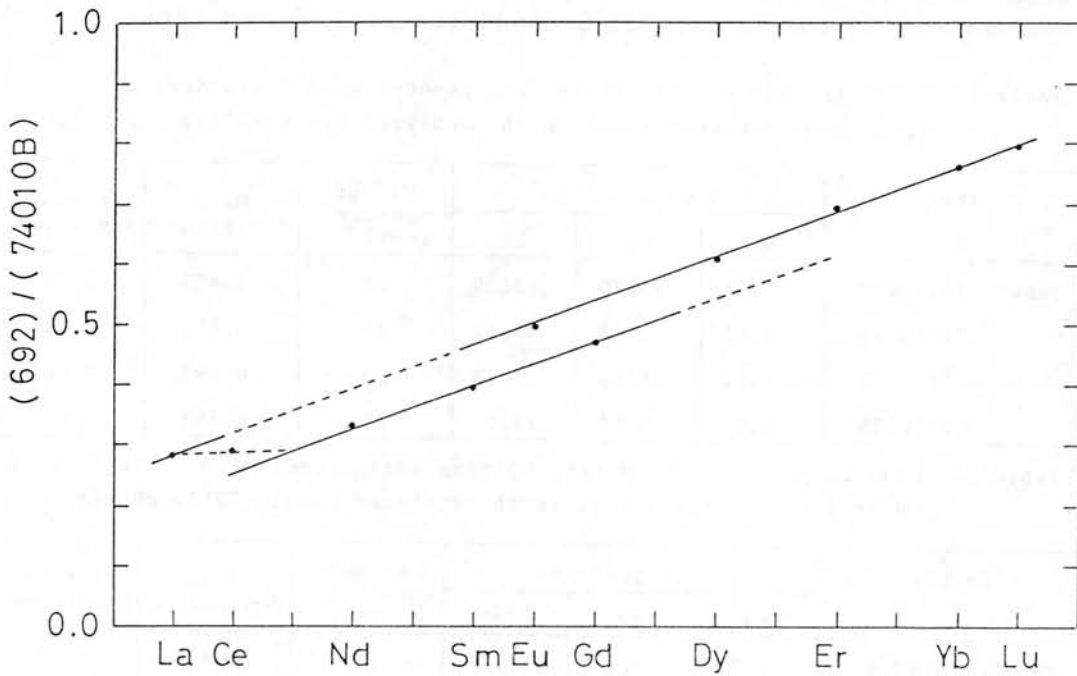


Fig. 2. REE abundance ratio pattern of Y692 relative to Y74010B.

16-1

HOMOGENEITY OF THE YAMATO-75110 CHONDRITE

Matsumoto, Y., Hayashi, M.^{*}, Daishi, M.^{*} and Miura, Y.

Department of Mineralogical Sciences and Geology, Faculty of Science, Yamaguchi University, Yamaguchi 753

^{*} Research Institute of Industrial Science, Kyushu University, Hakozaki, Higashi-ku, Fukuoka 812

The Yamato-75108 to -75257 chondrites are considered to be originally one meteorite which was broken into many fragments (Matsumoto, 1978; Matsumoto et al., 1979, 1980). Electron microprobe studies have been made on the olivine and orthopyroxene in four different sampling areas (such as Nos. 90, 91, 93 and 95) within the Yamato-75110 chondrite which is selected from the above many fragments.

Mean composition, mean deviation, and percent mean deviation of the iron contents of the olivines are shown in Tables 1 to 3; and those of the orthopyroxenes are shown in Tables 4 to 6. Analytical data in Tables 2 and 5 are from the olivines and orthopyroxenes in "matrix"; in Tables 3 and 6, from the minerals in "chondrule". Tables 1 and 4 show analytical data of those minerals both in the matrix and the chondrule, of which result should correspond to those of whole area in the "chondrite".

The value of % M.D. for the olivine in this chondrite is ranging from 2.02 to 2.98; but that in the matrix is taken from 1.79 to 2.12; and that in chondrule, from 0.88 to 2.05. The values of % M.D. for the orthopyroxene in this chondrite is changing from 2.38 to 5.27; but that in the matrix, from 2.15 to 7.17; and that in the chondrule, from 2.12 to 4.43.

Therefore, the above values of % M.D. of the olivine and orthopyroxene depend both on matrix and chondrule, and also on each sampling area. Such a chemical variety of the Yamato-75110 chondrite is observed clearly in this study.

Table 1. Mean compositions of Olivine and percent mean deviations of their iron concentrations in the analyzed Yamato-75110 chondrite.

Sample No.	Mean composition			No. of measurements	Mean deviation	% Mean deviation
	Ca	Mg	Fe			
Yamato-75110.90	0.01	76.39	23.60	30	0.477	2.02
-75110.91	0.01	76.48	23.51	20	0.498	2.12
-75110.93	0.02	76.69	23.28	19	0.693	2.98
-75110.95	0.00	76.09	23.91	22	0.493	2.06

Table 2. Mean compositions of Matrix Olivine and percent mean deviations of their iron concentrations in the analyzed Yamato-75110 chondrite.

Sample No.	Mean composition			No. of measurements	Mean deviation	% Mean deviation
	Ca	Mg	Fe			
Yamato-75110.90	0.00	76.28	23.72	20	0.427	1.80
-75110.91	0.01	76.13	23.86	10	0.505	2.12
-75110.93	0.00	77.29	22.70	11	0.407	1.79
-75110.95	0.00	76.40	23.60	12	0.483	2.05

Table 3. Mean compositions of Chondrule Olivine and percent mean deviations of their iron concentrations in the analyzed Yamato-75110 chondrite.

Sample No.	Mean composition			No. of measurements	Mean deviation	% Mean deviation
	Ca	Mg	Fe			
Yamato-75110.90	0.03	76.60	23.37	10	0.456	1.95
-75110.91	0.00	76.82	23.16	10	0.331	1.43
-75110.93	0.06	75.86	24.08	8	0.212	0.88
-75110.95	0.00	75.72	24.28	10	0.497	2.05

Table 4. Mean compositions of Orthopyroxene and percent mean deviations of their iron concentrations in the analyzed Yamato-75110 chondrite.

Sample No.	Mean composition			No. of measurements	Mean deviation	% Mean deviation
	Ca	Mg	Fe			
Yamato-75110.90	1.44	77.82	20.73	18	1.092	5.27
-75110.91	1.03	78.82	20.14	20	0.501	2.49
-75110.93	1.33	78.81	19.86	20	0.472	2.38
-75110.95	1.23	78.33	20.45	22	0.739	3.61

Table 5. Mean compositions of Matrix Orthopyroxene and percent mean deviations of their iron concentrations in the analyzed Yamato-75110 chondrite.

Sample No.	Mean composition			No. of measurements	Mean deviation	% Mean deviation
	Ca	Mg	Fe			
Yamato-75110.90	1.23	77.58	20.90	11	1.499	7.17
-75110.91	1.26	78.41	20.33	10	0.563	2.77
-75110.93	1.43	78.81	19.76	10	0.513	2.60
-75110.95	1.47	78.46	20.07	12	0.431	2.15

Table 6. Mean compositions of Chondrule Orthopyroxene and percent mean deviations of their iron concentrations in the analyzed Yamato-75110 chondrite.

Sample No.	Mean composition			No. of measurements	Mean deviation	% Mean deviation
	Ca	Mg	Fe			
Yamato-75110.90	1.32	78.21	20.47	7	0.551	2.69
-75110.91	0.81	79.24	19.96	10	0.423	2.12
-75110.93	1.23	78.80	19.97	10	0.433	2.17
-75110.95	0.94	79.3	19.96	10	0.925	4.43

#17-1

STUDY ON SOME MINERALS IN ALHA77015 (L3) CHONDRITE

Hirokazu FUJIMAKI, Ken-ichiro AOKI, Ichiro SUNAGAWA, Mikio MATSU-URA
Faculty of Science, Tohoku University, SENDAI

For preliminary experiments we have analyzed olivines and Ca-poor pyroxenes by an electron-probe microanalyzer using an energy-dispersive system. This system can simultaneously determine all the elements contained in the analyzed point except for lighter elements than fluorine.

It was found that some olivines and Ca-poor pyroxenes contain sulfur or sulfur oxides. Neither sulfur nor sulfur oxides could not be detected under the microscope. Fig. 1 shows a scanning profile of sulfur ($K\alpha$) obtained by our conventional wavelength-dispersive analytical system. The profile demonstrated homogeneous distribution of sulfur in the Ca-poor pyroxene. The representative results for some olivines and Ca-poor pyroxenes are given in Table 1 together with atomic ratios calculated based on 4 oxygen atoms and 4 oxygen+sulfur atoms for the olivines, and 6 oxygen atoms and 6 oxygen+sulfur atoms for the Ca-poor pyroxenes. All the calculation results differ from theoretical stoichiometric formulae of olivine and pyroxene. These data show that sulfur is contained as submicroscopic dusty inclusions and is not contained in substitution for oxygen or other cations.

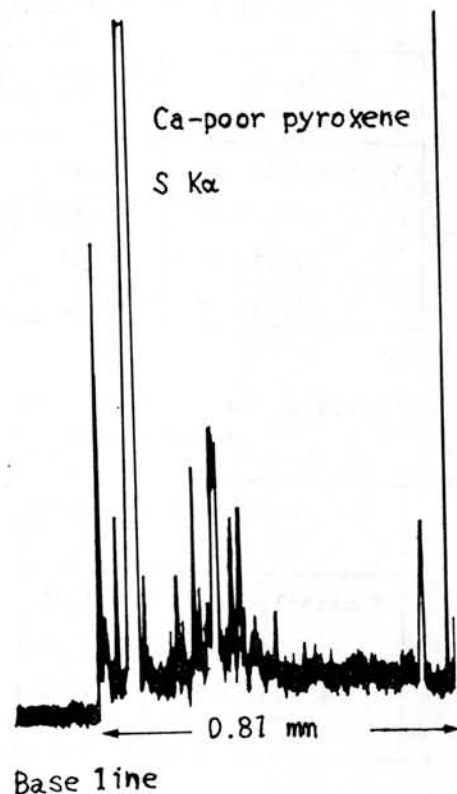


Fig.1

Table 1 shows also representative analytical results for troilites. Some troilites have strictly stoichiometric formulae and others not strictly stoichiometric formulae. These may also result from submicroscopic dusty inclusions.

It is highly probable that only selected electron-probe data have been reported in papers and many other data being regarded as analytical error and neglected from the reports.

Table 1. Representative analytical results of olivine, pyroxene and troilite.

	Pyx-1		Pyx-2		Tr-1	Tr-2 (wt%)
	01-1	01-2	1.43			
Na ₂ O	31.45	24.75			63.54	61.69
MgO	0.40	0.17	26.78	20.02		1.11
Al ₂ O ₃	36.54	34.17	0.74	1.34		0.17
SiO ₂	0.17		55.04	51.98		0.80
K ₂ O	0.15	0.77				0.80
CaO	0.65	0.74	0.44	1.24		0.16
TiO ₂	0.57	0.57				
Cr ₂ O ₃	30.30	34.63	0.61	0.64	36.70	35.26
MnO	0.15	4.11	0.23	0.95	100.24	99.99
FeO	0.18		15.75	21.70	49.85	47.91
NiO	0.27					1.72
S	0.36		0.25			0.14
Σ	100.2	100.6	99.6	99.6	50.15	47.70
Na	1.271	1.0477	0.1044	0.1044		
Mg	0.013	0.0057	1.444	1.1259		
Al	0.991	0.9701	0.032	0.0596		
Si	0.0061	0.0061	1.991	1.9604		
K	0.005	0.0234	0.017	0.0503		
Ca	0.0065	0.0064	0.0014	0.0014		
Ti	0.014	0.0167	0.018	0.0192		
Cr	0.013	0.0137	0.007	0.0301		
Mn	0.687	0.8223	0.476	0.6844		
Fe	0.003	0.0939	0.0177	0.0176		
Ni	2.997	3.0060	3.985	4.0357		
S	0.0096	0.0096	0.0177	0.0176		
Σ	100.7	100.8	99.7	99.9	0.63	0.63
Na	100.2	100.6	100.7	100.8	100.0	
Mg	1.0424	1.0452	0.1044	0.1044	0.1041	0.1036
Al	0.0056	0.0057	1.1258	1.1258	1.1226	1.1185
Si	0.9654	0.9677	0.0596	0.0596	0.0594	0.0594
K	0.0060	0.0061	1.9602	1.9602	1.9546	1.9479
Ca	0.0232	0.0233	0.0503	0.0503	0.0502	0.0499
Ti	0.0064	0.0064	0.0014	0.0014	0.0014	0.0014
Cr	0.0165	0.0166	0.0192	0.0192	0.0191	0.0189
Mn	0.0136	0.0136	0.0301	0.0301	0.0300	0.0300
Fe	0.8184	0.8203	0.6843	0.6843	0.6824	0.6801
Ni	0.0935	0.0936	0.0177	0.0176	0.0176	0.0176
S	0.0096	0.0096	4.0530	4.0414	4.0273	
Σ	3.0006	3.0081	0.50	0.50		

#18

MAJOR CHEMICAL COMPOSITION OF MATRICES OF UNEQUILIBRATED ORDINARY CHONDRITES

Ikeda, Y.*, Kimura, M.* and Takeda, H.**

*: Ibaraki Univ., Mito 310, **: Tokyo Univ., Tokyo 113.

The chemical compositions of matrices of ALH-76004, Y-74191, ALH-77015 and ALH-77299 were analysed using defocused beam of an electron-probe microanalyser. The matrix, here, is defined to be an aggregate of very fine-grained materials (less than micron size), which fills interstitial spaces between chondrules, lithic fragments and/or mineral fragments.

The chemical compositions of matrices of unequilibrated ordinary chondrites are distinct from those of E- and C-chondrites. The matrices of O-chondrites are poorer in SiO_2 and lower in Mg/Fe ratio than those of E-chondrite (Y-691), and are richer in SiO_2 than those of C-chondrites.

The chemical compositions of matrices of unequilibrated O-chondrites are different from those of chondrules in the same chondrites, and the former is lower in Mg/Fe ratio and poorer in SiO_2 than the latter. The major normative minerals of matrices are ferrous olivine and sodic plagioclase with small amounts of pyroxene, troilite and so on. The chemical compositions of matrices of O-chondrites support the low temperature condensate as origin of the matrix discussed by Larimer and Anders (1967).

PETROLOGY OF CHONDRULES IN ALHA77015 (L3) CHONDRITE

Nagahara, H.

Geological Institute, University of Tokyo, Hongo, 113 Tokyo

More than three hundred chondrules in ALHA77015(L3) chondrite were studied under the microscope in three thin sections, and the chemical compositions of the chondrules and their constituent minerals and glasses were determined by electron microprobe analysis.

Size of the chondrules ranges from 0.1 to 1.3mm in radius; their distribution pattern closely resembles those of Bjurbole (L4) and Chainpur (LL3) chondrites (Martin and Mill, 1976). They are classified into four groups by the textures and into three groups by the mineral assemblages. Bulk chemical composition of chondrules is extremely variable, especially in SiO₂, MgO and FeO. There is a reciprocal relation between SiO₂ content and MgO and FeO contents in general; however it is not so remarkable as in the case of the "equilibrated chondrites" (Nagahara, 1979). The abundances of Al₂O₃, CaO and TiO₂ are nearly equal to those of the "cosmic abundance", and show positive correlation among them. For most chondrules, volatile element Na is not depleted compared to refractory elements, such as Al, Ca and Ti; that is, the ratio of volatile/refractory is close to the cosmic ratio. These facts indicate that the chondrules were heated up to relatively low temperatures at which volatiles had scarcely been lost.

Some chondrules contain two types of olivine; one is irregular anhedral crystal which shows dirty appearance with "reverse zoning" (core is iron rich and rim is magnesian), and the other is small euhedral crystal around the former and shows clear appearance with "normal zoning" (core is magnesian and rim is iron rich). The former is thought to represent a relic mineral which was not completely melted at the time of chondrule formation and cited as the core of the chondrule. On the other hand, the latter is thought to have crystallized later from the liquid. These chondrules strongly support the remelting of pre-existing materials as the process of chondrule formation (i.e. Wasson, 1972; Kieffer, 1975).

Chemical compositions of olivine and pyroxene are controlled by the bulk composition of each chondrule; the Mg/Mg+Fe ratio of olivine and pyroxene depend on the bulk composition. In general, CaO in olivine and Al₂O₃ in pyroxene are affected by the crystallization temperature or cooling rate of liquid, and they are useful for the estimation of cooling history. But in this chondrite, they depend on the contents of these elements within the chondrule, and have no relation to texture of each chondrule. Exceptionally Al₂O₃ content in pyroxene with radial texture is less than those with porphyritic texture. These observations suggest that the cooling rate at which chondrules crystallized and internal texture was formed was not so variable. Therefore the difference in maximum temperature or the other kinetic factors should be considered for chondrules with different

#19-2

textures and with nearly equal composition. This is also suggested by the fact that the textures are not controlled only by SiO₂ content.

The above discussions are consistent with the results of experiments of reproducing chondrules (Tsuchiyama et al., 1980 and 1981; Nagahara and Tsuchiyama, in prep.)

REFERENCES

- Kieffer, S.W. (1975); *Science*, 189, 333-340.
Martin, P.M. and Mills, A.A. (1976); *EPSL*, 33, 239-248.
Nagahara, H. (1979); *Mem. Natl. Inst. Polar Res. Spec. Issue* 15, 78-109.
Tsuchiyama, A., Nagahara, H. and Kushiro, I. (1980); *EPSL* 48, 155-165.
—, — and — (1981); *GCA* submitted.
Wasson, J.T. (1972); *Rev. Geophys. Space Phys.*, 10, 711-759.

PETROLOGY OF ALHA77015 CHONDRITE

Mikio MATSU-URA, Ichiro SUNAGAWA, Ken-ichiro AOKI, Hirokazu FUJIMAKI
Faculty of Science, Tohoku University, SENDAI

The bulk chemical compositions of 55 chondrules and 12 matrix points in the ALHA77015 (L3) chondrite were analyzed by the defocussed beam of an electron-probe microanalyzer using an energy-dispersive analytical system.

The range of the chemical compositions of the chondrules and matrix are given in Table 1.

The chemical compositions of the chondrules are considerably variable, whereas those of the matrix are relatively constant, as shown in Fig. 1. There is a distinct compositional gap between the chondrules and the matrix. Fig. 2 shows

	chondrules			matrix		
	max	min	av	max	min	av
Na ₂ O	3.31-	0.35	1.70	1.69-	0.59	0.96
MgO	49.15-	13.36	29.43	26.15-	20.32	22.08
Al ₂ O ₃	6.60-	0.55	3.29	3.75-	1.83	2.23
SiO ₂	58.24-	38.68	47.84	37.76-	33.29	36.07
K ₂ O	0.41-	0.00	0.11	0.39-	0.00	0.13
CaO	4.27-	0.29	1.93	2.28-	0.14	0.96
TiO ₂	0.20-	0.00	0.08	0.11-	0.00	0.04
Cr ₂ O ₃	0.70-	0.15	0.47	0.99-	0.37	0.54
MnO	0.70-	0.00	0.33	0.63-	0.37	0.49
FeO	23.33-	5.22	13.09	37.92-	31.47	35.09

the compositional relationships between the chondrules and the matrix. The matrix are enriched in MnO and FeO, whereas the chondrules are enriched in Na₂O, CaO and Al₂O₃. It would therefore be difficult to produce the matrix by fragmentation from the chondrules.

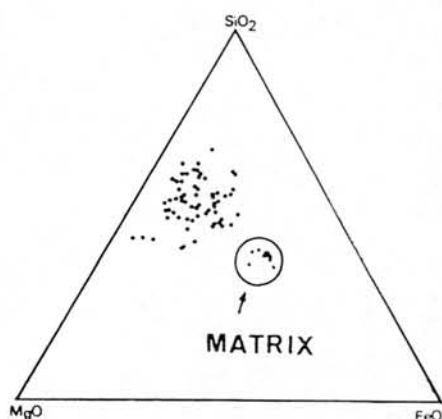


Fig. 1

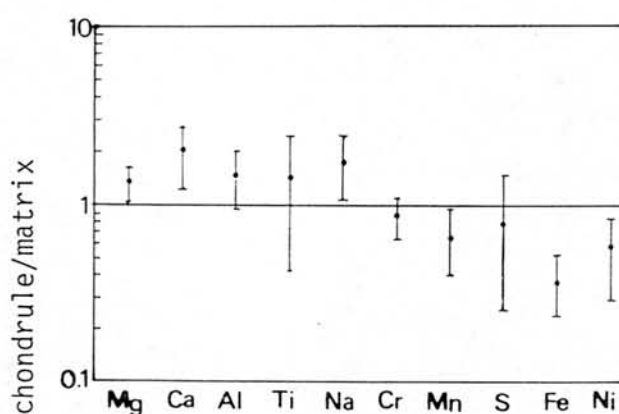


Fig. 2

In the chondrules Na is correlated with Al as shown in Fig. 3. The correlation coefficient for the Na-Al relation is +0.65. The volatilization temperature of Na is much lower than that of Al. Therefore, the data show that Na and Al behaved as NaAlSi₃O₈ component. The direct condensation model

#20-2

for origin of chondrules as liquid droplets from a tenuous solar nebula cannot explain the Na-Al correlation of the chondrules.

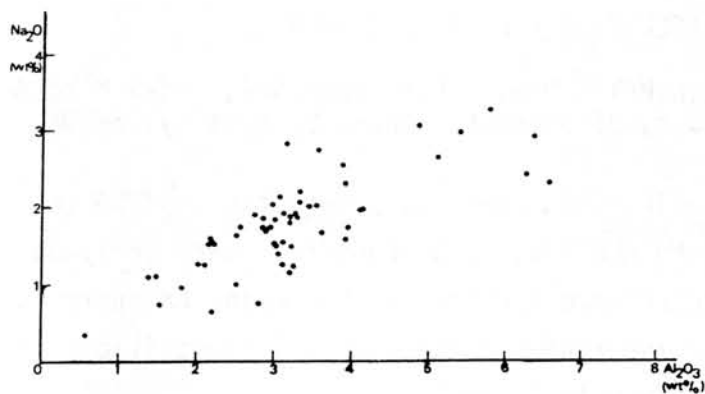


Fig. 3

EXPERIMENTAL REPRODUCTION OF TEXTURES OF CHONDRULES; II EFFECT OF RESIDUAL CRYSTALS.

Tsuchiyama, A. and Nagahara, H.

Geological Institute, University of Tokyo, Hongo, Tokyo, 113

Recently, the textures of chondrules have been reproduced by crystallizing melts of three different chondrule compositions with cooling rates ranging from 400 to 200°C/min and it has been concluded that some chondrule textures can be formed with cooling rates about 100°C/min (Tsuchiyama et al., 1980). On the other hand, it has been known that textures are also strongly affected by nucleation kinetics of crystals (eg. Lofgren, 1980). In the present study, crystallization experiments in which melts with and without crystals were cooled were conducted in order to investigate effects of the nucleation kinetics.

Experimental methods were similar to those in the previous experiments. Finely powdered starting materials of two chondrule compositions were used; sample 1 is a mixture of minerals and sample 2 is Yamato 74115 from which metallic iron was removed. Diameter of each crystal ranges from <1µm to a few tens µm. The starting materials were pressed into pellets and attached to Pt wire loops. After the charges were held at various temperatures ranging from superliquidus to subliquidus temperatures for 2 min, they were cooled to about 1200°C with cooling rates 100-50°C/min and then quenched into water. During cooling, partial pressure of oxygen varies from 10⁻⁹atm(1600°C) to 10⁻¹²atm(1200°C) in a constant H₂/CO₂ gas stream. In order to examine presence or absence of preexisting crystals before cooling, the charges were quenched immediately from the initial temperature.

Results are shown in Fig.1, where columns indicated by C and Q show the cooling experiments and the immediate quenching experiments respectively. The liquidus temperature of olivine of the starting materials are about 1440°C and 1580°C for the samples 1 and 2 respectively. The textures produced in the cooling experiments with initial temperature greater than the liquidus temperature were strikingly different from those with initial temperature less than the liquidus temperature for both the starting materials; the former is spinifex texture with fine radial and/or barred olivine crystals, whereas the latter is porphyritic or microporphyritic texture with equant olivine and probably pyroxene crystals. With increasing the initial temperature to superliquidus condition, the width of the olivine crystals becomes finer, and finally with the initial temperature greater than about 1560°C, no crystal crystallizes for the sample 1. On the other hand, with decreasing the initial temperature to subsolidus condition, the size of the equant crystals becomes smaller from a few hundreds to a few µm. With the initial temperature near the liquidus, the textures different from those found in the superliquidus and subliquidus runs were formed.

If chondrules were formed by local heating of pre-existing materials, porphyritic texture would be expected to form when the chondrules once not completely melted. In fact, porphyri-

#21 - 2

tic texture is a dominant texture in chondrules with various bulk chemical compositions. This suggests that maximum temperature of the local heating process was not so high; it was occasionally less than the liquidus temperature of chondrules. This is also consistent with the experimental results on sodium volatilization (Tsuchiyama et al., 1981). If the liquidus temperature of chondrules was sufficiently low and the maximum temperature was greater than the liquidus temperature by 100°C or more, glassy chondrule was also expected to form.

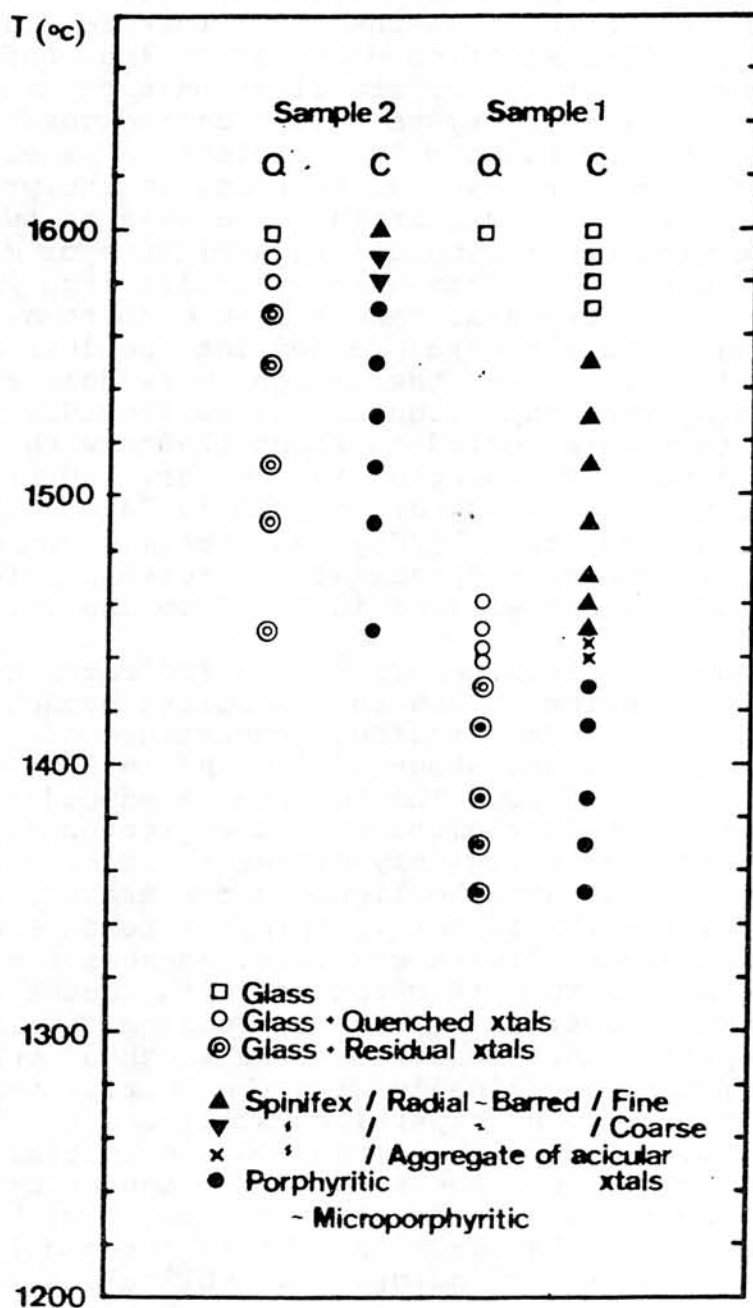


Fig.1 Results of the present experiments.

CHEMICAL AND PETROLOGICAL STUDIES OF ALHA77302 METEORITE

Fukuoka, T.¹⁾, Ishii, T.²⁾, Nakamura, N.³⁾, and Takeda, H.⁴⁾

1) Dept. of chemistry, Gakushuin University, Mejiro, Toshima-ku, Tokyo 171. 2) Ocean Research Institute, University of Tokyo, Minamidai, Nakano-ku, Tokyo 164. 3) Dept. of Earth Sciences, Kobe University, Rokkodai-cho, Nada-ku, Kobe 657. 4) Mineralogical Institute, University of Tokyo, Hongo, Bunkyo-ku, Tokyo 113.

ALHA77302 meteorite is a polymict eucrite which was collected in the Allan Hills region by U.S.-Japan team during the 1977-78 Antarctic field season. A consortium study of this meteorite is now in progress. The study include chemical, petrological, mineralogical, age determination, and stable isotope studies. We report here some chemical and petrological results as a part of the study.

Sliced meteorite sample (approximate 1 cm thick) was provided from National Institute of Polar Research. After mapping of the sample surfaces by photographs, over 20 of clasts, phenocrysts and matrices were separated from the sample specimens. The abundances of 15 major, minor, and trace elements (Fe, Cr, Co, Au, Ba, Sc, La, Ce, Sm, Eu, Tb, Yb, Lu, Hf, and Ta) in two matrices, one fusion crust, ten clasts, three pyroxene phenocrysts, and one feldspar phenocryst have been determined by INAA (instrumental neutron activation analysis). The abundances of 14 minor and trace elements (K, Rb, Sr, Ba, La, Ce, Nd, Sm, Eu, Gd, Dy, Er, Yb, and Lu) in a matrix have been determined by isotope dilution method using mass spectrometer. Petrological study have been carried out on a clast. The results of INAA and isotope dilution analysis are shown in table 1.

The meteorite specimens had included carbonaceous chondrite-like clasts which were recognized with the naked eye observations. The results of INAA of these clasts do not show chemical evidences for carbonaceous chondrite. Because the clasts do not contain high concentrations of siderophile elements, e.g. Co, Ni, Au, and Ir. Although howardite, mechanical mixture of eucrites and diogenites, include chondritic component, there is no evidence of chondritic component in polymict eucrite, ALHA77302 in this study, because of no determination of Ir and Ni, and low concentrations of Co and Au. The chondritic normalized REE (rare earth elements) patterns of matrices and clasts are generally similar to the eucrite patterns of previous works, but the patterns of some clasts and matrices show possible positive Ce anomalies. The REE pattern of a low iron pyroxene may show negative Ce anomaly.

The results of petrological investigation of pyroxene textures suggest the clast C (in Table 1) was formed under rapid cooling condition. Therefore, the bulk chemical compositions of the clast give the chemical compositions of liquid phase of magma at a certain time of magmatic evolution.

Table 1. Chemical compositions in matrices, clasts, and phenocrysts.

Sample	Wt mg	FeO %	Cr ppm	Co ppm	Au ppb	Ba ppm	Sc ppm	La ppm	Ce ppm	Sm ppm	Eu ppm	Tb ppm	Yb ppm	Lu ppm	Hf ppm	Ta ppm
Matrix A	12.1	19.0	3200	6.87	15	-	30.3	2.72	11.5	1.40	0.628	0.32	1.48	0.30	1.58	0.31
B	11.9	12.4	1860	5.88	31	34	29.4	3.38	12.5	2.16	0.798	0.38	2.3	0.35	3.1	0.43
C ¹⁾	6.3					37		2.00	5.87	1.40	0.532		1.56	0.238		
Fusion crust	5.4	19.7	2700	9.00	24	39	29.9	3.46	10.4	1.86	0.595	0.31	1.63	0.33	1.99	0.35
Clast A	9.3	15.2	2260	4.87	64	47	34.9	2.71	11.6	1.66	0.656	0.25	1.50	0.29	2.4	0.30
B	17.1	14.8	1620	5.90	21	52	23.2	5.38	14.2	2.29	0.965	0.35	1.79	0.29	1.37	0.26
C1	8.6	7.9	1010	14.2	28	21	21.6	2.41	5.6	1.13	0.700	0.40	1.71	0.26	3.2	0.46
C2	10.2	22.1	2980	7.30	-	53	35.1	4.37	10.8	1.93	0.743	0.31	1.82	0.37	1.90	0.31
C2)		14.4	1910	11.1	-	35	27.8	3.31	8.0	1.50	0.720	0.36	1.76	0.31	2.6	0.39
D	10.9	12.3	1650	16.7	27	56	33.6	6.97	18.5	3.44	1.06	0.60	3.2	0.53	4.5	0.55
E	14.1	19.8	2630	6.54	33	17	33.1	3.08	10.9	2.08	0.721	0.32	1.70	0.33	2.6	0.26
F	6.1	24.0	4010	9.24	41	69	48.2	5.42	21.7	3.25	1.11	0.54	2.7	0.48	3.9	0.34
G	4.5	17.9	2360	6.05	-	25	29.8	3.15	9.5	1.49	0.562	0.29	1.53	0.30	1.59	0.30
H	1.31	20.1	3230	5.37	9	102	27.5	2.97	13.3	1.59	0.637	0.22	1.45	0.30	1.61	0.23
I	2.87	21.1	3340	8.38	-	28	27.0	1.91	8.4	1.25	0.440	0.22	0.99	0.24	1.16	0.15
J	1.91	18.5	2380	6.51	11	70	28.5	4.00	15.5	2.11	0.695	0.39	1.95	0.43	2.5	0.30
Pyroxene A	0.83	32.4	2560	8.95	8	-	38.5	1.94	-	1.47	0.044	0.39	3.0	0.66	1.43	-
B	0.69	9.27	500	8.64	-	-	52.9	9.36	18.7	6.92	0.295	1.35	11.1	2.23	1.29	-
C	0.30	20.8	5030	13.8	7	20	16.3	1.52	-	0.138	0.062	0.071	0.24	0.082	-	0.18
Feldspar A	0.50	0.25	28	2.44	10	78	0.26	1.21	1.51	0.132	0.506	0.013	0.115	0.017	-	-
Errors (%)		1	1	1-2	10-50	15-70	1	5-20	5-10	2-10	3-7	4-20	5-15	3-15	4-10	10-30

1) Values obtained by isotope dilution method using mass spectrometer.

The values also show 622 K, 0.704 Rb, 78.0 Sr, 4.20 Nd, 1.89 Gd, 2.41 Dy, and 1.50 Er in ppm.

2) Weight mean of clast C1 and C2.

Sr-Ba Systematics in Antarctic Ca-rich Achondrites

Naoki ONUMA and Masataka HIRANO
Department of Chemistry
University of Tsukuba

Large divalent cations, Sr²⁺ (1.17A) and Ba²⁺ (1.36A) are considered to be sensitive geochemical indicators for elucidation of magma genesis. These elements are contained, not in the major phases (olivine, pyroxenes, metallic iron and troilite), but in the accessory mineral (feldspar) and in the interstitial material (glass) of primitive planetary constituent such as chondritic meteorites.

This fact suggests that small amounts of partial melting produce strong enrichment of Sr and Ba in the melt, since the accessory phases are among the first components to enter the melt. Increasing the degree of partial melting dilutes Sr and Ba contents with the addition of Sr and Ba-poor phases. Thus, a series of melts derived from different degree of partial melting of a common source material make a Sr-Ba systematics through source material in a Sr/Ca-Ba/Ca diagram.

We have developed a new analytical method for simultaneous determination of Ca, Sr and Ba in silicate rocks by Inductively Coupled Plasma - Optical Emission Spectrometry (ICP-OES). The method has

Table 1 Ca, Sr, Ba Abundances of Eight Eucrites*

	Ca(ppm)	Sr(ppm)	Ba(ppm)
Bereba	71500	74.7	28.6
Jonzac	71600	74.6	29.0
Juvinas	73000	77.1	30.2
Moore County	67500	63.9	18.6
Nuevo Laredo	73100	80.5	39.3
Pasamonte	72300	75.0	29.1
	73200	78.0	28.6
Sioux County	73900	75.9	27.2
Stannern	74000	87.8	53.0

* Tera et al (1970)

large dynamic range (Ca:10⁴, Sr:10⁵, Ba:10⁵), and low detection limit (Ca:13ppb, Sr:0.2ppb, Ba:0.7ppb). Accuracy and Precision of the method obtained by JB-1 standard rock are as follows :

Ca: 66900±1010 ppm (certified value=66300 ppm), Sr: 439±7.6 ppm (c.v.=435 ppm), Ba: 493±9.0 ppm (c.v.=490 ppm). The results of seven Antarctic Ca-rich achondrites are presented in Table 2, along with Table 1 of eight eucrites obtained by an isotope dilution method (Tera et al., 1970).

Table 2 Ca, Sr, Ba Abundances of Seven Antarctic Eucrites

	Ca(ppm)	Sr(ppm)	Ba(ppm)
Y-74450	68400	73.7	40.1
Y-75011	68500	74.5	40.5
Y-75015	70600	76.3	39.8
Y-76005	67300	71.5	33.8
ALHA-78040	69400	72.8	32.6
ALHA-78132	61100	62.7	30.5
ALHA-77005	21000	6.2	2.4
	20200	6.3	2.3

These reliable data from 15 Ca-rich achondrites are plotted in the Sr/Ca-Ba/Ca diagram shown in Figure 1. Eight eucrites (○) consist of a Sr-Ba systematics, and six Antarctic Ca-rich achondrites (●) fall on the Sr-Ba systematics, indicating the Antarctic achondrites belong to eucrites. However, one Antarctic Ca-rich achondrite (ALHA-77005) does not fall on the systematics, suggesting its uniqueness.

In Figure 1, chondrites (x) and an Antarctic diogenite (o) are also plotted. Data are from Tera et al. (1970) for chondrites, Masuda & Tanaka (1978) for Sr & Ba of the diogenite, and Shima & Shima (1973) for Ca of the diogenite, respectively.

#23 - 2

Note that, chondrites are located near an intersection of the eucrite systematics and the tie line of ALHA 77005 and Y-692.

Figure 1 suggests that eucrites are derived from a common source material by partial melting. The common source material may be a planetary material with chondritic constituent. ALHA 77005 (unique) and Y-692 (diogenite) may be residual solid produced by partial melting of the planetary material.

References

- Masuda and Tanaka (1978):
Mem. Natl. Inst. Polar Res.,
Spec. Issue, 8, 229.
Shima and Shima (1973);
Meteoritics 8, 439.
Tera et al. (1970); Proc.
Apollo 11 Lunar Sci., Conf.,
2, 1637.

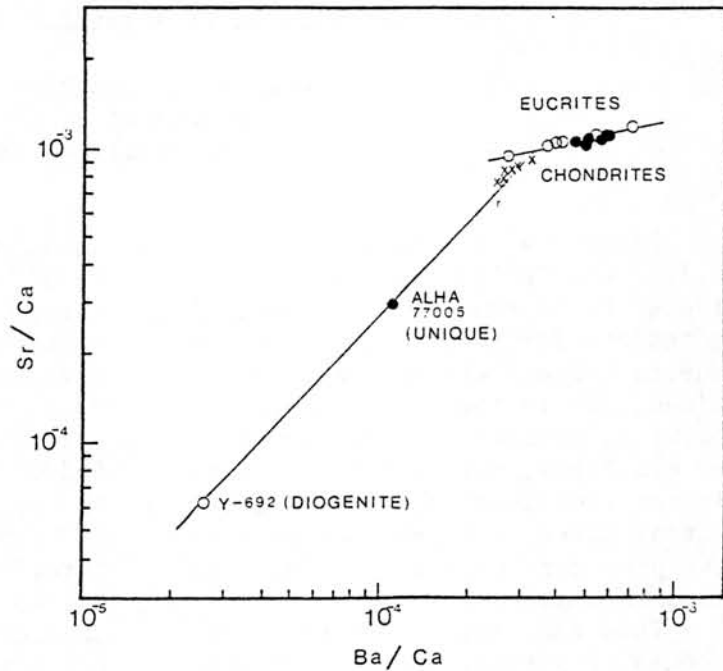


Fig. 1. Sr/Ca-Ba/Ca diagram for achondrites (O●) and Chondrites (X) (●: This work O & X: Others)

REE, Ba, Sr and Rb abundances in some unique Antarctic achondrites

Hiroshi Shimizu and Akimasa Masuda

Department of Earth Sciences, Faculty of Science, Kobe University

Rare-earth elements (REE), Ba, Sr and Rb were determined for seven Antarctic achondrites including some unique ones. The achondrites analyzed are Y-74450 (eucrite), ALH-77256 (diogenite), ALH-78113 (aubrite), ALH-77219 (mesosiderite), Y-74123 (ureilite), ALH-77257 (ureilite) and ALH-77005 (unique). REE, Ba, Sr and Rb were determined by a mass spectrometric stable isotope dilution technique. The REE patterns normalized by Leedy chondrite (Masuda et al., 1973) are shown in Figs. 1 and 2. Also in Fig. 2, are shown REE patterns for mineral separates, prepared from the unique achondrite ALH-77005 by heavy liquid.

The Y-74450 eucrite shows a negative Eu anomaly and a positive Ce anomaly. The ALH-77256 diogenite has the highest contents of REE among Antarctic diogenites analyzed thus far. REE pattern of ALH-78113 aubrite shows that points for La, Nd, Sm, Dy and Er lie on a single linear line, and that points for Ce, Eu and Gd deviate from the La-Nd-Sm-Dy-Er line. Further, a point of Yb for this ALH-78113 deviates from a Er-Lu line. The REE pattern of ALH-77219 mesosiderite appears to be composed of two rectilinear lines having an inflection point at Gd, with a positive Eu anomaly. Two ureilites, Y-74123 and ALH-77257, show curved patterns having a minimum position at Nd or Sm, with the exception of Eu, and having maximum at Lu. The REE curve for the ureilites appears to be upward concave for light REE segment and to be upward convex for heavy REE segment. REE pattern for whole rock sample of ALH-77005 unique achondrite shows S-shaped one and has a positive Ce anomaly. This Ce anomaly is also observed in the two mineral separates ($3.35 < d < 3.40$ and $3.55 < d < 3.60$) from the ALH-77005. REE, Ba and Sr concentration ratio patterns of the two mineral separates from ALH-77005 relative to ALH-77005 whole rock sample are markedly simple (see Fig. 3) in spite of their complicated chondrite-normalized patterns.

#24 - 2

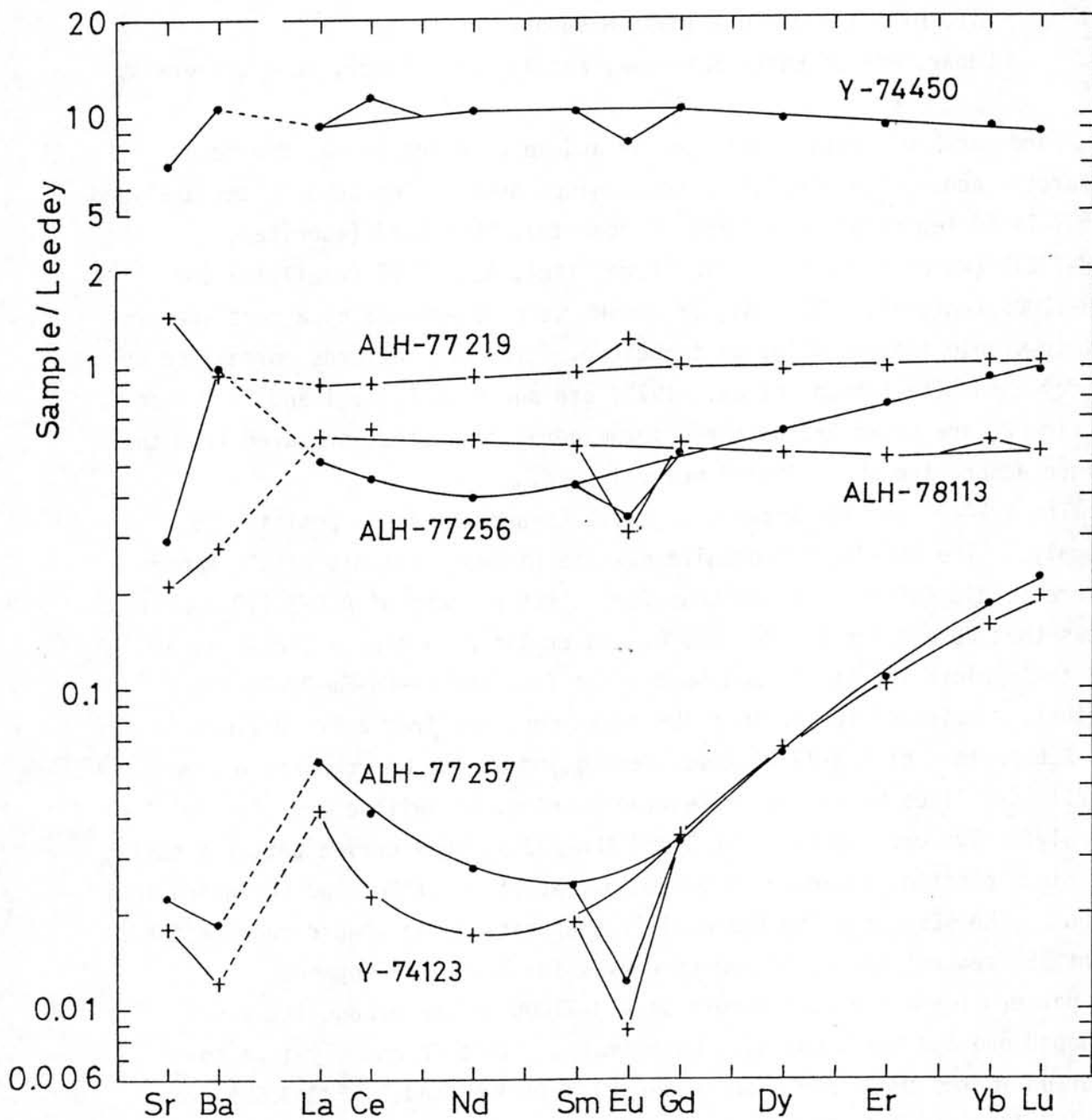


Fig. 1. Leedeey-normalized REE patterns plus Sr-Ba patterns; the normalizing value, 11.1 ppm, for Sr is from Gopalan and Wetherill (1971).

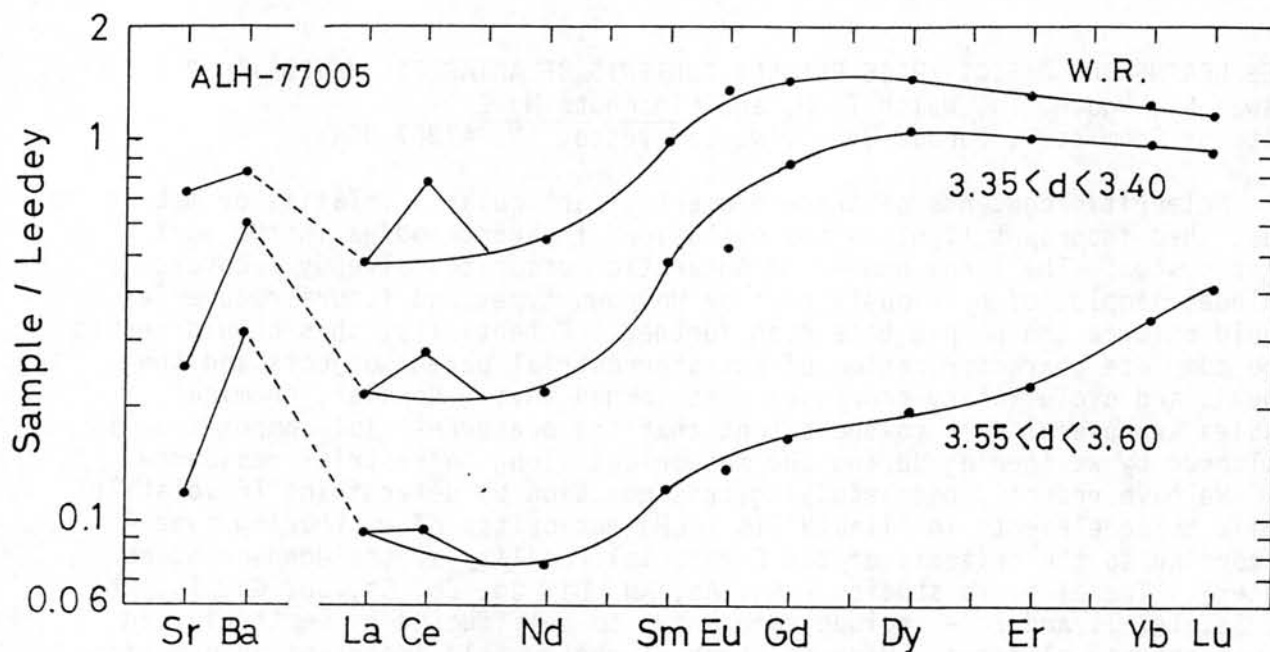


Fig. 2. Leedeey-normalized REE patterns plus Sr-Ba patterns, for ALH-77005 whole rock and two mineral separates.

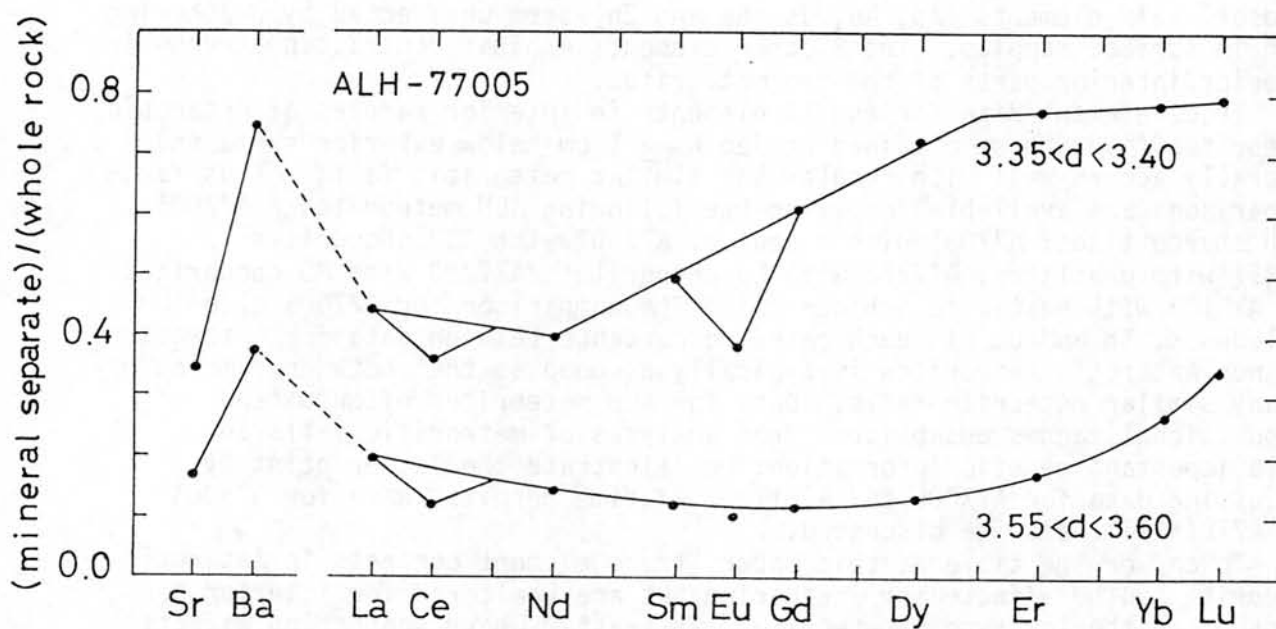


Fig. 3. REE, Ba and Sr concentration ratio patterns of two mineral separates relative to whole rock sample, for ALH-77005.

DOES WEATHERING AFFECT TRACE ELEMENT CONTENTS OF ANTARCTIC METEORITES?

Biswas S., Ngo H. T., Walsh T. M. and Lipschutz M. E.

Dept. of Chemistry, Purdue Univ., W. Lafayette, IN. 47907 USA

Meteoritic contents of trace elements, particularly volatile or mobile ones, shed important light on the evolution of parent bodies in the early solar system. The large number of Antarctic meteorites already recovered includes samples of previously rare or unknown types and future recoveries should enlarge the sample base even further. Potentially, this should permit more complete characterization of extraterrestrial parent objects and the genetic and evolutionary processes that formed them. However, chemical studies are useful only to the extent that the preterrestrial composition is unaltered by weathering during the meteorites' long terrestrial residence.

We have recently been studying this question by determining 16 volatile/mobile trace elements in Allan Hills (ALH) meteorites of weathering type A (according to the criteria of the Curatorial Facility at the Johnson Space Center). The elements studied - Ag, As, Au, Bi, Cd, Co, Cs, Cu, Ga, In, Rb, Sb, Se, Te, Tl and Zn - include some known to be affected by weathering in more temperate climates. Many of these elements yield important information on the pre-terrestrial thermal evolutionary histories of meteorites. Meteorites studied included representatives of previously rare types. We examined weathering effects by comparing trace element data for: interior and exterior samples of the same ALH meteorites; and interior samples of ALH meteorites with results for falls of similar type. We found significant Cs and Rb enrichments in the exterior samples of ALH A77257 ureilite and A77278 L3 chondrite and attribute this to deposition of wind-borne oceanic aerosol. Six elements (As, Au, Cs, Ga and Zn) seem unaffected by weathering even in surface samples. The 8 other elements exhibit contrasting trends in exterior/interior parts of the two meteorites.

Trace element data for the 16 elements in interior samples of Antarctic meteorites (i.e. those obtained at depths ≥ 1 cm below exterior surfaces) generally accord well with results for similar meteoritic falls. Thus far, comparisons are available involving the following ALH meteorites: A77005 with shergottites; A77081 with Acapulco; A77307 with C3V chondrites; A77257 with ureilites, A77278 with L3 chondrites; A77299 with H3 chondrites; and A78113 with enstatite achondrites. The comparison for A77005 also includes K, Th and U. In each case, concordance between data for Antarctic and non-Antarctic meteorites is typically as good as that between samples of any similar meteorite falls. Data for ALH meteorites often extend compositional ranges established from analyses of meteoritic falls and yield important genetic information; we illustrate the latter point by discussing data for A77005 and A78113. If time permits, data for A76004 and A77219 will also be discussed.

To answer the title of this paper, trace element contents in Antarctic meteorite can be affected by weathering but are unaltered for interior portions of weathering type A meteorites, at least. Where weathering effects can be detected, they generally involve elemental loss by leaching but contents of alkali metals reflect contamination. With proper collecting and curating procedures, data obtained from Antarctic meteorites are as reliable as those determined for meteoritic falls. This result is especially gratifying since it indicates that the scientific potential of the Antarctic Collection is even higher than previously thought.

25 - 2

Acknowledgement. This research was supported in part by NASA grant NGL 15-005-140. Travel to attend this Symposium was supported in part by a grant from the Barringer Crater Company.

#26-1

MAGNESIUM ISOTOPIIC RATIOS OF YAMATO METEORITES

Nishimura, H. and Okano, J.
College of General Education, Osaka University, Toyonaka,
Osaka 560.

Excess of magnesium 26 has been reported by several investigators [1] in relation to the in situ decay of extinct ^{26}Al ($\tau_{1/2}=7.2\times 10^5$ y) for Al-Ca rich inclusions in the Allende carbonaceous chondrite. This ^{26}Al is thought to be synthesized during explosive carbon burning at supernova explosion, and to be injected less than about 10^6 years prior to the solidification of the minerals in the inclusion. If this is the case, ^{16}O , ^{20}Ne and ^{24}Mg might be produced at the same time. The isotopic anomaly of ^{16}O has been found in the Allende and other carbonaceous chondrites by CLAYTON et al. [2].

We have measured the isotopic abundance ratios of magnesium in Allende with the ion microprobe mass analyzer (IMMA), and detected the ^{26}Mg excess of about 30 % above normal for one Al-rich white inclusion.

Furthermore, Al-poor portions of the Yamato and Allende meteorites have been analyzed in order to find the remnant of ^{24}Mg which might be injected in the similar way of pure ^{16}O injection.

A preliminary result is reported in the following.

A Hitachi IMA 2A ion microprobe mass analyzer was used. 17 keV O_2^+ ion were used as primaries. The diameter and the current of the primary ion beam were ca. $100\ \mu\text{m}$ and $3\times 10^{-7}\ \text{A}$, respectively. Analyses were done at Al-poor portion at which the concentration ratio of Al/Mg was less than about 0.1. Mass scanning was carried out over the mass range of 24 to 27 about 60 times at each portion.

Samples used were Yamato 74082, Yamato 74097, Yamato 74155, Yamato 74445, Yamato 74495, Yamato 74190, Yamato 74159, Yamato 74640 and Allende meteorites.

A preliminary result was shown in Fig.1. The ordinate and the abscissa are Δ_{25} and Δ_{26} , respectively. These values are

calculated from the raw secondary ion intensities of $^{24}\text{Mg}^+$, $^{25}\text{Mg}^+$ and $^{26}\text{Mg}^+$ according to the following equation.

$$\Delta m = \left(\frac{({}^m\text{Mg}/{}^{24}\text{Mg})_{\text{met}}}{({}^m\text{Mg}/{}^{24}\text{Mg})_{\text{ref}}} - 1 \right) \times 1000 \quad (m=25, 26)$$

where $({}^{25}\text{Mg}/{}^{24}\text{Mg})_{\text{ref}}=0.12663$ and $({}^{26}\text{Mg}/{}^{24}\text{Mg})_{\text{ref}}=0.139805$ from SCHRAMM et al. [3].

In Fig.1, are also shown the data for the Allende matrix with home made IMMA. These data are corrected for the mass discrimination of the apparatus. A following point is given from the results.

Almost all plotted points appear to fall on the straight line with the slope of 1 instead of a mass fractionation line. This may indicate that pure ^{24}Mg isotope was added at the stage of the injection of the synthesized elements at the explosive carbon burning.

REFERENCES

- [1] C.M. Gray and W. Compston, *Nature*, 251 (1974) 495-497.
 T. Lee, D.A. Papanastassiou and G.J. Wasserburg, *Geophys. Res. Lett.*, 3 (1976) 41-44.
 G.J. Wasserburg, T. Lee and D.A. Papanastassiou, *Geophys. Res. Lett.*, 4 (1977) 299-302.
 T. Lee, D.A. Papanastassiou and G.J. Wasserburg, *Astrophys. J.*, 211 (1977) L107-L110.
 T. Lee, D.A. Papanastassiou and G.J. Wasserburg, *Geochim. Cosmochim. Acta*, 41 (1977) 1473-1485.
- [2] R.N. Clayton, L. Grossman and T.K. Mayeda, *Science*, 182 (1973) 485-488.
- [3] D.N. Schramm, F. Tera and G.J. Wasserburg, *Earth Planet. Sci. Lett.*, 10 (1970) 44-59.

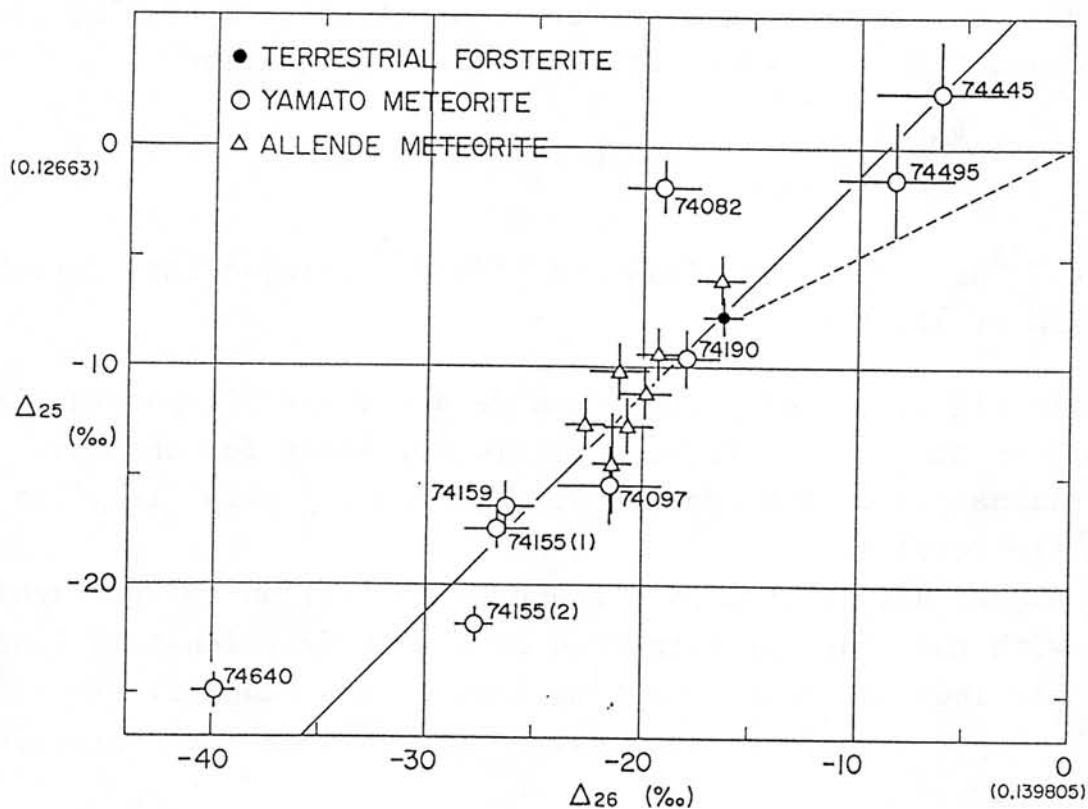


Fig. 1 Deviation, Δ_{25} , as a function of Δ_{26} . The values are calculated from the equation in the text. Dashed line indicates a normal mass fractionation line with the slope of 1/2 through the reference point.

COSMOGENIC ^{53}Mn IN YAMATO AND ALLAN HILLS METEORITES.

K. Nishiizumi, M. Imamura*, J. R. Arnold and M. Honda**

Dept. of Chem., B-017, Univ. of Calif., San Diego, La Jolla, CA 92093

*Institute for Nuclear Study, Univ. of Tokyo, Tokyo, Japan

**Institute for Solid State Physics, Univ. of Tokyo, Tokyo, Japan

We have measured cosmic ray produced ^{53}Mn ($t_{1/2} = 3.7 \times 10^6$ y) in over one hundred Yamato and Allan Hills meteorites [1-5 and this work]. Table 1 shows 47 new ^{53}Mn results obtained by neutron activation analysis since the last symposium along with meteorite class and recovered mass. This ^{53}Mn survey program of Antarctic meteorites provides us with the information described below.

(1) Multi-stage irradiation

It is known that two Antarctic meteorites, Y7301 and ALHA 76008, have two-stage (or multi-stage) irradiation histories [2,3] which are described using several cosmogenic radioactive nuclides and rare gases. Y74028 and Y74116 are new candidates for multi-stage irradiation. Both of the meteorites have low ^{53}Mn (60 and 64 dpm) and longer ^{40}K exposure age, 5-8 My [6]. It seems likely that they are part of the same fall, even though they were found 2.5 km apart. Another possible candidate for multi-stage irradiation is Y74094 (H6) which has the lowest ^{53}Mn value, 31 dpm, among 75 Yamato meteorites. It is also possible for Y74094 to have a normal short exposure age. If so, this low value indicates less than a 0.9 My exposure age of this object. Figure 1 shows the histogram of the ^{53}Mn content of Yamato and Allan Hills ordinary chondrites. At least 4 of the 5 meteorites, with less than ~ 100 dpm as discussed above, have multi-stage bombardment histories. Such a ^{53}Mn survey provides important statistical information concerning the meteorite bombardment studies.

(2) Terrestrial age

It is very interesting to measure the terrestrial age of Antarctic meteorites in order to understand the meteorite accumulation mechanism. We have demonstrated that ^{36}Cl ($t_{1/2} = 3.0 \times 10^5$ y) is one of the best isotopes for this study [5,7]. The terrestrial ages are lying, so far, between 10^4 and 7×10^5 y. Typical values are $2-4 \times 10^5$ y. The terrestrial age affects the ^{26}Al ($t_{1/2} = 7.2 \times 10^5$ y) activity appreciably, but not that of ^{53}Mn . In fact the histogram of ^{26}Al values in Antarctic meteorites is shifted from the histogram excluding Antarctic meteorites [8]. On the other hand, the histogram of ^{53}Mn in both sets of meteorites is quite similar [4]. Using both ^{53}Mn and ^{26}Al values, one may be able to estimate the terrestrial age of the object. For example ALHA 77015, 77162, 77260 have similar ^{53}Mn and ^{26}Al (36-37 dpm [8,9]). The terrestrial age is estimated to be $3-4 \times 10^5$ y, probably they are from the same fall. The pair ALHA 77112 and 77114 also have similar ^{53}Mn and ^{26}Al (42 and 38 dpm [9]) and the age is calculated to be $2-4 \times 10^5$ y.

(3) Pair meteorites

Several showers are well known among Yamato meteorites [10], for example the Y74194, 74459, 75034, 75108 series and especially the diogenite group including Y74013. These showers are understood also from field and physical observation. But many pairs, assuming they exist, will be identified only by measuring several cosmogenic nuclides including ^{53}Mn in addition to the physical and mineralogical characteristics. For example, the ^{53}Mn activity

#27 - 2

level in Yamato diogenites is close to 440 dpm, which also suggests these objects are a part of the same shower fall.

A more detailed discussion will be given in separate papers along with data on other cosmogenic nuclides.

REFERENCES:

- [1] Nishiizumi, K., et al (1978) Mem. Natl. Inst. Polar Res. Spec. Issue, 8, 209-219.
- [2] Nishiizumi, K., et al (1979) ibid, 12, 161-177.
- [3] Imamura, M., et al (1979) ibid, 15, 227-242.
- [4] Nishiizumi, K., et al (1980) ibid, 17, 202-209.
- [5] Nishiizumi, K., et al (1981) Earth Planet. Sci. Lett. (in press)
- [6] Nitoh, O., et al (1980) Mem. Natl. Inst. Polar Res. Spec. Issue, 17, 189-201.
- [7] Nishiizumi, K., et al (1979) Earth Planet. Sci. Lett. 45, 285-292.
- [8] Evans, J. C., et al (1979) Proc. Lunar Planet. Sci. Conf. 10th, 1061-1072.
- [9] Evans, J. C. (1980) private communication
- [10] Yanai, K. (1979) (compiled) Catalog of Yamato Meteorites.

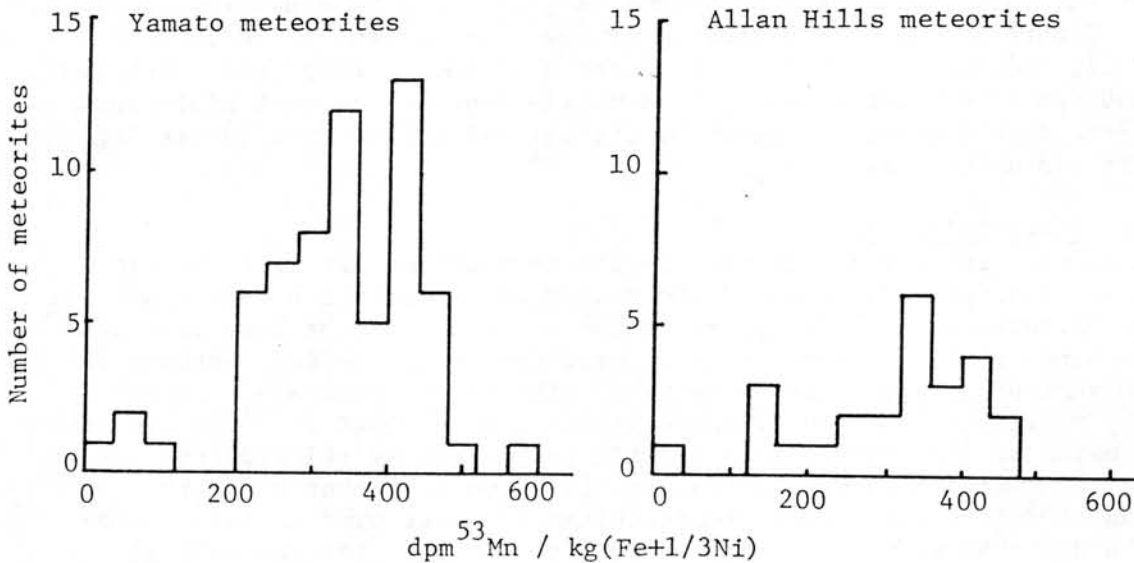


FIGURE 1. A histogram of the ⁵³Mn content of 63 Yamato and 25 Allan Hills ordinary chondrites [1-5 and this work]. The values have not been corrected for undersaturation.

TABLE 1

		Recov- ered mass	dpm ⁵³ Mn/kg (Fe+1/3Ni)			Recov- ered mass	dpm ⁵³ Mn/kg (Fe+1/3Ni)
Class	(kg)			Class	(kg)		
Yamato 74001	H5	0.246	351+16	Yamato 74471	H6	0.086	476+21
74002	LL5	0.070	218+10	74491	H4	0.135	406*
74007	L6	0.162	433+19	74497	H6	0.301	428+19
74015	L5	0.088	404+18	74605	L	0.581	413*
74028	L	0.090	60+4	74609	H5	0.257	265*
74035	L6	0.116	430*	74648	D	0.186	444+21
74073	H4	0.030	253+12	74650	L6	0.163	380+17
74094	H6	0.867	31*	75015	Eu	0.167	460+21
74106	H6	0.147	339+18	75017	L6	0.087	410*
74107	H6	0.114	370+16	75289	L5	0.051	322+15
74108	H6	0.139	360+16	ALHA 77004	H4	2.230	323*
74110	H3	0.090	285*	77015	L3	0.411	162+8
74115	H6	1.045	336*	77167	L3	0.611	137+7
74117	L5	0.080	240+11	77260	L3	0.744	150+8
74120	L5	0.091	419+18	77285	H6	0.271	397*
74125	D	0.107	449+20	77294	H5	1.351	411*
74144	L5	0.141	281+13	77302	Eu	0.236	433*
74165	L4	0.203	311+14	78112	L6	2.485	349*
74174	L4	0.021	211+10	78114	L6	0.808	354*
74348	H4	0.024	279*	78115	H6	0.848	335*
74375	H4	0.093	208+10	78130	L6	2.733	389*
74455	L6	0.114	278+13	META 78001	H4	0.624	432*
74459	H6	1.720	453*	PGPA 77006	iron		587*
74462	H6	0.205	386+17				

*Preliminary value

Extraterrestrial history of antarctic meteorites
recorded in the cosmogenic nuclides

M. Imamura, M. Honda¹, K. Nishiizumi², O. Nitoh, and N. Takaoka³

Institute for Nuclear Study, University of Tokyo, Tanashi, Tokyo 188, ¹The Institute of Solid State Physics, University of Tokyo, Roppongi, Minato-ku, Tokyo 106, ²Department of Chemistry, B-017, University of California-San Diego, La Jolla, California 92093, U.S.A., ³Department of Earth Sciences, Faculty of Science, Yamagata University, Yamagata 990.

Cosmic rays produces a variety of nuclides with half-lives ranging years to ∞ in the surface of the meteoritic object in space. These nuclides can provide a unique information on the history of the meteorite: the time scale and the extent of shielding during the exposure. A number of investigations on the cosmogenic nuclides in meteorites have been reported. Most of them have been directed to the specific interest in a small number of meteorites rather than the statistical information. This trend was partly due to the difficulty in obtaining meteorite samples. A great number of meteorites found in Antarctica are suited to such a statistical study. Since we started a systematic study on cosmogenic nuclides in antarctic meteorites a few years ago, the data have been accumulated to the level which is comparable to those of non-antarctic meteorites.

In this report, we summarize the data on ⁵³Mn, ²⁶Al, ³⁶Cl, ⁴⁰K, ²¹Ne and other isotopes, and try to draw some pictures of the extraterrestrial history of (antarctic) meteorites.

(i) Exposure ages can be calculated from cosmogenic ²¹Ne and ⁴⁰K contents. Distribution of the preatmospheric size can be estimated indirectly from the frequency distribution of the ⁵³Mn saturation values. No differences has been found between antarctic meteorites and non-antarctic ones.

(ii) If the meteorite is a break-up fragment which was originally located within 2-3m in the surface of the parent body, a two(or multi)-stage exposure history is recorded. One can find such a object as it contains less radio-activities than are expected from the stable nuclides. Multi-exposure histories have been found in at least 4 antarctic meteorites out of 11 meteorites with 2nd(or last)-stage exposure ages less than 5 million years(Table 1). This probability seems to be consistent with the case for the ordinary chondrites excluding antarctic ones(2 out of 11 cases surveyed). The probability of about 30% suggests that they are from the objects or craters with diameters of several tens of meters, on the average. We will also discuss on the 1st-stage exposure ages which are the ages of meteorite parent bodies.

(iii) To specify the time of the collision break-up event, the depth effect of the production rate of each nuclides must be taken into account. ²¹Ne production rate decreases with the decrease of the shielding for a small to medium sized meteorite. Depth dependence can be monitored by the ⁵³Mn saturation values since ²¹Ne is produced by similar nuclear reactions to ⁵³Mn. Fig. 1 shows the dependence of saturation ⁵³Mn upon ²¹Ne/⁴⁰K ratio. The production rate of ⁴⁰K is expected to remain nearly constant except in large objects. We will show ⁵³Mn-²¹Ne method to be useful in correcting the exposure ages for the shielding effect.

Table 1. Cosmogenic nuclides in some antarctic meteorites with low ^{53}Mn content.

Name	Class	^{53}Mn (dpm/kg)*	^{26}Al (dpm/kg)	^{36}Cl (dpm/kg)*	^{40}K age (my)	^{21}Ne age (my)	$\frac{^{22}\text{Ne}}{^{21}\text{Ne}}$	Type of exposure
Y-691	E4	182+9				2	1.11	single-stage
Y-7301	H4	101+6	29+2	18+2	8+1	13	1.12	multi-stage
Y-74028	L	60+4			5.4+1			} (shower)
Y-74116	L	63+3			7.6+1	7**	1.10**	
Y-74094	H6	31**				0.9**	1.10**	multi-stage
Y-74115	H4	255+15				4**	1.13**	} (shower ?)
Y-74193	H4	205+9			4+1	3**	1.25**	
Y-74375	H4	208+10			2+1			single-stage
Y-75028	H3	237+10				2**		single-stage
A-768	H6	22+3	11+1	9+1	1+<1	2	1.08	multi-stage
A-77015	L3	162+8				2.3**		} (shower)
A-77167	L3	137+7				1.6**		
A-77214	L3	152+8	56+6	17+1	2+1			single-stage
A-77260	L3	130+8	37+2			1.3**		} (shower)
A-77272	L6	215+11	35+4	7+1	5+1			

* dpm/kg Fe. ** preliminary data.

(Footnote) Exposure ages are not corrected for the shielding effect. Source of the data: Evans(1978, 1980), Nagao and Takaoka(1979), Nishiizumi et al. (1978, 1979, 1980, 1981), Nitoh et al.(1980), Shima et al.(1973), and Takaoka and Nagao(1978, 1981).

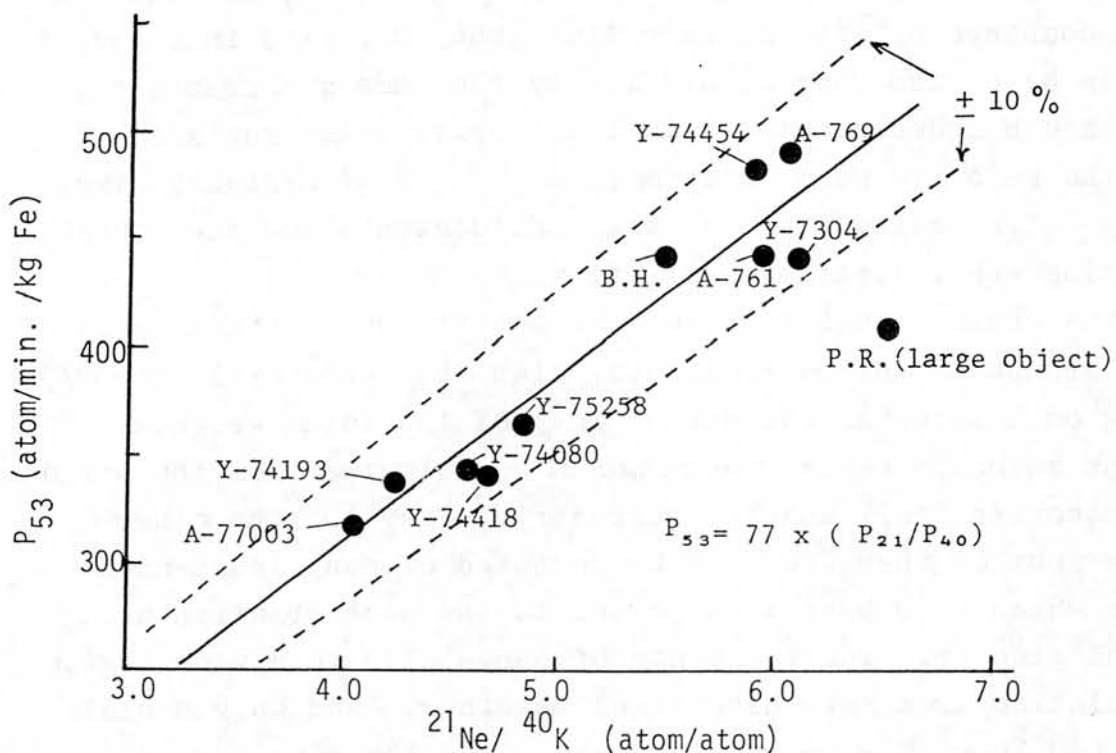


Fig. 1.

TERRESTRIAL HISTORY OF ANTARCTIC METEORITES
RECORDED IN THE COSMOGENIC NUCLIDES

Masatake HONDA, Inst. for Solid State Physics, Univ. of Tokyo

By some mechanisms which have not been well explored yet, Antarctic meteorites have naturally been concentrated in bare ice areas of Antarctica, and the quantities as well as the number of species of the fragments of the stone meteorites are impressively large. Based on the studies of cosmogenic nuclides in these samples, we may extend our discussions to the following problems:

(1) The terrestrial ages are distributed thus far between 10^4 and $7 \cdot 10^5$ y, or $2 \cdot 10^5$ y on the average. The age seems to correspond to the mean life of the meteorites in Antarctica.

(2) Their occurrences are indicating already the following that each group of 10 to more than 100 small fragments which were recovered in a small narrow area could be attributed to the same fall. In general, a pairing among the fragments could be confirmed by the classification, the terrestrial age, the exposure age and such things as the contents of radiogenic and trapped components, etc. At the same time many unpaired independent fragments have also been identified by the same measurements.

(3) Although independent small meteorite falls may also be found, the majority seem composed of ordinary size, 10 - 10^4 kg. stone meteorites, as the ^{53}Mn contents and the $^{22}\text{Ne}/^{21}\text{Ne}$ ratios are indicating statistically.

On the whole, local falls of the meteorites on the ablation area, or groups of paired fragments, might be responsible for $\sim 2/3$ (depending on a material balance of ice) of the total weights. The amount seems to be in the range of estimates from the world annual meteorite fall and the terrestrial age. On the other hand, the rest of them seem to be composed of many independent fragments which have been transported to the same ablation area by a local glacier. The fragments of many falls in a wide region of accumulation area have been mixed together. And only a small fraction (10^{-2}) of them have been exposed on the blue ice as their representatives.

Name	dpm/kgFe		Expos.age my		Name	Class	dpm/kg		Expos.age my	
	53Mn	40K	40K	21Ne			53Mn	26Al	40K	21Ne
Y692	diag.	429		31 ^s	Y74155	H4	255			4.4
Y74011	"	525			156	H		35*		
13	"	401		32	(193	H4-5	205		4.2	2.5
37	"	422			(375	H4	208		2.4	
97	"	421		35	Y74190	L6	436			22 ^k
125	"	449			75097	L4	424			21
136	"	449			102	L6	452			22
648	"	444			108	L4	407			22
Y74459	H6	453		28	271	L6	424			19
462	H6-5	386	31		A761	L6	443		34	33 ^w
471	H6	476	29		3	"	431			34
491	H4	406			A77015	L3	162			2.2
492	H3		31		164	"		44		
497	H5-4	428	28		167	"	137			1.6
Mt.Bldr a	H4-5	394		4.9	214	"	152	56	2	
b	H6-5	355		4.3 ^w	249	"		37		
Y74116	L	63	7.5	7.3	260	"	150	37		1.2
028	L5-6	60	5.4							

53Mn: dpm/kgFe+1/3Ni, ±5% (Nishiizumi et al., 1979-1981)

26Al: (Evans et al., 1979, 1980); *(Komura, 1979)

40K: (Nito et al., 1980, 1981)

21Ne: ±10% (Takaoka, Nagao, 1979-1981), w:(Weber et al., 1980)

s:(Shima et al., 1973)

k:(Kamaguchi, 1978)

29 | 2

30

U-Pb and Lu-Hf Systematics of Antarctic Meteorites.

D.M. Unruh, P.J. Patchett, and M. Tatsumoto
U.S. Geological Survey, MS 963, Box 25046, Denver, Colorado U.S.A.

U-Pb systematics of AH 77278 (L or LL3) and Lu-Hf systematics of AH 77302 (eucrite) will be discussed. AH 77278 contains 1 ppm pb, whereas Mezö-Madaras (L3) contains 5 ppm Pb and Bishunpur (L or LL3) 0.37 ppm, although all three meteorites contain about 11 ppb U. The high Pb content of AH 77278 relative to Bishunpur is consistent with enrichments of other volatile elements observed in this meteorite (Biswas et al., 1979). However, the Pb content is well within the range of reported values for type 3 ordinary chondrites; thus the data are consistent with McSween and Wilkening's (1980) observation that AH 77278 is not one of the most unequilibrated ordinary chondrites yet found.

The U-Pb relationships and young model $^{207}\text{Pb}/^{206}\text{Pb}$ age of ~4480 m.y. for this meteorite suggest a complex terrestrial history, involving about 50 ppb terrestrial Pb contamination and perhaps Pb and/or U loss due to leaching. It is not known if Pb contamination occurred in the field, or was induced during sawing for allocation. Troilite, hand-separated from AH 77278, contains 28 ppb, and 0.14 ppb U and $^{206}\text{Pb}/^{204}\text{Pb}$ of 12.41, which is more radiogenic than that (9.94) of the whole rock; therefore troilite Pb could not be used to evaluate the initial Pb composition. Instead the troilite date have been used to approximate the isotopic composition of the terrestrial Pb contaminant. The terrestrial-Pb corrected concordant $^{207}\text{Pb}/^{206}\text{Pb}$ age is 4512 m.y., which is still quite young compared to the ~4550 m.y. ages commonly found in minimally contaminated chondrites.

The Lu-Hf data of AH 77302 also deviate from the 4.55 b.y. trend of eucrites indicating the possibility of preferential leaching of elements or isotopes under antarctic conditions.

References:

- Biswas, S., Ngo, H. T., and Lipschutz, M. E. (1979), *Meteoritics* 14, 350.
McSween, H. Y., Jr., and Wilkening, L. L. (1980), *Meteoritics* 15, 193-199.

Rb-Sr and Sm-Nd systematics of the Antarctic chondrites (ALHA-74640, Y-76009) and achondrite (ALHA-77302)

Noboru NAKAMURA*, Akihiro ITO*, Akimasa MASUDA* and Mitsunobu TATSUMOTO*

*Department of Earth Sciences, Faculty of Science, Kobe University; **U.S. Geological Survey, Denver

In a recent study (1), we have determined a 4.0 b.y. impact metamorphism age of the Modoc chondrite (L6) by the Sm-Nd method. The Sm-Nd results for Modoc suggest that the Sm-Nd method can potentially determine the precise time of relatively late heavy impact event as well as early thermal metamorphism in the chondritic parent body.

In the present work, we have examined Sm-Nd systematics of additional two L-6 chondrites (Yamato 76009 and Bruderheim). Rb-Sr analyses for ALHA-74640 and -77302 meteorites are also in progress at Kobe University (Sm-Nd analyses were carried out using facilities of U.S.G.S., Denver).

Mineral separates from two L-6 chondrites show rather small variation in $^{143}\text{Nd}/^{144}\text{Nd}$. Except for phosphate fraction of Bruderheim, five data points (combined for mineral data of two chondrites) define linear array on $^{147}\text{Sm}/^{144}\text{Nd}$ vs. $^{143}\text{Nd}/^{144}\text{Nd}$ plot within rather narrow range (see Fig. 1). The slope of the regression line corresponds to an age of 4.58 ± 0.22 (2 σ) b.y. The age may be interpreted as the time of early thermal metamorphism in the parent body as typically found for most equilibrated chondrites, although the age value can not be resolvable from formation age of meteorite. Deviation of Bruderheim phosphate from the regression line suggests that Sm-Nd system of the meteorite was partially disturbed by later impact(s).

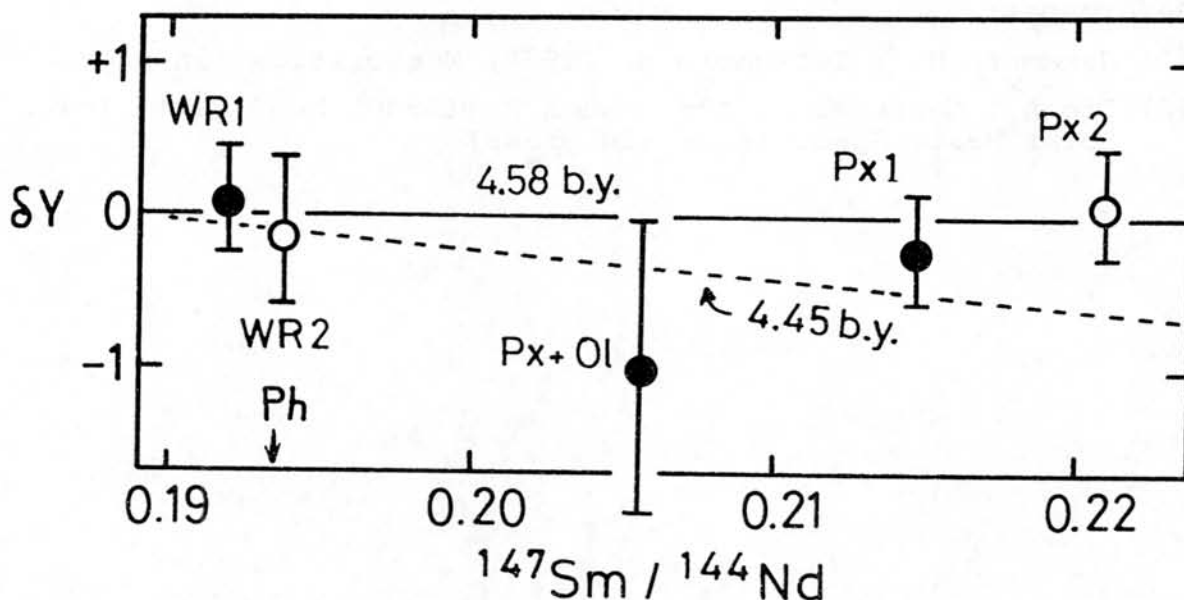


Fig. 1. Sm-Nd evolution diagram for Y-76009 (●) and Bruderheim (○) chondrites. δY represents fractional deviations in parts in 10^4 of $^{143}\text{Nd}/^{144}\text{Nd}$ ratio from the 4.58 b.y. evolution. (Ph=Phosphate; WR=Whole rock; Px=Pyroxene; Px+Ol=Mixture of pyroxene and olivine)

#31 - 2

Table 1. Sr isotopic composition of standards and meteorites*

Standard	$^{87}\text{Sr}/^{86}\text{Sr}^{**}$	Meteorite	$^{87}\text{Sr}/^{86}\text{Sr}^{**}$
NBS 987 Sr (0.5 micro-grams)	0.71002 ± 6	Y-74640 (H6)	0.75112 ± 13
	0.71000 ± 7	ALHA 77302 (eucrite)	0.69885 ± 7
	0.71000 ± 10	Allegan (H5)	0.73235 ± 5
E & A (0.8 micro-grams)	0.70796 ± 5		

* Sr isotopic composition measured using Faraday cage and Cary 401 MR electrometer at Kobe University.

** Errors are 2σ (mean) and correspond to last digits.

The mass spectrometric system for Sr isotopic measurement at Kobe University has been recently modified to an on-line desk-top computer controlling system using a new electrometer (Cary 401 MR) and YHP 9835. Preliminary results of Sr isotopic measurement for standards and meteorites (see Table 1) suggest that present precision of $^{87}\text{Sr}/^{86}\text{Sr}$ ratio is 0.007-0.01% which is several times better than our previous values (2), and that $^{87}\text{Sr}/^{86}\text{Sr}$ ratio for NBS 987 Sr standard obtained at 300 mv scale appears to be slightly (2 parts per ten thousands) lower than the recommended value of 0.71014.

References:

- (1) Nakamura N. & Tatsumoto M. (1980) Meteoritics (in press)
- (2) Ito A., Nakamura N. and Masuda A. (1980) Mem. Natl. Inst. Polar Res., Spec. Issue (in press)

^{40}Ar - ^{39}Ar AGES OF ANTARCTIC METEORITES
 Ichiro KANEOKA and Minoru OZIMA
 Geophysical Institute, University of Tokyo

^{40}Ar - ^{39}Ar method has been applied on six meteorites found in Antarctica in order to investigate their chronological aspects. They include Y-74191(L3), Y-75258(LL6), Y-74450 (Eucrite), Y-7308(Howardite), Y-74037(Diogenite) and Allan Hills-765(Eucrite). Each sample was wrapped in Al-foil and stacked in a quartz ampoule paired with two standard samples (MMhb-1, hornblende, K-Ar age: 519.5Ma). Samples were irradiated in the JMTR reactor of the Tohoku University and received a total fast neutron fluence of about 10^{19} nvt/cm². Ar was extracted and purified following a conventional procedure. Ar isotopes were measured on a Reynolds type mass spectrometer with a Farady cup. All necessary corrections including blanks were done to calculate an age.

The sample Y-74191 shows a disturbed age spectrum indicating lower ages in the lower and higher temperature fractions. Although this meteorite contains relatively large amount of trapped components, both the age spectrum and the total ^{40}Ar - ^{39}Ar age suggest radiogenic Ar loss from this meteorite.

On the other hand, the sample Y-75258 shows a plateau-like age spectrum of about 4.5 b.y. At the highest temperature (1600°C), an apparent age exceeds 4.6 b.y., but it probably reflects an artifact caused by neutron irradiation effect and/or insufficient correction procedures.

The sample Y-74450 also shows a plateau-like age spectrum, but the age seems to be rather young of about 3.8 b.y. Hence, the age should reflect some secondary disturbance(s) on the parent body for this meteorite. Such a relatively young age is often found for achondrite(s), which suggests that the parent body(ies) of achondrites might have located at different circumstances than that of ordinary chondrites.

The sample Y-7308 indicates an inversed age spectrum having very high ^{40}Ar - ^{39}Ar ages of more than 4.6 b.y. in the lower temperature fractions and low ^{40}Ar - ^{39}Ar ages of less than 4.0 b.y. at higher temperatures. Such a spectrum may be interpreted as a redistribution of Ar isotopes in the sample caused by neutron irradiation effect.

The sample Allan Hills-765 seems to show a plateau-like age spectrum in the higher temperature fractions. However, the apparent age is rather young of less than 3.8 b.y. This may also suggest a rather later event on the parent body of achondrites.

Although the ^{40}Ar - ^{39}Ar age of the sample Y-74037 was tried to calculate, any reliable value could not be obtained, since it contains little amount of radiogenic ^{40}Ar .

Present results suggest that meteorites found in Antarctica have very different histories one another.

#33 - 1

RARE GAS STUDIES OF THE ANTARCTIC METEORITES

Nagao, K.¹⁾, Saito, K.²⁾, Ohba, Y.²⁾ and Takaoka, N.²⁾

1) Okayama University of Science, 2) Yamagata University

Twenty four antarctic meteorites were mass spectrometrically analyzed for rare gas isotopic and elemental compositions. Preliminary results on rare gas compositions, cosmic-ray exposure ages (T_3 , T_{21}), and gas retention ages (T_4 , T_{40}) were listed in Table 1. Though Kr and Xe concentrations were determined, they were not presented in Table 1.

Cosmic-ray exposure ages were calculated with the production rates of $P_3=2.48 \times 10^{-8}$ (H-, L-ch.), $P_{21}=0.466 \times 10^{-8}$ (L-ch.), and $P_{21}=0.433 \times 10^{-8}$ (H-ch.) ccSTP/g/my.¹⁾ However, for some samples with high cosmogenic $^{22}\text{Ne}/^{21}\text{Ne}$ ratios, a depth dependence of production rate, P_{21} , was corrected with the empirically determined correlation between cosmogenic $^{22}\text{Ne}/^{21}\text{Ne}$ and $^3\text{He}/^{21}\text{Ne}$ ratios.²⁾ Cosmic-ray exposure ages determined in this work show the general behavior characteristic for H- and L-chondrites. A very long exposure age of about 95my (T_{21}) was obtained for Y74035(L6) chondrite. The age is the longest among the ages for chondrites analyzed to date. (One achondrite is known to have a long exposure age of about 110my.³⁾) Y74094, AHL77015, AHL77167 and AHL77260 showed the short exposure ages of 1~2my.

U/Th-He and K-Ar ages showed characteristic features for H- and L-chondrites. K-Ar ages for H-chondrites distribute between 3 and 4.5 by. Whereas, the ages for L-chondrites show two clusters. K concentrations were measured for nine samples by a method of flame photometry. For other samples, U and K concentrations were assumed to be similar to the averaged values for H- and L-chondrites.

Y75028(H3) chondrite is a gas-rich meteorite. Appreciable amounts of solar type He and Ne were detected. Rare gas concentrations are similar to those for the gas-rich meteorites composed of dark-light structure.

Rare gas compositions indicate that some meteorites can be grouped as follows: 1) Y74155 and Y74193, 2) Y74364, Y74371 and Y74418, 3) Y74605, Y75097, Y75102, Y75108 and Y75271, and 4) AHL77015, AHL77167 and AHL77260. These were presumably disrupted from the parent meteorites at the entry into earth's atmosphere or on the earth. This grouping is concordant with that proposed by Honda (personal communication) based on the concentrations of cosmogenic radioactivities. Y74605 in group 3 was found at the area 15km north-east of the area where other samples in group 3 were found. If the meteorites in group 3 were come from a shower, the meteorite shower might be in a direction from north-east to south-west or in an opposite direction.

References

- 1) Herzog and Anders, G.C.A. 35 (1971) 605. 2) Nishiizumi et al., E.P.S.L. 50 (1980) 156. 3) Kirsten et al., G.C.A. 27 (1963) 13.

Table 1.
Rare gas compositions, cosmic-ray exposure ages and gas retention ages. (Preliminary)

Meteorite	$^4\text{He}^*$	$\frac{^3\text{He}}{^4\text{He}}$	$^{21}\text{Ne}^*$	$\frac{^{22}\text{Ne}}{^{21}\text{Ne}}$	$\frac{^{20}\text{Ne}}{^{22}\text{Ne}}$	$\frac{^{36}\text{Ar}^*}{^{36}\text{Ar}}$	$\frac{^{38}\text{Ar}}{^{36}\text{Ar}}$	$\frac{^{40}\text{Ar}}{^{36}\text{Ar}}$	# T ₃	# T ₂₁	\$ T ₄	\$ T ₄₀	K (ppm)
Y74094 (H6)	2600	0.00068	0.37	1.20	1.00	0.79	0.24	8800	0.7	1.2	3.0	4.6	
Y74115 (H6)	2000	0.012	3.4	1.16	0.91	0.78	0.67	6700	10	9.5	4.3	4.3	
Y74155 (H4)	1800	0.0059	1.9	1.13	0.87	1.6	0.31	2800	4	4.8	4.2	3.6	1020
Y74193 (H4)	1700	0.0062	1.1	1.25	0.84	0.8	0.46	7800	4	4.0	4.0	4.0	1100
Y74364 (H5)	1580	0.0095	2.1	1.25	0.86	2.5	0.32	2000	6	7.7	3.8	3.8	1050
Y74371 (H5)	1400	0.013	2.8	1.13	0.87	1.5	0.60	4500	7	7.0	3.5	4.2	1030
Y74418 (H6)	1280	0.014	2.3	1.18	0.85	0.7	0.60	8400	7	6.8	3.3	4.2	920
Y74459 (H6)	1200	0.051	12	1.06	0.87	1.7	1.12	2700	24	28	2.7	4.0	
Y75028 (H3)	29000	0.00049	1.7	15.2	11.5	38	0.19	65		2			
Y74035 (L6)	2930	0.063	40	1.12	0.83	3.6	1.14	1800	80	95	3.9	4.6	
Y74077 (L)	2800	0.074	42	1.14	0.84	6.8	0.65	1400					
Y74080 (L6)	1700	0.048	17	1.10	0.86	1.7	1.1	4000	33	36	3.0	4.5	
Y74080 (L6)	1340	0.097	16	1.19	0.84	1.4	1.2	3890					
Y74116 (L5)	937	0.11	16	1.21	0.81	1.7	1.2	3070	48	49	1.5	4.0	
Y74362 (L6)	1200	0.12	18	1.19	0.83	1.6	1.24	2900					
Y74454 (L5)	720	0.013	3.4	1.10	0.95	1.0	0.36	2400	3.5	7	1.8	2.9	
Y74605 (L)	690	0.036	6.6	1.12	0.85	1.4	0.67	4400	10	15	1.5	3.9	1180
Y75097 (L4)	1490	0.012	3.2	1.07	0.88	(1.7)		7800	7	7	3.2	(4.7)	1070
Y75102 (L6)	400	0.10	11	1.09	0.87	1.3	0.78	350	20	23	0.46	1.0	
Y75108 (L4)	362	0.12	9.9	1.07	0.84	1.8	0.66	124	18	21	0.41	0.47	1080
Y75271 (L4)	289	0.16	10	1.08	0.85	2.1	0.92	128	18	22	0.17	0.7	
AHL77003 (H3)	429	0.10	10	1.08	0.87	2.8	0.43	85	17	22	0.61	0.45	1200
AHL77015 (L3)	360	0.12	9.1	1.09	0.86	2.2	0.55	100	17	19	0.42	0.6	
AHL77167 (L3)	2100	0.016	4.4	(1.20)	147			18	11	10	4.4	3.0	
AHL77260 (L3)	1550	0.0034	1.1	(2.4)	95			34	1.6	2.3	3.4	3.7	
	1100	0.0034	0.77	(2.7)	105			33	1.3	1.6	2.6	3.5	
	760	0.0039	0.6	(2.4)	98			33	1	1	1.9	3.3	

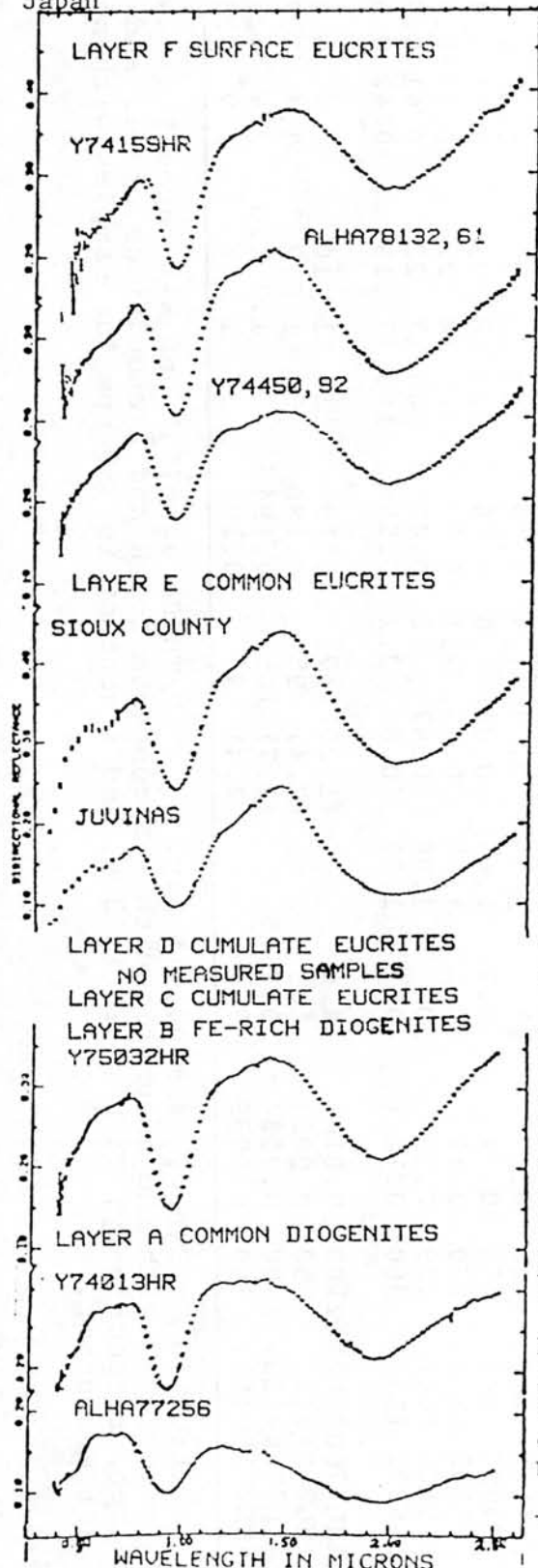
Unit: * 10^{-8} ccSTP/g, # m.y., \$ b.y. U/Th-He ages (T_4) and K-Ar ages (T_{40}) were calculated with the assumptions that U contents for H and L chondrites are 12 and 15 ppb, respectively, Th/U ratio is 3.6, and K content is 850 ppm for samples with no data of K content.

#34 - 1

THE LAYERED CRUST MODEL AND THE SURFACE OF VESTA

McFadden, L.A., Gaffey, M.J., Hawaii Institute of Geophysics, University of Hawaii, Honolulu, Hawaii 96822

Takeda, H., Mineralogical Institute, University of Tokyo, Hongo, Tokyo 113, Japan



We have measured the reflectance spectra of some meteorites which are representative of the proposed layered crust model of the howardite parent body (Takeda et al., 1979; Takeda, 1979). From these data the spectral variations which correlate with the mineralogical differences in the layers can be defined. The reflectance spectrum of the asteroid 4 Vesta can then be examined to determine which layer predominates on the surface, and which, if any other layers, are exposed.

Experimental Techniques. The meteorite samples vary in weight and grain size distribution from 0.2-10g and from fine powder <math><50\mu\text{m}</math>, to one whole rock sample, which does not affect the present discussion. Each meteorite was measured on the laboratory spectrometer described in Singer (1981) and McFadden et al. (1980). The angle of incident light was

Results. The reflectance spectra of the meteorite specimens representing the howardite parent body layers all contain the 0.9 and

Discussion. The diogenite layer A and B can be distinguished from the eucrite layers C-F by the difference in the 0.9 and

Fig. 1 - Layered crust model reflectance spectra

to distinguish between eucrites, diogenites, or howardites (Gaffey, 1976).

The quantitative analysis of band position, depth, and width will permit discrimination between each discrete layer. In order to detect the presence of two different pyroxene compositions, (which is necessary to distinguish between layers E and F, for example) we need to resolve a total of four pyroxene bands. The capability for our gaussian curve fitting techniques has not yet been thoroughly tested in this regard. The high precision spectra presented here and the available well characterized pyroxene mineralogy will provide an excellent standard for developing these techniques.

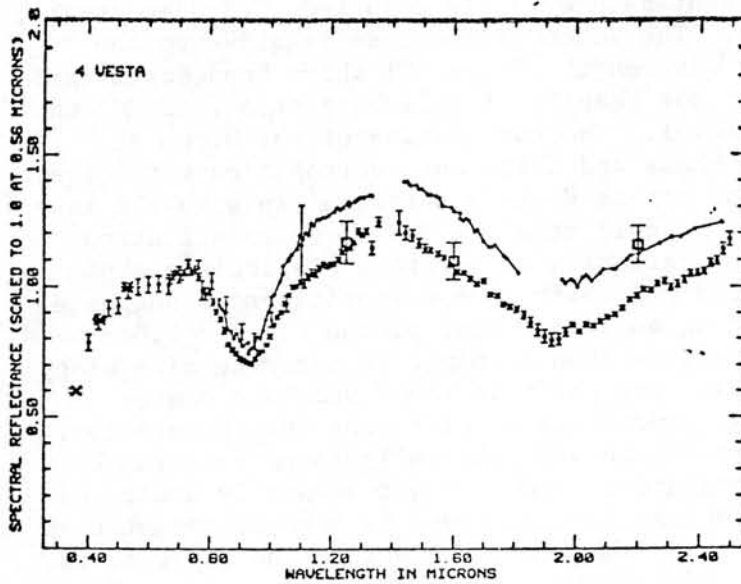
Application of the Layered Model to Vesta - Results. Recent telescopic measurements of the reflectance spectrum of Vesta were made with the same In-Sb system used in the lab. Internal errors are 0.5%, the dominating errors of a few percent represented by the error bars in Figure 2 are systematic in the solar calibration.

Absorption features due to pyroxene at 0.92 and 1.94 μ m and in the 1.25 μ m region due to plagioclase are present as previously reported (McFadden et al., 1979, and Feierberg et al., 1980). The Vesta reflectance relative to the average as a function of time and wavelength (Figure 3) shows band depth variations of up to 7 \pm 2% contradicting the results of Feierberg et al. (1980) who reported no variations at the 2% level. The correlation of the 0.9 μ m and 1.25 μ m band depth with rotational phase and their anti-correlation with albedo indicates a particle size variation across Vesta's surface. This result is consistent with the conclusions of Degewij et al. (1979) from polarization measurements. The possibility of a variation in pyroxene/plagioclase abundance greater than 10% is eliminated. A shift in band positions is suggested by looking at the relative absorption on either side of the 0.9 and 2.0 μ m band minima. If the bands do change position then a change in pyroxene mineralogy on a hemispheric scale is indicated. The shift in the 0.9 μ m band can be verified with higher precision measurements using different instrumentation.

Discussion. There are differences between the reflectance spectrum of Vesta and those of eucrites and howardites which are not presently understood in mineralogical terms. The plagioclase band in Vesta is more prominent than in eucrites and the band position is at shorter wavelength. The shape of the UV absorption below 0.7 μ m is most characteristic of howardites, not eucrites. We would expect the reflectance spectrum of cumulate eucrites with a higher plagioclase to pyroxene ratio to have a more prominent 1.25 μ m plagioclase band. Measuring such a eucrite and quantifying the absorption band parameters of the Vesta spectrum should provide further explanation. We can constrain the size of a significant diogenite provenance at the surface by assuming that the spectral contribution of a pyroxene component is proportional to the surface area of that component. An increasing diogenitic component would result in a band shifted to shorter wavelengths and a smaller bandwidth. Initially the plagioclase band would become more prominent. At 80% diogenite the plagioclase band would be very shallow (Gaffey and McCord, 1977). Less than a 30% component is not detectable. Since we see no abundance variation larger than 10% and the plagioclase band is strong, an upper limit on a diogenite provenance is approximately 40%. This would be a global characteristic which we cannot presently distinguish from a global cumulate eucrite surface. Further work is needed, but it is easier to have a global cumulate eucrite layer than to expose large areas of deep crust homogeneously across the surface of Vesta. Indeed this cumulate surface would support the hypothesis that impact debris is not retained on the surface of Vesta and over the age of the solar system tens of kilometers have eroded away from the surface of Vesta, according to the layered crust model.

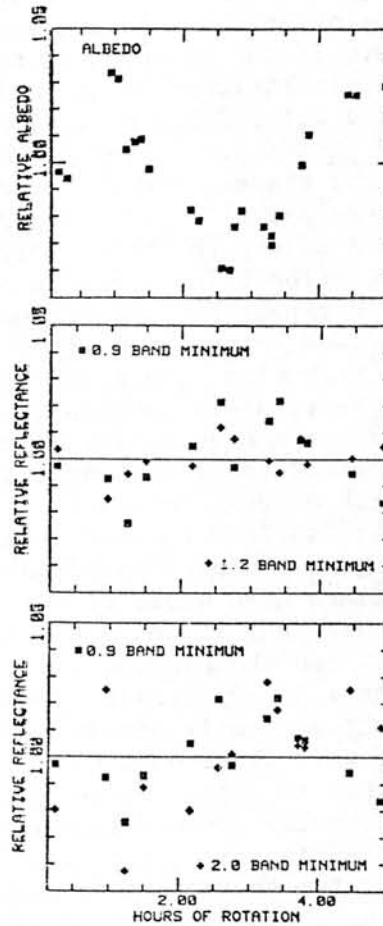
34 - 3

Degewij, J., et al. (1979) Icarus 40, 364-374.
 Feierberg, M.A., et al. (1980) Geochim. Cosmichim. Acta. 44, 513-524.
 Gaffey, M.J. (1976) J. Geophys. Res. 81, 905-920.
 Gaffey, M.J. and McCord, T.B. (1977) Comets, Asteroids, Meteorites, A.H. Delsemme, 199-218.
 McCord, T.B., et al. (1970) Science 168, 1445-1447.
 McFadden, L.A., McCord, T.B. (1978) BAAS 10, 601.
 McFadden, L.A., et al. (1980) 13th Lunar and Planetary Symposium, Tokyo, Japan, 273-280.
 Singer, R.B. (1981) J. Geophys. Res., in press.
 Takeda, H. (1979) Icarus 40, 445-470.
 Takeda, H., et al. (1978) Proc. Lunar Planet. Sci. Conf. 9th, 1157-1171.
 Takeda, H., et al. (1979) Mem. Nat. Inst. Polar Res. Spec. Issue 13, 82-108.
 Veeder, G.J. (1978) Astron. J. 83, 651-663.



†Fig. 2 - Reflectance spectrum of Vesta 0.3-2.5 μ m. Solid line from Feierberg et al., 1980, squares JHK data from Veeder et al., 1978, X's UBV, Triad file, unconnected points from McCord et al., 1970 (0.3-0.8 μ m), and new data presented here (0.8-2.5 μ m).

→Fig. 3 - Anti-correlation of albedo with relative band depth. Vertical scale is 0.95-1.05.



PREFERRED ORIENTATION OF PHYLLOSILICATE IN Yamato-74642 AND 74662 (C2)

Fujimura, A., Kato, M. and Kumazawa, M.

Dept. Earth Sciences, Nagoya Univ., Nagoya

Preferred orientation of the constituent mineral grains is one of the unique orientation-dependent textures to characterize a polycrystalline rocks, since it provides an information on the physical conditions under which the component materials were coagulated and the resulted aggregate has evolved at the later stages. In the previous textural study of Murchison (C2) meteorite (Fujimura et al., 1980), we have examined the preferential orientation distribution of $\langle 001 \rangle$ of phyllosilicates in the matrix. The result indicated that $\langle 001 \rangle$ axis of phyllosilicate (presumably (002) of serpentine) showed very weak preferred orientation of uniaxial type. Such a texture is well interpreted as caused by sedimentation under weak gravity field and/or the slight uniaxial compaction due to burial following the sedimentation. The present work is an extension of the previous one to Yamato 74642 and 74662 (both C2), in order to see whether such type of preferred orientation of phyllosilicates is common characteristics of carbonaceous chondrite or not. The size of the samples provided by Antarctic meteorite laboratory, NIPR, are so small that the final determination of the preferred orientation is not successfully made yet. This paper is an interim report on the subject.

Yamato 74642

A thin section sample (ca. 100 μm thick, 3.5x3.5 mm^2) is worked out from a supplied chondritic chip. An ordinary 2θ scanning of the X-ray diffraction does not show any significant peak, which could be attributed to the possible phyllosilicates in the chondrite. This feature makes a significant contrast to that for Murchison meteorite, for which a large diffraction peak at 7.2 Å ((002) of serpentine) appears. Numbers of trials have been made to increase the diffraction intensity and signal to noise ratio (fixed time scanning, angular oscillation, increase of X-ray power, choice of divergent and limiting slits, choice of wave length of X-ray, etc.). By adopting the very appropriate measuring conditions, the presence of very small diffraction peak was recognized at $d \approx 7.4$ Å, which may be identified with (002) of serpentine group minerals as in the case of Murchison. The intensity data of X-ray diffraction of 7.4 Å are collected by means of a pole figure goniometer in the geometrically possible range of solid angle for transmission method. The preliminary

#35 - 2

result of the data analysis (absorption correction and the removal of background) showed that the intensity of 7.4 Å diffraction was certainly orientation-dependent, indicating the presence of preferred orientation of phyllosilicate in the matrix of this chondrite.

Yamato 74662

Although the diffraction peak at $\sim 7 \text{ \AA}$ is recognized better in this sample than in Yamato 74642, the size of supplied chondritic chip is much smaller, and the reliable determination of preferred orientation is facing with a considerable difficulty.

Reference

Fujimura, A., Kato, M. and Kumazawa, M.: Preferred orientation and its formation conditions of phyllosilicate in Murchison meteorite (C2) (in Japanese). The fifth symposium on Antarctic Meteorites (programme and abstracts), NIPR, Tokyo, 1980

ORGANIC MATTER IN CARBONACEOUS CHONDRITES FROM THE ANTARCTIC
Cyril Ponnampерuma and R. K. Kotra
University of Maryland, College Park, Maryland 20742

In the study of chemical evolution we are interested in the organic molecules which may have been formed before the appearance of life on earth. The only source of prebiotic organic matter available for analysis are the carbonaceous chondrites. The Murchison meteorite provided the first unambiguous evidence for extraterrestrial organic molecules. This finding has been extended to two other meteorites, the Murray and the Mighei.

The recent discoveries in the Antarctic by the Japanese Polar Expeditions have opened up a new era of study for carbonaceous chondrites. The number of samples available for analysis has almost doubled. Besides, the meteorites have been found in pristine conditions clean of terrestrial contamination.

We have examined three of these samples, the Yamato, 74662, the Allan Hills, 77306 and Allan Hills 77307. The discovery of a whole range of organic molecules has given us new insights into the cosmic nature of chemical evolution.

THE STRUCTURES OF OLIVINES IN YAMATO-74 METEORITES

Yamaji, M. and Matsumoto, T.

Department of Earth Sciences, Faculty of Science,
Kanazawa University, 1-1 Marunouchi, Kanazawa, Ishikawa 920

The crystal structures of eight olivines from four YAMATO-74 chondrites (Y-74354, 74371, 74191, 74155) have been studied using X-ray diffraction data and those site occupancies of Iron and Magnesium cations for M1 and M2 sites have been determined by least squares method. The lattice constants, d_{301} values and compositions are tabulated in Table 1. Those compositions (Fo mol %) in it were calculated from d_{301} values using Yoder and Sahama's equation (1957), $\text{Fo (mol \%)} = 4233.91 - 1494.59 \times d_{301}$.

The olivine structure is based on hexagonal close packing of oxygen atoms with Mg^{2+} and Fe^{2+} cations occupying half of the distorted octahedral voids (M1 and M2), and Si atoms occupying one-eighth of the tetrahedral sites. The average M1-O and M2-O distances of those olivines are 2.106-2.113(Å) and 2.135-2.144(Å), respectively.

The terrestrial and lunar olivines show the site preference of Fe^{2+} cations in M1 site. The chondritic olivines analysed in this study show the slight site preference of Fe^{2+} cations in M2 site except one sample, even though they show the disordering tendency.

Table 1. Cell data for olivines†

sample	a(Å)	b	c	d_{301}	Fo(mol %)
74354-41	10.265(2)	6.008(1)	4.771(1)	2.781	Fo ₇₇
* 74354-70	10.268(2)	6.010(1)	4.770(1)	2.781	Fo ₇₇
74354-71	10.266(2)	6.009(2)	4.771(1)	2.781	Fo ₇₇
* 74371-16	10.244(3)	6.002(2)	4.777(5)	2.778	Fo ₈₂
74191-1	10.232(6)	5.993(3)	4.760(2)	2.772	Fo ₉₀
74191-2	10.254(2)	6.003(4)	4.764(3)	2.777	Fo ₈₃
74191-3	10.258(3)	6.005(4)	4.764(2)	2.778	Fo ₈₂
74155-1	10.239(5)	5.998(4)	4.762(1)	2.774	Fo ₈₈

† Cell data determined by X-ray single crystal diffraction method.

* Yamaji, M. & Matsumoto, T., Mem. Natl Inst. Polar Res., Spec. Issue (1980).

The numbers in parentheses represent calculated standard deviations, for 10.265(2) read 10.265±0.002.

[The text in this section is extremely faint and illegible. It appears to be a multi-paragraph document, possibly a report or a letter, but the specific content cannot be discerned.]

39

HISTORIC RECORDS OF METEORITES IN CHINA AND THEIR TIME-SERIES ANALYSIS

Chang Shuyuen (Department of Geology, Peking University)

Yu Zhi-Jun (Peking petroleum college)

China has a rich historic records of astronomy data. The authors had taken part in the work of establishing Table of historic records of astronomic phenomenon in China headed by Peking Astronomical Station. The table included: eclipse of the sun, eclipse of the moon, comet, nova, spot, polar light, meteorites, meteor, stream, queer sound from heaven, tides etc.

The earliest record of meteorites appeared in 2133 B.C. But it was not very accurate & systematic. Since 1479 (the 15th year of Chen Hua Min dynasty) such records increased considerably and systematically, including many local records.

There are many vivid descriptions about the phenomenon, the falling-position, the genesis, and the classifications of the meteorites.

Besides, the observation of the falling-times, the numbers, The size, The shape of meteorites, and its relationships with other natural phenomenon also began.

The distribution of ancient meteorites is uneven. As a result of direct observation, there was a high tide of the falling in the 17th century. Approximately at the same time, there was a pike of volcano, earthquake and storm.

The result of the time-series analysis for 580 items of data shows the falling of meteorites in China has a long cycle of 240 years and a short cycle of 60 years. The calculation was done on computer for two intervals of time, one was from 620 - 1499, altogether 880 years, the other was from 1479 - 1920. The results of the two intervals are in harmony. We analyzed the frequencies of the falling in one year and in ten years, which results in the same conclusion.

The witness meteorite falls in USA also prove the cycle of 60 years.

THE FISSURE OF KIRIN METEROITE

Chang Shuyuen

Department of Geology, Pkein University

Through observations by eyes and microscope, there are many fissures in the Kirin Meteorites. They may be divided into two kinds: filled with dark materials and nonfilled. The former included shear and tansion. The latter are fresh.

Conjugate shear fissure, filled with dark meteorails, are widely spread in Kirin meteorite. The morphological characteristics are similar to that of the shear joints in the terres traial rocks. It is not generated by the force of impact but by the tectonism.

It is very interesting that the same shear fissure is also seen in other meteorites, such as those in pictures of Ramdohr. P published in 1973.

SHAPE OF THE METEORITES

Hasegawa, H.

Dept. of Physics, Fac. of Science, Kyoto Univ. Kyoto 606

Shape of the meteorites was described by the ratio of shorter axial length to the longer axial length for each meteorites. About one thousand Yamato meteorites were used for analysis. The distribution of the axial ratio was similar to that of the high velocity impact fragments of basalt of Fujiwara's experiment¹⁾. In detail, the former was rather broad and the latter has a peak at the axial ratio of 0.7~0.8. For 29 fragments of diogenite, a different tendency was found. They are comparatively rounded, the average value of the ratio being slightly higher.

- 1) A. Fujiwara, G. Kamimoto and A. Tsukamoto, Nature, 227, 602, (1978).

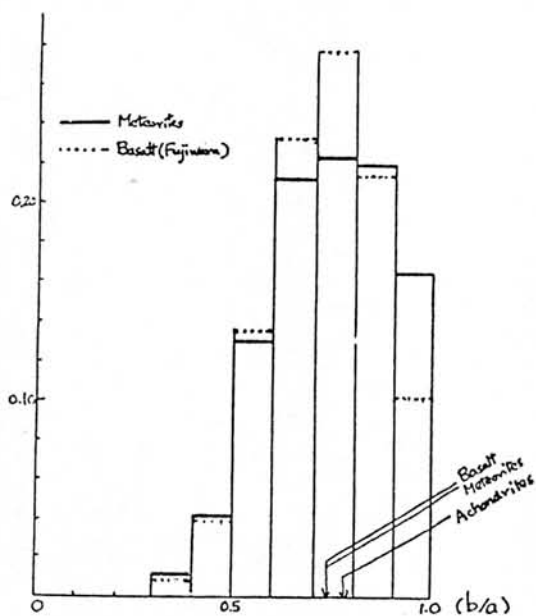


Fig. 1. Distributions of axial ratio (b/a) of Yamato meteorites (ordinary chondrite) and basalt fragments.

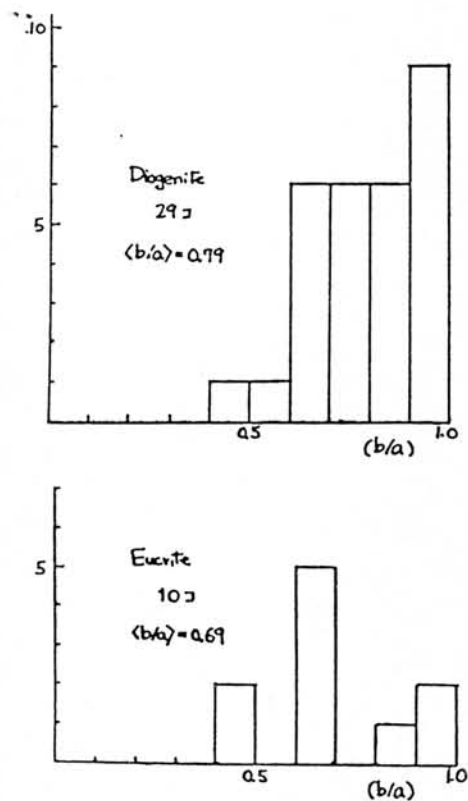


Fig. 2. Distribution of axial ratio of Yamato achondrites.

THE COMPOSITION OF NATURAL REMANENT MAGNETIZATION OF AN
ANTARCTIC CHONDRITE, ALHA-76009 (L6)

MINORU FUNAKI¹⁾, TAKESI NAGATA¹⁾ AND KAN'ICHI MOMOSE

1) Natl Inst. Polar Res. 2) Shinshu University

The natural remanent magnetization (NRM) of individual chondrule of the Allende C₃-chondrite was experimentally studied by Lanoix et al (1978) and Sugiura et al.(1979). Their results have shown that the NRM directions of individual chondrules are widely scattered, suggesting that these chondrules acquired the thermoremanent magnetization (TRM) before their assembling into the chondrite. ALHA-76009 L₆ chondrite comprises a number of fairly large broken pieces, the total weight of which is about 400 kg. Since a considerably large piece of this chondrite is available for studying the composition of NRM in fair detail, NRM characteristic of the bulk chondrite, individual chondrules, matrix parts and metallic grains are separately examined.

From a large piece of ALHA-76009 L₆ chondrite (7 kg in weight), 3 pieces of bulk chondrite, 11 chondrules, 9 pieces of matrix part and 12 grains of metal larger than 1 mm in mean diameter have been picked up, where the orientation of each picked-up specimen relative to the mother chondrite piece is measured. The basic magnetic properties of typical samples of each group, such as saturation magnetization (I_s), saturation IRM (I_R), coercive force (H_c) and remanence coercive force (H_{rc}) at room temperature, together with the original NRM intensity (I_n), are summarized in Table 1.

sample	weight gm	I _n x10 ⁻⁴ emu/gm	I _s emu/gm	I _R emu/gm	H _c Oe	H _{rc} Oe	
Bulk	0.157	22.1	9.73	0.34	92	2700	
chondrule	x-1	0.031	0.86	3.67	0.059	115	2210
	x-2	0.019	0.86	3.50	0.091	95	1770
	y-3	0.017	0.80	1.30	0.016	101	1270
	z-1	0.025	2.75	1.51	0.068	176	2650
	z-2	0.022	0.32	2.44	0.028	48	980
	z-1	0.032	54.2	0.99	0.012	45	940
matrix	C-1	0.018	6.7	5.68	0.27	132	1810
	C-2	0.020	35.0	9.73	0.80	114	2610
	C-3	0.015	75.5	12.75	0.35	45	1140
metal grain	B-1	0.0042	24.8	157	0.38	7.0	63
	B-2	0.0022	26.9	171	0.28	5.0	63
	B-3	0.0083	71.6	127	0.53	13.5	147
	B-4	0.014	15.6	81	0.18	0.6	135
	B-5	0.022	14.2	150	0.28	6.0	97

Table 1. Basic magnetic properties of the bulk chondrite, chondrules, matrix and metallic grains of ALHA-76009 L₆ chondrite.

#42 - 2

(a) NRM of bulk chondrite. The AF-demagnetization characteristics of NRM of all 3 bulk specimens show that their NRM is unstable with respect to both intensity and direction, though their TRM acquired by cooling from 750 °C in a magnetic field of 0.5 Oe is fairly stable against the AF-demagnetization.

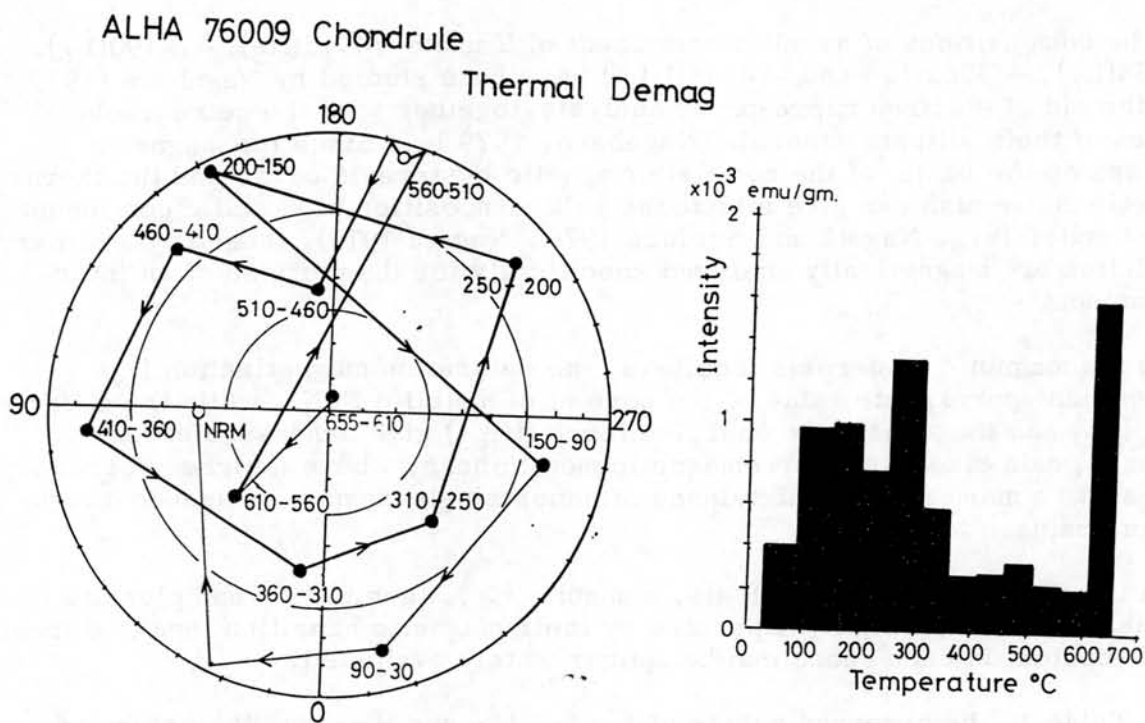
(b) NRM of chondrules. The directions of the original NRM and NRM after AF-demagnetizing up to 140 Oe peak of individual chondrules are widely scattered over almost the whole spherical coordinate surface, but their NRM is fairly stable against the AF-demagnetization. The thermal demagnetization of their NRM has suggested a tendency that the partial TRM acquired during cooling through a temperature range, $\Delta T = T_i - T_{i-1}$, is steadily rotated with a decrease in temperature T_i , as shown in Fig.1 for example. These results may suggest that NRM of individual chondrules was acquired as TRM while they were making precessional motions in the presence of a magnetic field before their assembling into the mother chondrite.

(c) NRM of matrix. The NRM directions of 9 matrix parts origin of their NRM, but are clustered within a limited range as indicated by $\alpha_{95} = 27^\circ$. Their NRM is stable against the AF-demagnetization up to at best 160 Oe peak. These results may suggest that the matrix NRM is due to a certain mechanism for a loosely defined magnetic orientation such as the depositional remanent magnetization (DRM).

(d) NRM of metallic grains. The NRM directions of 12 metallic grains larger 1 mm in mean diameter are at random within the chondrite and their NRM is extremely unstable against the AF-demagnetization with respect to both intensity and direction, as expected from their very small values of H_c . The apparently unstable bulk NRM of ALHA-76009 chondrite may be mostly due to the unstable NRM of these metallic grains of large size.

This work may be the first study of the composition of NRM of an ordinary chondrite which consists of chondrules, matrix and considerably large metallic grains. As critically reviewed by Nagata (1979 a), the Allende C₃ chondrite appears to possess a reasonably stable NRM as the whole, whereas the bulk NRM of ALHA-76009 L6 chondrite is extremely unstable (Nagata 1979 b). In both chondrites, however individual chondrules possess a stable NRM, the direction of which is widely scattered within the mother chondrites, Summarizing the results of the present study, it seems likely that chondrules in chondrites were formed and magnetized before assembling into the chondrites, and the

matrix NRM of chondrites would be either DRM acquired in the process of matrix accretion or TRM acquired in a later process of metamorphism in the presence of a certain magnetic field in both possible cases



MAGNETIC ANALYSES OF METALLIC PHASES OF YAMATO-74115
(H₅), -74190(L₆), -74354(L₆), -74362(L₆) and -74646(LL₆)

T. Nagata and M. Funaki

National Institute of Polar Research

The compositions of metallic component of Yamato-74115(H₅), -74190(L₆), -74354(L₆), -74362(L₆) and -74646(LL₆) have been studied by Nagahara (1979 a) with the aid of electron micro-probe analysis, together with the petrographical studies of their silicate minerals (Nagahara, 1979 b). Since the magnetic analyses on the basis of the complete magnetic hysteresis curve and the thermo-magnetic curve also can give rise to the bulk composition of metallic component of meteorites (e.g. Nagata and Sugiura 1976, Nagata 1979), these five ordinary chondrites are magnetically analyzed specifically for the purpose of an inter-comparison.

In the magnetic hysteresis analysis, the saturation magnetization (I_s) presents an approximate value of the content of metallic FeNi, while the coercive force (H_C) and the remanence coercive force (H_{RC}) give a measure of the dominant grain size of the ferromagnetic metal phase, where a higher coercivity represents a more relative abundance of minor single-domain or pseudo-single domain grains.

In the thermo-magnetic analysis, kamacite (α), taenite (β) and plessite ($\alpha + \beta$) phases can be distinctly separated by their magnetic hausion temperatures, and Ni-content in each phase can be approximately evaluated.

In Table 1, the observed values of I_s , I_R , H_C and H_{RC} and the estimated abundances of α -, β - and $\alpha + \beta$ - phases in the term of I_s of the five chondrites are summarized, together with Nagaharas results of the Ni-content spectra of individual metallic grains.

As for Yamato-74115, -74354 and -74362, Nagahara's analyses gave measurements of a reasonably large number of metallic grains. Compared with the magnetic analysis, it may be concluded that Yamato-74115 (H₅) and -74354 (L₆) contain mostly kamacite and plessite phases, whereas the metallic components of Yamato-74362(L₆) comprise kamacite, taenite and plessite.

The number of metallic grains analyzed by Nagahara for Yamato-74190 and -74646 does not seem to be sufficiently large. It appears almost certain, however, that the metallic components of Yamato-74646(LL₆) are composed mostly of plessite and/or taenite, the kamacite phase is none or little. A considerable difference between the magnetic analysis and the micro-probe one appears in Yamato-74190(L₆). Since kamacite is the major metallic phase in the magnetic analysis whereas taenite and/or plessite phases of Ni-content 32% are only a detected phase in the micro-probe analysis, additional special magnetic analyses have been further carried out to check this discrepancy.

Table 1. Composition of Metallic component

	Yamato					unit	
	-74115(H ₅)	-74354(L ₆)	-74362(L ₆)	-74190(L ₆)	-74646(LL ₆)		
(Magnetic parameters)							
I _S	23.9	21.8	9.5	9.2	3.2	emu /gm	
I _R	0.60	0.71	0.36	0.02	0.026	"	
H _C	26	66	84	6	20	Oe	
H _{RC}	89	2,620	1,995	91	406	"	
(Thermo-magnetic analysis)							
I _S (α)	19.7	17.3	4.7	5.5	(1) ~ 0	(2) 0.7	emu /gm
I _S ($\alpha + \beta$)	4.2	4.5	2.7	0.6	2.7	0.2	"
I _S (β)	~ 0	~ 0	2.1	3.1	0.5	2.3	"
(Nagahara's analysis)							
2 - 8 % Ni	((64))	4	(13)	0	0		
8 - 14 "	6	(23)	((22))	0	0		
14 - 20 "	7	((78))	(11)	0	0		
20 - 26 "	7	(16)	3	0	((7))		
26 - 32 "	((54))	2	1	0	2		
32 - 38 "	4	12	(9)	((9))	((6))		
38 - 44 "	1	5	0	((9))	((6))		
44 - 50 "	0	0	1	4	1		
50 - 56 "	0	0	1	0	0		
Total	143	140	61	22	22		

Remarks: (()) > 25%, 25% > () > 10%.

References:

- Nagahara, H. (1979 a) Mem. Nat'l. Inst. Polar Res., Spec. Issue. No.15, 111-122.
 Nagahara, H. (1979 b) Mem. Nat'l. Inst. Polar Res., Spec. Issue. No.15, 77-109.
 Nagata, T. (1979) Phys. Earth Plan. Inter. 20, 324-341.
 Nagata, T. and Sugiura, N. (1976) Mem. Nat'l. Inst. Polar Res., Ser C. No.10, 30-58.

PALEOINTENSITY OF ANTARCTIC ACHONDRITES

Takesi NAGATA

National Institute of Polar Research

A possible electromagnetic field and its variations are considered to be one of the most critical problems with respect to the formation and evolution of the early solar nebula system. For this reason, evaluations of the magnetic paleointensity have been attempted for various kinds of meteorite. As critically reviewed by Nagata (1979), however, no fully satisfactory result of the meteorite paleointensity has ever been obtained, though several results obtained for carbonaceous chondrites and achondrites appear to be almost reliable. The main difficulty in paleointensity studies on meteorites is concerned with a non-reproducibility in the thermal change of ferromagnetic characteristics of Fe-Ni-P-C₀ metals or magnetites. (It has been ascertained that iron and stony-iron meteorites must be excluded from the objects of paleointensity studies, because of a very small magnetic coercivity of their metallic parts.)

In a previous work (1980), some aspects of the paleointensity of Antarctic achondrites were examined, resulting in a provisional conclusion that the paleointensity for achondrites is 0.1 Oe or less, and those achondrites whose metallic component consists mostly of kamacite, such as eucrite and ureilite, can give rise to a relatively reliable estimation of the paleointensity.

In the present work, the paleointensity characteristics of these ureilites and an eucrite, Yamato-74123, -74130 and -74659 (Ur) and Yamato-75011, are newly examined by means of the NRM/ARM method. New results are summarized in the following table, together with the previous ones.

Since the NRM/ARM method can evaluate only the upper limit of paleointensity. (Nagata 1980), a certain calibration of the NRM/ARM method with the aid of the standard Koenigsberger-Thellier method will be necessary. In the present work, a comparison of the paleointensity data obtained by the ARM/NRM method with these obtained by the Koenigsberger-Thellier method is demonstrated for ALHA77302 (Eu) and 77257 (Ur).

Achondrite	NRM	Paleointensity
Yamato-74123 (Ur)	8.8×10^{-4} emu/gm	0.34 Oe
-74130 (Ur)	4.0×10^{-4} "	0.051 "
-74659 (Ur)	2.1×10^{-4} "	0.28 "
-75011 (Eu)	6.8×10^{-6} "	0.048 "
(previous results)		
ALHA-77005 (Eu)	3.6×10^{-5} "	0.010 "
-77302 (Eu)	4.1×10^{-6} "	0.049 "
-78040 (Eu)	6.4×10^{-6} "	0.060 "
-77257 (Ur)	5.4×10^{-4} "	0.089 "

References:

- Nagata, T. (1979) Phys. Earth Planet. Inter. 20, 324-341.
 Nagata, T. (1980) Mem. Nat'l. Inst. Polar Res. (In press).

#45

SPECTRAL REFLECTANCE(250-2500nm) of POWDERED SAMPLES OF ANTARCTIC METEORITES

Miyamoto, M., Mito, A., Takano, Y. Pure and Applied Sciences, College of General Education, Univ. of Tokyo, Meruro-ku, Tokyo 153, and Fujii, N. Dept. of Earth Sciences, Kobe Univ., Nada-ku, Kobe 657, Japan.

Spectral reflectance measurements of asteroids have increased rapidly and the resolution and wavelength coverage(visible-near IR) are available for the comparison between these astronomical data and the laboratory spectral reflectance data of meteorites or various mineral assemblages(e.g. Gaffey and McCord 1977). It is possible that the surface of small bodies such as asteroids or meteorite parent bodies are covered with the very thin layer(a regolith layer) of fine grain materials.

In order to examine the change of the reflectance spectra of the powdered samples of olivines and meteorites, the spectral reflectance measurements were made with a Beckman UV 5240 spectrophotometer using an integrating sphere. The spectra(250-2500nm) were recorded on a chart and in digital form on a floppy disc for computer processing. Preliminary examination was made of olivine(San Carlo, Arizona), Yamato-75258(LL6) and ALHA77231(L6).

It has been known that the albedo increases by pulverization of the sample, but the amount of this change is dependent on the mineral assemblages contained in the sample, and that whether the absorption feature becomes deep or not with the diminution of particle size depends on the mineral species contained in the sample(Adams and Filice 1967).

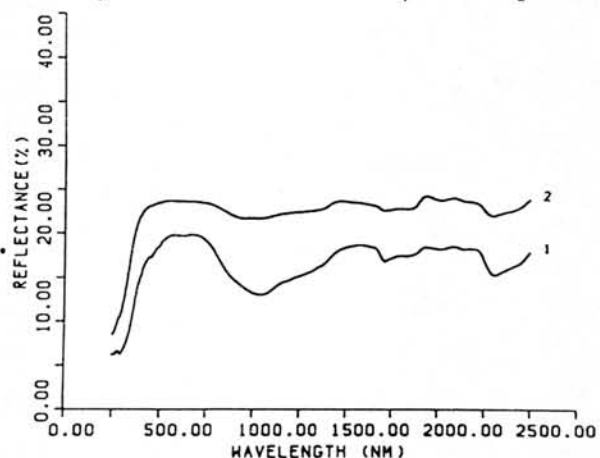
The results of the powder samples($<46\mu$) of the olivine and the ordinary chondrites(Y75258,ALHA77231) revealed that the depth of the absorption band(ca.1000nm) becomes shallow and the curvature of the spectral reflectance around ca.400nm is raised with the diminution of particle size. Therefore, the shape of the reflectance spectra gradually becomes 'flat' in the range of ca.400-1000nm with the diminution of particle size. The absorption feature in the range of ca.1000-2500nm varies slightly with the size of the samples. These features are enhanced for the very fine-grain($<46\mu$) fraction(Fig.1).

The reflectance spectra of 1 Ceres (or 2 Pallas) reported by Feierberg et al.(1980) shows the flat curve in the region of ca.500-2500nm, a small broad peak at ca.400-500nm, and steep drop off at wavelength less than ca.400 nm. The spectral reflectances of these asteroids seem to have many points of resemblance(e.g. its flatness and drop off less than 400nm) to those of powder samples of meteorites(e.g. ordinary chondrites). Though the albedo of these asteroids is lower than that of the powder sample, we note that a small amount of opaque minerals or metallic components or low reflectivity materials(e.g. carbon black) is effective on lowering the albedo and depressing other spectral features(Johnson and Fanale 1973).

It is necessary to examine in more detail the effect of pulverization of meteorites or mineral assemblages (including very fine-grain fractions $<ca.50\mu$) in order to identify exactly the surface materials of these asteroids.

Fig.1 Spectral reflectance curve of Y-75258.

- 1: coarse grain
- 2: powdered($<46\mu$)



A CLASSIFICATION OF SOME YAMATO-75 CHONDRITES (III)

Miura, Y. and Matsumoto, Y.

Department of Mineralogical Sciences and Geology, Faculty of Science, Yamaguchi University, Yamaguchi 753

The Yamato-75108 to 75257 chondrites are considered to be originally one meteorite which would be broken into many fragments (Matsumoto, 1978; Matsumoto et al., 1979, 1980).

Chemical compositions of the olivines and orthopyroxenes in four chondrites (Yamato-75135, 136, 140, 271) have been determined by using a JEOL JXA-50A electron probe X-ray microanalyzer.

Analytical data of three chondrites (Yamato-75135, 136, 140) of which mass weights are 98.1, 62.8 and 35.9g, respectively are shown in Tables 1 to 4. Table 1 shows frequency distribution of iron contents of olivines and orthopyroxenes in the Yamato-75 chondrites. Tables 2 and 3 show mean composition of the olivines and orthopyroxenes, mean deviation and percent mean deviation of their iron contents in the Yamato-75 chondrites. It is found in Tables 2 and 3 that the three chondrites of Yamato-75135, 136 and 140 which are classified as an L4-5 type show similar iron content and percent mean deviation.

Yamato-75271 chondrite of which mass weight is 1797.5g did not be classified yet. Analytical data in Tables 1 to 3 and microscopic observation show that the Yamato-75271 chondrite is tentatively classified as an L4-5 type.

Plagioclases in the Yamato-75 chondrites are Ab-rich feldspars from oligoclase to andesine as shown in Table 4.

Table 1. Frequency distribution of iron contents of olivines and orthopyroxenes in some Yamato-75 chondrites

Atomic % Fe	Olivine					Orthopyroxene				
	22	23	24	25	26	19	20	21	22	23
Sample No.	Percent of Measurements					Percent of Measurements				
Yamato-75135(93)	-	11.8	76.5	11.7	-	9.1	45.5	45.5	-	-
-75136(93)	-	9.1	36.4	36.4	18.1	-	-	81.8	9.1	9.1
-75140(50)	-	-	33.3	66.7	-	8.3	33.4	50.0	8.3	-
-75271(91)	10.0	30.0	40.0	20.0	-	12.5	50.0	37.5	-	-

#46 - 2

Table 2. Mean compositions of olivines and percent mean deviations of those iron contents in the analyzed Yamato-75 chondrites

Sample No.	Mean composition			No. of measurements	Mean deviation	% mean deviation
	Ca	Mg	Fe(%)			
Yamato-75135(93)	0.01	75.58	24.41	17	0.318	1.30
-75136(93)	0.05	74.81	25.14	11	0.466	1.85
-75140(50)	0.00	74.86	25.14	12	0.299	1.19
-75271(91)	0.16	75.59	24.25	10	0.726	2.99

Table 3. Mean compositions of orthopyroxenes and percent mean deviations of those iron contents in the analyzed Yamato-75 chondrites

Sample No.	Mean composition			No. of measurements	Mean deviation	% mean deviation
	Ca	Mg	Fe(%)			
Yamato-75135(93)	1.16	78.07	20.77	11	0.475	2.29
-75136(93)	1.00	77.25	21.75	11	0.485	2.23
-75140(50)	1.16	77.76	21.08	12	0.573	2.72
-75271(91)	0.83	78.51	20.66	8	0.416	2.01

Table 4. Plagioclase composition in the analyzed Yamato-75 chondrites

Sample No.	Or	Ab	An (mol. %)
Yamato-75135(93)	1.2	85.1	13.7
	12.5	67.1	20.4
-75136(93)	9.3	76.4	14.3
-75140(50)	3.5	84.0	12.5
-75271(91)	1.8	55.3	42.9
	19.5	55.2	25.3
	8.6	75.6	15.8
-75110(90)*	4.3	53.6	42.1
	9.7	55.0	35.3
-75110(93)*	5.8	53.7	40.5

* Matsumoto et al. (1981)

PHYSICAL PROPERTIES OF METEORITES

Kiyoshi Yomogida and Takafumi Matsui
Geophysical Institute, University of Tokyo

Physical properties of meteorites may represent some formation condition of meteorites. However, a few data on physical properties of meteorites are available. We have measured porosity, thermal diffusivity and elastic constants of meteorites. Because, these quantities are considered to be important in revealing a nature of meteoritic parent bodies.

The new porosity data are obtained for 5 ordinary chondrites (ALHA-77288, -77294, -78251, -78103 and META-78003). In order to avoid the secondary effect such as impact and erosion on the porosity of meteorites, fresh samples with few cracks were chosen. The porosity, ϕ , is estimated by the relation, $\phi = 1 - \rho_0/\rho_{\text{bulk}}$, where ρ_0 is the intrinsic density and ρ_{bulk} is the bulk density. The intrinsic density, ρ_0 , is measured by the helium pycnometer and the bulk density, ρ_{bulk} , by the modified Archimedes method. (The details of these methods were shown in Matsui et al. (1980).) It must be noted that the porosity calculated by this method is in good agreement with that of the crushed sample but gives higher value (about 20%) than that obtained by the usual method such as water-saturated method. The results are listed in Table 1. The porosities of these chondrites are mostly smaller than that of loose sand and correspond to that of tuff, so that consolidation must have proceeded under the condition of no available water.

Fig. 1 shows the thermal diffusivity of meteorites measured in this study. We used the modified Angstrom method (see Matsui and Osako (1979)). The accuracy of these measurements is estimated to be less than $\pm 10\%$. The measurements have been conducted in vacuum condition (below 10^{-3} mmHg). The low thermal diffusivity of ALHA-76009 is noticed. It may be due to its high porosity (19.6%). For ALHA-77231 measurements were conducted for three mutually perpendicular directions. Thermal diffusivities do not differ significantly between directions. Data of the elastic constants will also be reported.

Table 1. Densities and porosity.

SAMPLE	TYPE	VOLUME (cm ³)	WEIGHT (g)	DENSITY (g/cm ³)		POROSITY (%)
				bulk	intrinsic	
ALHA-77288	H6	4.88	17.340	3.55	3.75	5.1
ALHA-77294	H5	4.49	14.275	3.18	3.86	17.5
ALHA-78251	L6	6.06	18.820	3.11	3.71	16.2
ALHA-78103	L6	5.85	18.156	3.11	3.73	16.7
META-78003	L6	4.81	14.694	3.06	3.61	15.4

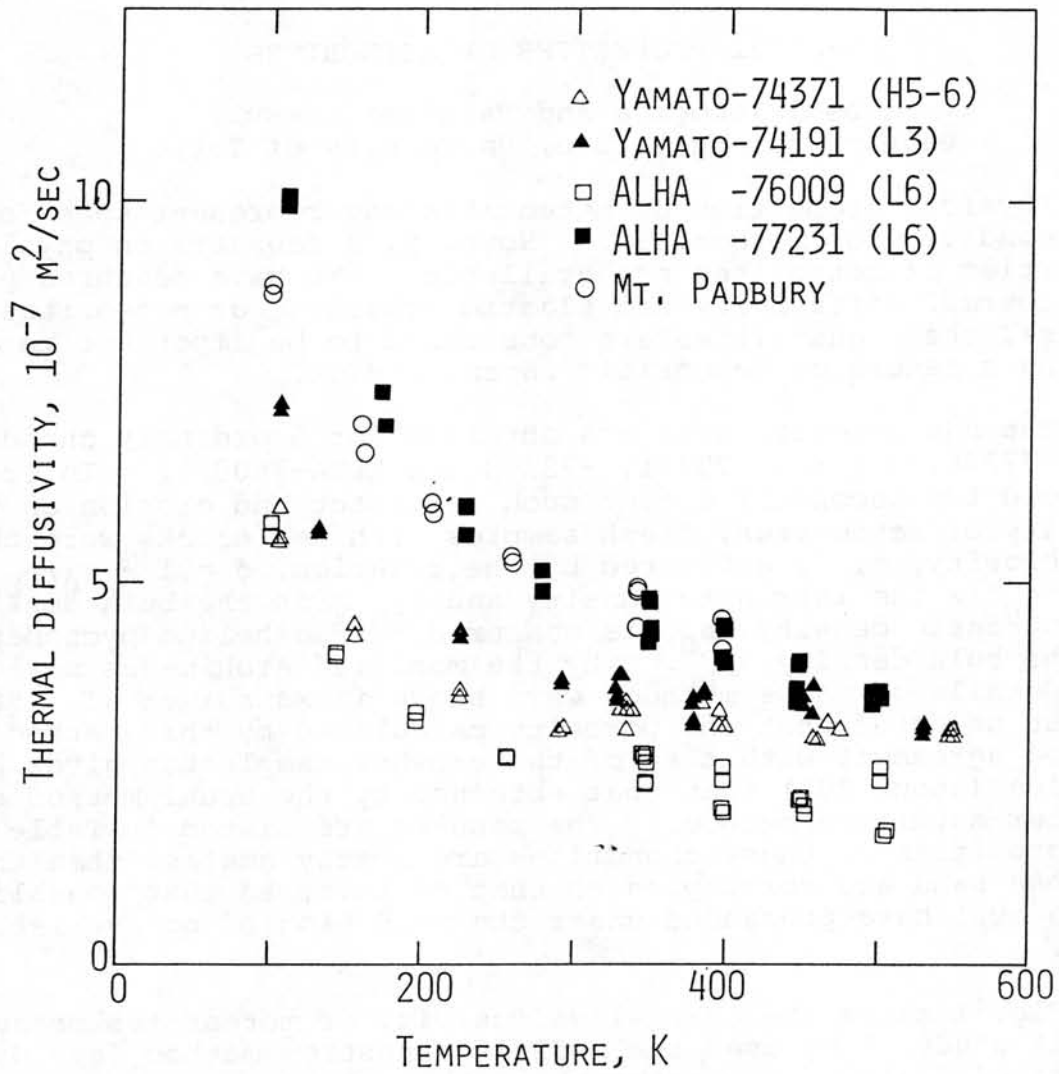


Fig. 1. Thermal diffusivity, k , versus temperature, T , for Yamato-74371, -74191, ALHA-76009, -77231 and Mt. Padbury.

REFERENCES

Matsui, T., Hamano, Y. and Honda, M. (1980)
Mem. Natl Inst. Polar Res., Spec. Issue, No. 17.
Matsui, T. and Osako, M. (1979)
Mem. Natl Inst. Polar Res., Spec. Issue, No. 15.

DISLOCATIONS IN OLIVINES FROM PALLASITE METEORITES

Karato, S.¹ and Matsui, T.²

¹ Ocean Research Institute, University of Tokyo,
Nakano, Tokyo 164, Japan

² Geophysical Institute, Faculty of Science,
University of Tokyo, Tokyo 113, Japan

Dislocation structures in olivines from Pallasite meteorites (Yamato-74044, Admire, Brehnam, New Port, Dora, Mount Vermon, Glorietta Mountain, and Eagle Station) are examined by the oxidation decoration technique. Two types of dislocation structures, (1) high temperature and/or low strain rate (HT-LS) type and (2) low temperature and/or high strain rate (LT-HS) type are observed. In general, the density of HT-LS type dislocations is low, 10^4 to 10^6 cm^{-2} , suggesting that relatively low stresses (less than 10 MPa) were acting in their parent bodies. The LT-HS type dislocations are observed in some meteorites associated with the HT-LS type dislocations. No evidence of annealing of the LT-HS type and the coexistence of these two types suggest that the LT-HS type dislocations were formed after the HT-LS type dislocations had been formed and that the strain associated with the event that resulted in the formation of LT-HS type dislocations may be low, less than about 1 %. These observations suggest that the LT-HS type dislocations were formed by a shock event. Stress-temperature conditions of a shock event are estimated from (1) the temperature dependence of the Peierls stress, (2) the time constant of the dislocation dipole collapse, and (3) the time constant of the cooling of meteorites. The results suggest that the shock event that has caused the dislocation multiplication occurred at relatively hot condition, indicating that the collision of parent bodies with hot interior may be responsible for the formation of LT-HS type dislocations.

#49-1

Mineralogy of the Matrix Phyllosilicates of Carbonaceous Chondrite by High Resolution Electron Microscopy

Junji AKAI
Faculty of Science, Niigata University

Carbonaceous chondrite is considered as one of the oldest material which offers informations about the origin of the solar system. The genesis of the phyllosilicate in the carbonaceous chondrite is not always ascertained. In this report, the author will describe mineralogical characters of the phyllosilicate in Yamato-74662 (C2). The results will be compared with those of Murchison Meteorite (C2) (Mackinnon et al. 1979; Akai, 1979, 1980).

Yamato-74662 is composed mostly of phyllosilicate. Minor amount of other minerals such as olivine, Fe-Mg pyroxene and Ca pyroxene etc. are scattered in the black phyllosilicate matrix as crystal fragments or chondrules. Another characteristic occurrence of phyllosilicate is that in amygdal cavity, where it makes relatively pure phyllosilicate aggregate. These phyllosilicates are yellowish brown and have almost no pleochroism. The inner wall of the amygdal cavity is rimmed by small grains of Ca pyroxenes. These textural features of amygdal cavity containing relatively pure phyllosilicate are very similar to those of the Murchison Meteorite.

The chemical compositions of the phyllosilicate are shown in Table 1.

Phyllosilicate can be morphologically classified into two types by high resolution electron microscopy; i) thick platy and ii) phyllosilicate with low crystallinity (tube? Fig.1). Both have 7 Å serpentine structure. New phyllosilicate (1:1:1×2 type) found in the Murchison Meteorite was not found. Thick platy phyllosilicate sometimes has noticeable character of high density of stacking disorder (Fig. 2 and 3). These features are also the same as those in the Murchison Meteorite. Another 11 Å layer structure and locally disordered structure composed of serpentine and brucite layers were found (Fig.4&5).

Table 1. Electron microprobe analysis of phyllosilicates in Yamato-74662 ^{cf.} Chemical Compositions (Murchison M)

	black matrix		(yellowish brown)				amygdal cav.phy.		green mat	Phyllosilicate A		Phyllosilicate B	
SiO ₂	25.1	25.1	35.6	32.7	29.1	31.9	17.5	12.7	28.3	23.7	23.9	15.8	16.9
TiO ₂	0.0	0.0	0.2	0.1	0.2	0.2	0.3	0.2	0.2	0.1	0.1	0.2	0.8
Al ₂ O ₃	4.5	4.1	3.0	2.4	6.2	5.4	26.4	40.1	4.1	4.9	3.8	20.8	21.4
Cr ₂ O ₃	0.3	0.2	0.6	0.5	0.1	0.1	0.1	0.0	0.8	0.0	0.0	0.1	0.0
FeO	45.1	44.8	33.8	31.1	47.0	33.4	25.6	17.7	31.6	47.3	41.6	18.0	22.2
MnO	0.2	0.2	0.1	0.2	0.2	0.1	0.1	0.0	0.2	0.2	0.2	0.1	0.1
MgO	11.4	11.8	17.2	19.4	10.4	12.1	16.3	17.9	12.5	9.8	13.3	20.8	15.1
CaO	0.4	0.3	0.6	0.3	2.2	6.3	1.7	2.0	5.5	0.2	0.1	0.6	0.2
Na ₂ O	0.3	0.1	0.1	0.2	0.3	0.2	0.1	0.0	0.4	0.1	0.2	0.0	0.0
K ₂ O	0.0	0.0	0.0	0.0	0.0	0.0	0.0	0.0	0.0	0.0	0.0	0.0	0.0
Total	87.3	86.6	91.2	86.9	95.7	89.7	88.1	90.6	83.6	86.3	83.2	76.4	76.7

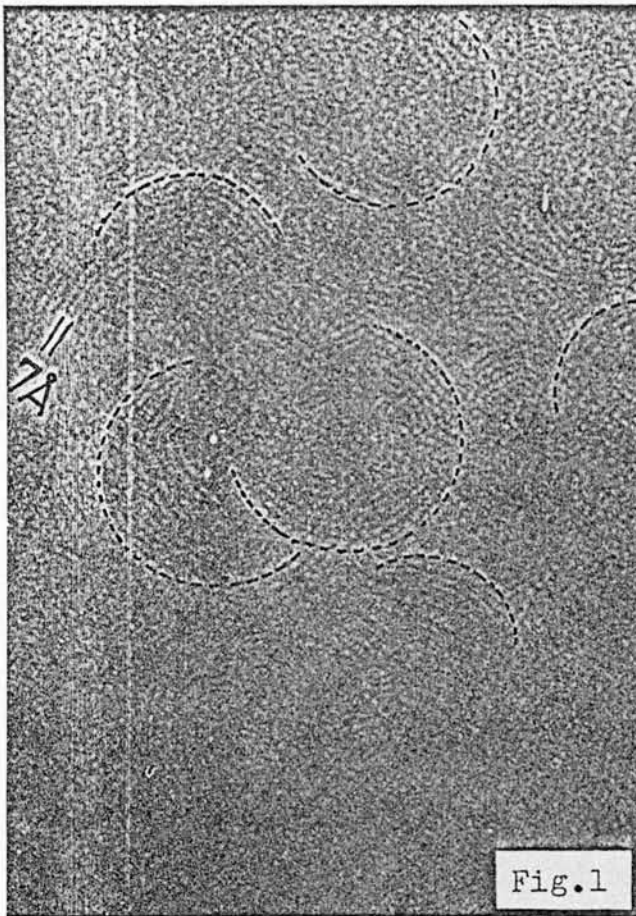


Fig.1

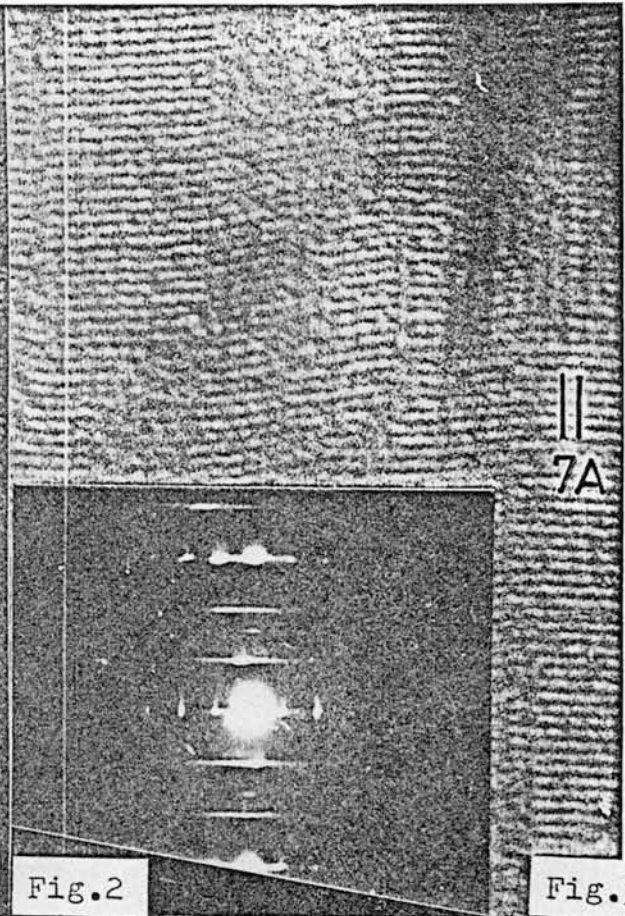


Fig.2

Fig.3

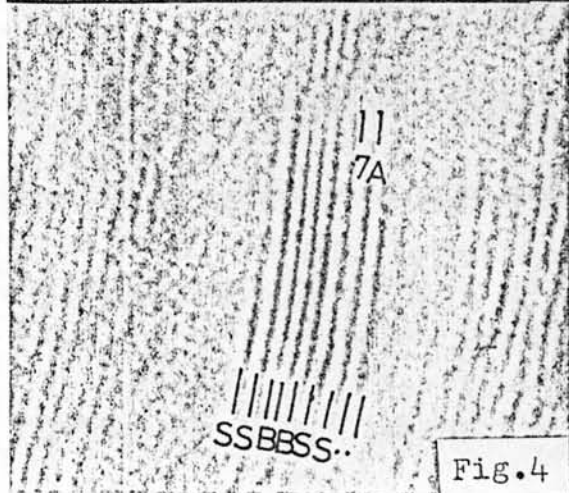


Fig.4

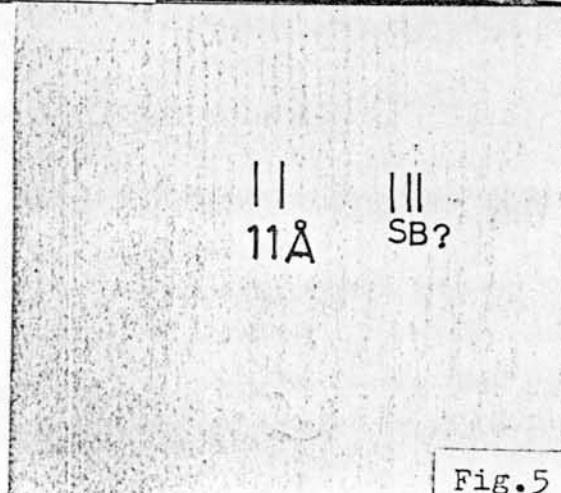


Fig.5

